On the applicability of geophysics for groundwater investigations in areas with lack of hydrogeological information. Examples from Mozambique

Chirindja, Farisse Joao

2018

Document Version:
Förlagets slutgiltiga version

On the applicability of geophysics for groundwater investigations in areas with lack of hydrogeological information. Examples from Mozambique

Farisse João Chirindja

LUND
UNIVERSITY

Coverphoto by Torleif Dahlin

Faculty of Engineering, LTH
Department of Engineering Geology

ISRN LUTVDG/(TVTG-1037)/1-49/ (2018)
ISBN 978-91-7753-190-6 (print)
ISBN 978-91-7753-191-3 (pdf)

Printed in Sweden by Media-Tryck, Lund University
Lund 2018

Dedication

To my family: Laura Mateus Chirindja, Nilton Tomo Chirindja, Lucia Farisse Chirindja and João Farisse Chirindja.

Acknowledgements

This thesis was completed with help and encouragement from many people. I am particularly grateful to:

Torleif Dahlin has been a truly great supervisor leading me in the right direction since my master's studies until he handed over the main supervision to Gerhard Barmen in 2018;

Gerhard Barmen and *Diniz Juizo* as co-supervisors always encouraged me during hard times with honestly zealous comments and tips to improve my knowledge and understanding of hydrogeological phenomena;

Richard Owen, Nils Perttu, Franziska Steinbruch and *Jan-Erik Rosberg* who co-authored my papers, for helpful discussions during the preparation and implementation of field work, interpretation of data and writing the papers;

The MFS students *Kristina Arvidsson, Li Stenberg, Erik Sjöstrand and Oskar Enkel, Björn Andersson, Tom Björkström, Elin Olsson and Sofia Hallerbäck,* for helping with field data collection, analysis and interpretation of field data;

SIDA/SAREC who have been the financer and supporter for the financing of this work during its full extension;

The colleagues at *Engineering Geology Division* in *Lund University* for friendship and help, as well as for making the department a wonderful place to study;

The G*eology Department of Eduardo Mondlane University* for great company during field work in Gorongosa National park and the Districts of Rapale and Mongicual;

The Eduardo Mondlane University students *Felix Uqueio, Manuel Nepuruarua and Eugenio José* for helping with field data collection.

And all the other wonderful people that I came into contact with during my thesis work. Thank you very much!

Popular science summary

In tropical climates where the rainfall is seasonal, surface water is depleted and rare during the dry season. As a consequence, during the dry season, groundwater is usually the main solution for water supply. One important way of locating potential sites to extract groundwater is the application of geophysical methods that measure the physical properties of the geological material. For the interpretation of hydrogeophysical data, usually additional reference data are needed either to calibrate the chosen geophysical model or to verify its hydrogeological interpretation. In many countries such information does not exist or it is not well organized, old reports are missing in the archives and data is not published in scientific journals.

The overall aim of this work is to improve the knowledge about the groundwater occurrence by using combinations of different geophysical methods and other methods in areas with little background information. A number of methods have been assessed regarding their applicability in solving real hydrogeological problems in Mozambique. The implemented methods are electrical resistivity tomography (ERT) which measure the resistance of ground to transport electrical current, magnetic resonance sounding (MRS) which measures the decay time after the water molecules have been excited, induced polarization (IP) which measures the decay time after the ground has been electrically charged and geophysical borehole logging (BL) which measures several properties in details within the boreholes. Other methods include slug tests, dilution tests and grain size analyses.

Since the 1960s vertical electrical sounding (VES) has been the dominant geophysical method in Mozambique for groundwater studies. As the name says, the method mainly gives information about the vertical variation of the resistivity of the subsurface. Therefore, ERT was used throughout the survey as this method measures both the vertical and lateral variation of the ground resistivity, and it can be adapted to different scales of surveying by varying the electrode separation. Reliable interpretation of ERT results requires access to relevant reference data. However, such data turned out to be very scarce and limited to observations close to the surface such as grain size analysis of dug samples. In order to partly compensate for this scarcity of information, ERT was used together with other geophysical methods in addition to the existing small amount of reference data.

For example, in the Urema floodplain in a part of Gorongosa National Park, the combination of different geophysical methods aimed to improve the understanding of a possible interaction between surface and ground water. The aquifer layers indicated by ERT results were also indicated by MRS, due to low resistivity and high free water content compared with clay layers with low resistivity and low free water content. MRS results may give indication of some hydraulic properties such as hydraulic conductivity, but the results were not fully exploited due to lack of other reference data.

The Mozambican government has invested heavily in borehole projects throughout the country to satisfy the populations' needs, aiming to achieve one of the Millennium Development Goals (more than 50% of population should have access to safe drinking water by 2015). But detecting the groundwater in consolidated rock areas has been challenging. Consequently many drilled boreholes were dry or only produced a limited water supply. The main reasons found, in this study, for the limited success of groundwater development are related to socio-economic and technical aspects.

The community members were asked to choose three preferable sites to drill a water well. The choice was not based on any scientific approach. Hence there was a tendency to have the well close to the leader´s house so that he or she may have it under their control which probably contributed a lot to the reported failures.

Combined ERT and MRS were used to identify the main reason for low possible groundwater extraction rates from some of the wells. MRS did not work well due to the low signal caused by low water content in combination with different types of noise, both natural and anthropogenic. Interpretation of ERT results compared to groundwater extraction rates from new boreholes showed that areas with a well-developed weathered layer have better potential

for groundwater extraction. Dry wells were drilled in places with a thin weathered layer according to the interpretation of the resistivity.

Combined ERT and measurements of IP was used to explain the salinity of groundwater in some boreholes. The interpretation of IP results, in terms of normalized chargeability, was useful to detect sediments with heavy mineral content. The dissolution of heavy minerals was interpreted as the reason for the salinity of groundwater in some boreholes. Unfortunately some models were not useful due to high residual error, which was caused by poor ground contact.

The borehole logging was performed combining sensors that measure the resistivity, magnetic susceptibility and natural gamma. As the pump was removed to perform the borehole logging, slug testing was also performed to describe the aquifer properties in the vicinity of the well.

The study indicated that the applied hydrogeophysical tools improved the knowledge about the hydrogeology in areas without reference information. In such conditions, the combination of two different methods is a recommended approach since this helps to reduce hydrogeological uncertainties.

Resumo da ciência popular

Em climas tropicais, onde a precipitação é sazonal, a água da superfície é escassa durante a estação seca. Como consequência, durante a estação seca, a água subterrânea é geralmente a principal solução para o abastecimento de água. Uma maneira importante de localizar locais potenciais para extrair água subterrânea é a aplicação de métodos geofísicos que medem as propriedades físicas do material geológico. Para a interpretação de dados hidrogeofísicos, geralmente são necessários dados de referência adicionais para calibrar o modelo geofísico escolhido ou para verificar sua interpretação hidrogeológica. Em muitos países essa informação não existe ou não é bem organizada, os relatórios antigos estão em falta nos arquivos e os dados não são publicados em revistas científicas.

O objetivo geral deste trabalho é melhorar o conhecimento sobre a ocorrência de águas subterrâneas usando combinações de diferentes métodos geofísicos e outros métodos em áreas com pouca informação de base. Vários métodos foram avaliados quanto à sua aplicabilidade na resolução de problemas hidrogeológicos reais em Moçambique. Os métodos implementados são a eletrorresistividade (ERT) que medem a resistência do solo para transportar corrente elétrica, ressonância magnética (MRS) que mede o tempo de decaimento após as moléculas de água terem sido excitadas, polarização induzida (IP) que mede o tempo de decaimento após o subsolo ter sido carregado eletricamente e diagrafia geofísica de furo (BL), que mede várias propriedades em detalhes dentro dos furos. Outros métodos incluem slug test, testes de diluição e análises granulométricas.

Desde a década de 1960, a sondagem elétrica vertical (VES) tem sido o método geofísico dominante em Moçambique para estudos de águas subterrâneas. Como o nome diz, o método dá principalmente informações sobre a variação vertical da resistividade do subsolo. Portanto, a ERT foi usada durante todo o levantamento, pois este método mede a variação vertical e lateral da resistividade do solo, e pode ser adaptado a diferentes escalas de levantamento variando a separação do eletrodo. A interpretação confiável dos resultados da ERT requer acesso a dados de referência relevantes. No entanto, esses dados são muito escassos e limitados a observações próximas à superfície, como a análise granulométrica de amostras superficiais. A fim de compensar parcialmente essa escassez de informações, a ERT foi usada em conjunto com outros métodos geofísicos, além da pouca quantidade existente de dados de referência.

Por exemplo, na planície de inundação de Urema, numa parte do Parque Nacional da Gorongosa, a combinação de diferentes métodos geofísicos teve como objetivo melhorar a compreensão de uma possível interação entre águas superficiais e subterrâneas. As camadas aquíferas indicadas pelos resultados da ERT também foram indicadas pela MRS, devido à baixa resistividade e alto teor de água livre, comparadas às camadas de argila com baixa resistividade e baixo teor de água livre. Os resultados da MRS podem indicar algumas propriedades hidráulicas, como a condutividade hidráulica, mas os resultados não foram totalmente explorados devido à falta de outros dados de referência.

O governo moçambicano investiu fortemente em projetos de poços em todo o país para satisfazer as necessidades das populações, visando atingir um dos Objectivos de Desenvolvimento do Milénio (mais de 50% da população deve ter acesso a água potável até 2015). Mas detectar as águas subterrâneas em áreas rochosas tem sido um desafio. Consequentemente, muitos furos perfurados estavam secos ou com produção limitada de água. As principais razões encontradas, neste estudo, para o baixo sucesso estão relacionadas a aspectos socioeconômicos e técnicos.

Os membros da comunidade foram convidados a escolher três locais preferenciais para perfurar um poço de água. A escolha não foi baseada em nenhuma abordagem científica. Portanto, havia uma tendência de ter o poço próximo à casa do líder, de modo que ele pudesse tê-lo sob seu controle, o que provavelmente contribuiu muito para as falhas relatadas.

ERT e MRS combinados foram usados para identificar a principal razão para as baixas taxas de extração de água subterrânea de alguns dos poços. A MRS não funcionou bem devido ao baixo sinal causado pelo baixo teor de água em combinação com diferentes tipos de ruído, tanto natural quanto antropogênico. A interpretação dos resultados da ERT em comparação com as

taxas de extração de água subterrânea de novos furos mostrou que as áreas com uma camada meteorizada bem desenvolvida têm melhor potencial para extração de água subterrânea. Poços secos foram perfurados em locais com uma fina camada meteorizada de acordo com a interpretação da resistividade.

ERT combinada e medições de IP foram usadas para explicar a salinidade das águas subterrâneas em alguns furos. A interpretação dos resultados de PI, em termos de cargabilidade normalizada, foi útil para detectar sedimentos com conteúdo mineral pesado. A dissolução de minerais pesados foi interpretada como a razão para o alto valor de conductividade eléctrica das águas subterrâneas em alguns furos. Infelizmente alguns modelos não foram úteis devido ao alto erro residual, que foi causada pelo mau contato com o solo. A diagrafia do furo foi realizada combinando sensores que medem a resistividade, suscetibilidade magnética e gama natural. Como a bomba foi removida para realizar a diagrafia do poço, slug tests também foram realizados para descrever as propriedades do aquífero nas proximidades do poço. O estudo indicou que a abordagem hidrogeofísica aplicada melhorou o conhecimento sobre a hidrogeologia em áreas sem informações de referência. Em tais condições, a combinação de dois métodos diferentes é uma abordagem recomendada porque ajuda a reduzir as incertezas hidrogeológicas.

List of Papers

Paper 1 Arvidsson K, Stenberg L, **Chirindja FJ**, Dahlin T, Owen R, Steinbruch F. (2011) A hydrogeological study of the Nhandungue river, Mozambique – A major groundwater recharge zone. Physics and Chemistry of the Earth, 36, 789-797

Paper 2 Chirindja FJ, Dahlin T, Perttu N, Steinbruch F, Owen R (2016) Combined electrical resistivity tomography and magnetic resonance sounding investigation of the surface-water/groundwater interaction in the Urema Graben, Mozambique. Hydrogeology Journal, 24 (6), 1583-1592

Paper 3 Chirindja FJ, Dahlin T, Juizo D (2017) Improving groundwater-well siting approach in consolidated rock in Nampula province, Mozambique. Hydrogeology Journal, 25(5), 1423-1435. DOI 10.1007/s10040017-1540-1

Paper 4 Chirindja FJ, Dahlin T, Juizo D, Steinbruch F. (2016) Reconstructing the formation of a costal aquifer in Nampula province, Mozambique from ERT and IP methods for water prospection. Published: Environmental Earth Sciences Journal, 76:36, DOI 10.1007/s12665-016-6364-0

The author's contributions to the papers

Paper 1 The author took part in field data collection with Arvidsson K and Stenberg L, supervised the field work together with Dahlin T, Owen R and Steinbruch F and contributed to the writing and discussion of the paper.

Paper 2 The author conceived the survey together with Dahlin T and Perttu N, participated in field data collection, processing and inversion of ERT data together with Dahlin T and MRS data with Perttu N. He wrote the paper with all the other co-authors, where he led the process.

Paper 3 The author participated in field data collection, together with students from Lund and Eduardo Mondlane University, as well as processing and inversion of ERT data together with Dahlin T. The author participated in the writing of the paper with all the authors and took the lead in the writing process.

Paper 4 All the authors conceived the study. The author acquired the field data together with students from Lund and Eduardo Mondlane University, and processed and inverted the data. He and Steinbruch F have written the entire article and produced the geological conceptual model with supervision of Dahlin T and Juizo D.

Related conference and journal papers

Chirindja FJ, Dahlin T, Perttu N, and Steinbruch F (2013) Combined ERT and MRS Investigation of Surface and Groundwater Interaction in a Part of Gorongosa National Park in Mozambique. WaterNet Conference, Dar Es Salaam, Tanzania.

Chirindja FJ, Sjöstrand E, Enkel O and Dahlin T (2013) Geophysical Investigations of a Rural Water Point Installation Program in Nampula Province, Mozambique. Near Surface Geoscience, Bochum, Germany.

Chirindja FJ, Andersson B, Björkström T, Dahlin T and Juizo D (2014) Geophysical Investigation of a Rural Water Point Installation Program in Nampula Province, Mozambique. SAGEEP 2014, Boston - USA.

Chirindja FJ, Rosberg JE, Dahlin T (2017) Borehole logs and slug tests for evaluating the applicability of electrical resistivity tomography for groundwater exploration in Nampula complex, Mozambique. Published: Water Journal (MDPI) 9:95, DOI: 10.3390/w9020095

Related Master thesis

Chirindja F and Hellman K (2009) Geophysical investigation in a part of Gorongosa National Park in Mozambique – A minor field study. Master thesis, IRSN LUTVDG/TVTG—5113—SE, 57 pp. Engineering Geology, Lund University, Sweden.

Table of content

1. Introduction

Groundwater is a natural resource that can supply water in areas where other options would be more expensive. Most of the drinkable groundwater is generally located in the shallow subsurface of the earth. This is an extremely important geological zone because it yields much of our water resources, supports agriculture and ecosystems and influences our climate (Hubbard & Rubin, 2005; MacDonald & Calow, 2009). This groundwater can be indirectly detected with many different geophysical methods. Furthermore the geophysical data can be used to characterize some hydrogeological properties of aquifers (Linde et al., 2006; Lubczynski & Roy, 2003).

The improvement of digital technology for acquisition and processing since the 90s facilitated the application of geophysics in this context. This improvement has been possible due to improved computational speed and capability associated with processing, inversion, modelling and visualization of geophysical data. The downside of this development is the cost of the equipment. The need of additional information (so-called ground-truth data) for the interpretation of geophysical results is also often over-looked.

Electrical, electromagnetic, magnetic, seismic and other geophysical methods are techniques applied for groundwater exploration that have been improved with time. Among those methods, the electrical method is widely used in groundwater exploration in many developing countries (Kellett et al., 2001; MacDonald et al., 2012; Moyce et al 2006; Muiuane, 1999; Reynolds, 1987).

In Mozambique, Vertical Electrical Sounding (VES) is up to now the main method used to explore for groundwater. The method has been successfully used in unconsolidated rock (about 1/3 of the country) but usually it encounters difficulties in hard rock areas (2/3 of the country). The reason is the assumption of the method that all subsurface layers are horizontal and homogeneous (Srivastava & Bhattacharya, 2006). However in cases where this assumption is not valid, the results can become misleading.

The situation is worsened when no additional data are available, which is normal in a developing country like Mozambique. Existing additional information such as geological and hydrogeological maps, pumping tests and water quality data are either out of date, questionable or do not exist at all. To overcome this problem a combination of two or three different geophysical methods with limited additional

reference information was tested in Mozambique in different geological environments.

1.1 Objectives

The overall objective of the research is to investigate how a combination of hydrogeophysical and other methods can improve the understanding of the hydrogeological conditions in areas with little background information. The investigation was based on answering questions concerning groundwater occurrence and recharge conditions using the Electrical Resistivity Tomography (ERT), Magnetic Resonance Sounding (MRS), Induced polarization (IP) and borehole logging methods.

The specific objectives are:

- To identify the groundwater recharge conditions in sedimentary unconsolidated rock. The assessment is based on a comparison of results from ERT and available geological information.
- To investigate the applicability of ERT and MRS for improving the understanding of the interaction between surface water and groundwater.
- To assess the applicability of ERT combined with IP in understanding basement aquifers and reasons for failure of groundwater production from newly drilled wells.
- To improve the interpretation of geophysical data with borehole logging and slug test results.

1.2 Limitations

This thesis is focused on the application of resistivity, magnetic resonance sounding and induced polarization methods for mapping of groundwater resources in Mozambique. Even though other geophysical methods for groundwater exploration do exist, the thesis is limited to the use of these methods as they are among the most widely used ones.

The methodology has been evaluated for Mozambican conditions. However, it is expected that all other countries with similar geology, climate and socio economic situation can fit in this approach.

1.3 Thesis structure

The thesis work is based on five field campaigns carried out in three different geological environments in Mozambique: two surveys in Sofala province and three in Nampula province. The field work has resulted in five published scientific papers. Four of them are appended to the thesis. In PAPER 1 and PAPER 2 the ERT was tested in a graben basin filled with unconsolidated sediments mainly sand and clay (in PAPER 2 ERT was combined with MRS). In PAPER 3 the combination of MRS and ERT was implemented in basement aquifers. As the MRS method did not work well, it was substituted by the Induced Polarization method (IP) in PAPER 4. The combination of ERT with other methods gave insufficient information for interpretation, therefore Chirindja et al. (2017b) performed borehole logging in an attempt to improve the interpretation of ERT models. Since the pump was removed from each borehole to perform the geophysical logging, slug tests were also performed to determine some hydraulic properties of the aquifers.

The summary part of the thesis has been written in order to introduce and emphasize the problems investigated in the different field campaigns and papers. It clarifies the specific contribution from each of them to get closer to the final objective of the project as described above. The summary part starts with a section about the geology and hydrogeology of Mozambique in general. The subsequent section describes briefly all the geophysical methods used in this study. In the next section, selected findings regarding the application and interpretation of chosen methods in situations with little additional information are brought up and discussed in relation to three case studies. In each case study, results from the field surveys are presented. Finally, the summary part ends with discussion and some general conclusions concerning the objectives and some proposals for future research.

2. Geology and hydrogeology of Mozambique

2.1 Background

Mozambique is located in the south-east part of Africa. In the north it borders with Tanzania, in the east with the Indian Ocean, in the west with Malawi, Zambia and Zimbabwe and in the south with South Africa and Swaziland. Mozambique has 10 provinces: Niassa, Cabo Delgado, Nampula and Zambezia in the north; Sofala, Tete and Manica in the center; and Inhambane, Gaza and Maputo in the south (Figure 1). The capital city is Maputo and it is located in the Maputo province.

A low-lying coastal belt characterizes the eastern parts of Mozambique. This coastal belt gets wider from north to south and covers about 50% of the country's surface area. The coastal plain rises to the west and meets the high plateau, 500 m to 1000 m above sea level. The terrain in Mozambique is relatively flat in general with a mountainous area to the northwest. In the western plateaus, several areas are dotted with granite inselbergs (Briggs, 2007).

The climate is tropical with two main seasons: wet and dry season. The wet season starts from October and goes to March and is characterized by high temperatures (mean temperature is 28 degrees centigrade) and rain. The dry season stretches from April to September with low temperatures (mean temperature is 23 degrees centigrade) and the absence of rain (Briggs, 2007).

Temperature and rainfall varies with the hottest and most humid parts along the northeastern coast and colder areas at higher altitudes in Niassa and Nampula provinces. Most parts of northeast and central Mozambique have an annual precipitation in excess of 1000 mm. The highland east of Malawi can experience almost 2000 mm annually. The South is much drier; in the interior of Gaza province, annual rain can be below 500 mm (Briggs, 2007).

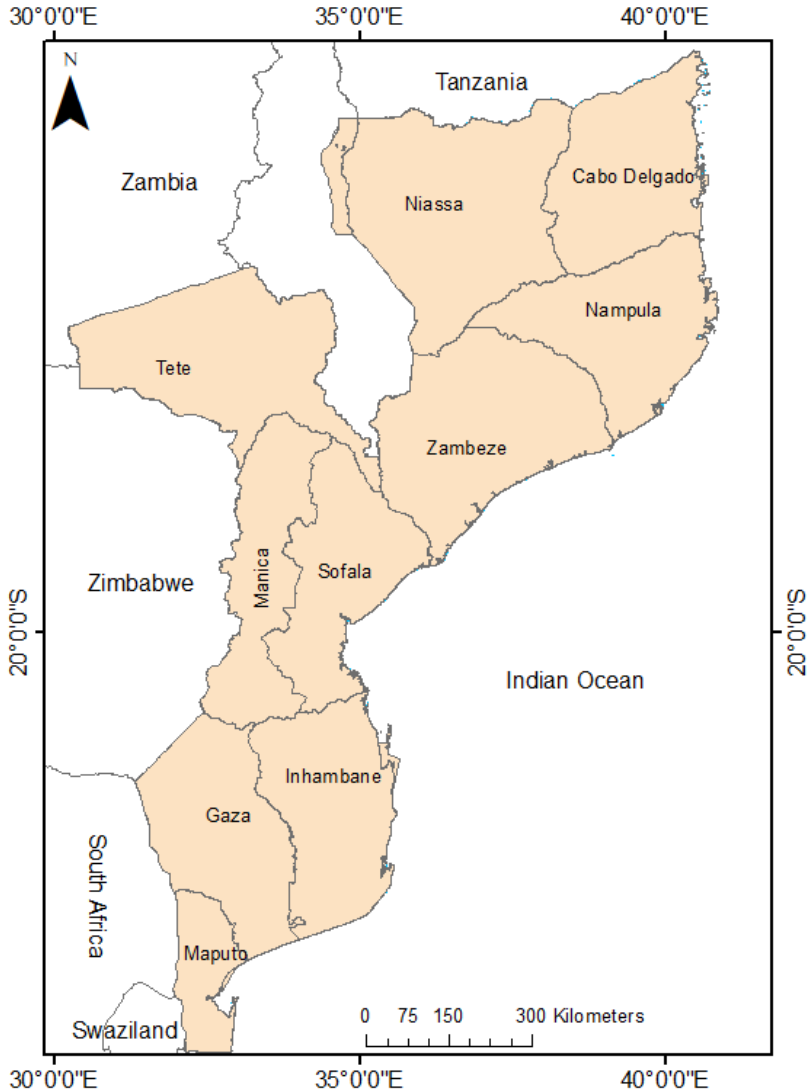

Figure 1. The provinces of Mozambique and boundary countries.

The earliest description of Mozambican Geology originates from Holmes in 1918 (Holmes, 1951) followed by Andrade (1929). After the independence (1975), the DNG (National Directorate of Geology) produced a Geological map (scale 1:1000000) in cooperation with different international organizations: Aquater (Italy), Bulgargeomin (Bulgaria), BRGM (France) and Hunting Geology & Geophysics Ltd (UK). Lächelt (2004) compiled the available information about the geology and economic potential of the mineral resources in Mozambique and GTK (2006) produced an up-dated geological map.

2.2 Geological evolution of Mozambique

Mozambique is divided in two different geologic-structural regions (Afonso, 1978; GTK, 2006; Lächelt, 2004): a Precambrian basement covering a surface area of about 534000 km^2 (2/3 of the country) and a Phanerozoic region of about 237000km^2 (1/3). The following description of geological evolution is based on Lächelt (2004).

The Precambrian basement in Mozambique consist of Archean units (3800 – 2500 Ma), Archean mobile belts and Proterozoic Units (2500 – 545Ma). These terrains are partially covered by Mesoproterozoic and Phanerozoic deposits and in some areas they were reworked forming new rock types. Igneous rocks such as granite and metamorphic rocks such as gneiss and greenstones compose the Archean areas. The Mesoproterozoic units, such as the Nampula complex, are the result of Mesoproterozoic-Neoproterozoic orogenic development of geosynclines on the east coast of Africa.

The Phanerozoic region is a platform cover that consists of:

1. Paleozoic – Mesozoic basins, also known as the Karoo basins system;
2. The Mesozoic-Cenozoic basins and volcanism, controlled by regional tectonic phenomena similar to the continental margin and therefore irregular in form;
3. The Quaternary covering deposits that continued during regional cycles with formation of recent deposits and the continuing evolution of the Mesozoic-Cenozoic basins taking place.

After the disintegration of the Gondwana super-continent (Mesozoic-Cenozoic), large continental basins were formed such as Rovuma, Mozambique-Kwazulu-Natal, Maniamba and Zambezi basins. The Post Gondwana Period consists of three main phases, which are disintegration, stabilization, and neo-rifting.

Disintegration of Precambrian and Phanerozoic units was active from 157 to 118 Ma resulting in the formation of the East African Rift System.

Stabilization was characterized by the expansion of continental margin basins, and the deposition of marly-argillaceous, shallow water sediments between 113 Ma and 35 Ma ago (Paleocene to Eocene).

Neo-rifting started 35 Ma ago and continues today. It is characterized by active tectonic movement that formed graben faults and the deposition of thick sediment layers (Lächelt, 2004). The Cheringoma-Urema Graben is one example of the Neo-rifting.

All these basins were filled by Quaternary sediments consisting mainly of colluvial, lacustrine, deltaic and alluvial deposits (Afonso, 1978; GTK, 2006;

Lächelt, 2004). The Quaternary period is characterized by a general regression eastwards of the Indian Ocean coastline.

2.3 Hydrogeology of Mozambique

Mozambique can be divided into four major hydrogeological provinces (Ferro & Bouman, 1987): 1. Unconsolidated aquifers; 2. Sedimentary basins; 3. Volcanic (and other igneous) terrains and 4. Basement complex and cratons.

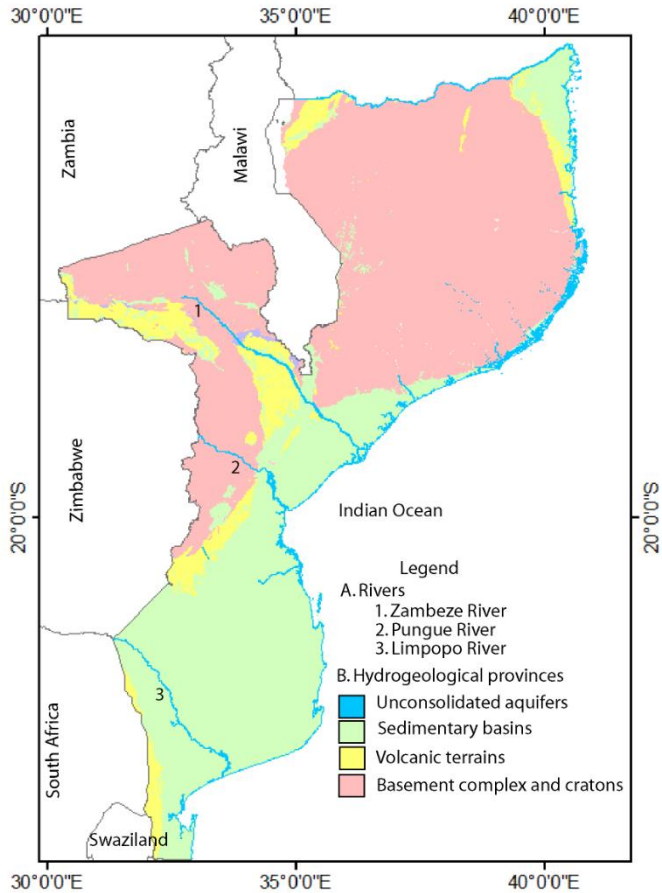

Figure 2. Schematic hydrogeological map of Mozambique (modified from Ferro & Bouman (1987))

Basement Complex rocks and cratons cover around 57% of the country (Figure 2) in the western part of the central region (largely part of the Zimbabwe Craton) and almost the entire region north of the Zambezi River. The area consists of mountains, upland and midland plateaus and an eastern strip of lowlands. The lowland has accumulating depositional relief whereas the plateaus and mountain areas are characterized by erosive landforms. Most of the midland plateaus have an inselberg style landscape.

Water-bearing formations of the basement complex are low productive (table 1), discontinuous and limited in extent. The productivity mainly depends on the thickness and texture of the weathered mantle. The ground water occurrences are associated with geologically weak zones, fractures and joints. These zones are associated with particular geological structures, like folds, faults and fractures, displaying relatively high permeability and porosity. The groundwater quality is good except in areas with high evaporation rates where it is salty.

The volcanic terrains are developed along the margins of sedimentary basins and the basement complex (Figure 2). They mainly consist of basalts, rhyolites and alkaline rocks, most of them originating from fissure eruptions. Primary and secondary fractures are the most important water-bearing features in these rocks. The weathered layer is generally less developed and rarely exceeds 10 m. It may be more developed in basalt terrains but since the material is very clayey, it is almost impermeable.

The volcanic rocks of Karoo system (basalts and ryolites) are classified as aquitards (table 1) because the weathered layer is less than 10 m. The potential zones for groundwater occurrence are encountered in fractures zones, in fault-breccias and along the dolerite intrusions. In general the groundwater quality is good except in contact with Mesozoic sedimentary rocks and Cenozoic marine sediments.

The sedimentary basins comprise mainly Cretaceous-Tertiary rocks, with small outcrops of older Mesozoic-Palaeozoic rocks. The most significant sedimentary basin is the Mozambique Sedimentary Basin. The sedimentary rocks form variably local/discontinuous to regional/continuous aquifers, typically with a mixture of intergranular (porous) and fracture/fissure permeability. The groundwater quality varies from brackish to fresh water (Table 1) as a consequence of the source of the sediments that form the rock i. e. from marine or continental sources.

Large areas of the country are overlain by unconsolidated sediments, particularly in river beds, valleys, dune fields and the coastal plain (Figure 2). The alluvium, aeolian dunes and marine sand are generally unconsolidated forming continuous aquifers. The groundwater from these sediments is saline in sand dunes and lagoons but has good quality in alluvial sand (table 1).

Table 1. General relationship of the different geological units, age, aquifer potentiality and water quality (Ferro & Bouman, 1987).

Eon	Era	Rock Unit	Aquifer potential	Water quality	Main hydrogeological classification
Phanerozoic	Cenozoic	Alluvium, aeolian dunes and marine sand	Unconsolidated sedimentary aquifers	Good water quality on alluvial aquifers and saline water in sand dunes, marine sand and lagoons	Aquifers
	Mesozoic	Sedimentary rocks of Karoo system	consolidated sedimentary aquifers (marine and continental sandstone)	Varies from brackish to fresh water	Aquifers
	Paleozoic	Volcanic rocks of Karoo system	Small, local and dispersed aquifers with limited productivity	Good	Aquifers/aquitards
Precambrian	Mesoproterozoic	Basement complex	Depends on development of weathered mantle	Good, except salty water in areas with high evaporation rate	Aquitards
	Proterozoic	Cratons	Very limited	Good (mineral water)	Aquitards

3. Geophysical methods applied for groundwater exploration

Geophysical methods measure the contrast in the physical properties of the sub-surface. Often no interpretation is done with raw data sets but is mainly done during and after the processing of the data. The processing for many methods, like ERT, IP and MRS, includes the inversion of measured data after bad data and noise removal and adjustment of the parameters of processing and inversion. After data processing, a simplified representation of the reality is given as a geophysical model.

Reference information is required to reduce ambiguity caused by the variability and overlap in the physical properties of the rocks. The physical properties can be interpreted in terms of geology, rock mass quality and hydrogeological characteristics. Methods such as resistivity and magnetic resonance sounding may contribute with estimations of hydraulic properties (permeability, porosity and water content) to create a groundwater model.

The short description of the theory in this chapter is only for the geophysical methods applied in this research. The selection of methods is described and motivated in chapter 1 and 4. These methods and also others useful for groundwater exploration are describe by for instance Hubbard & Rubin, 2005; Kirsch & Yaramanci, 2009 and also Møller et al., 2009. However each method has a different performance in different geological environments.

3.1 Electrical conductivity of earth materials

When the metallic ores and clay minerals are disregarded, only the water in fissures and pores can conduct the electric current in the ground. A general rule is that the more saturated the pore space, the better the conductivity. Hence generally one can say that hard rocks are bad conductors while pores, fissures, jointing and weathering increases the pore space for water, thus increasing the conductivity. In contrast, precipitation of minerals, compaction and metamorphism will decrease the pore space and thereby decrease the conductivity.

Groundwater is a natural electrolyte with a lot of ions present (Sharma, 1997). Therefore the concentration and mobility of the ions are the key factors in conductivity variations. The resistivity is a highly variable property, dependent on the characteristics of the rock formation being surveyed (Sharma, 1997). Due to this variation, there is no direct relationship between resistivity and lithology. A general classifications on how the resistivity varies from clays to fresh rock is presented in Figure 3.

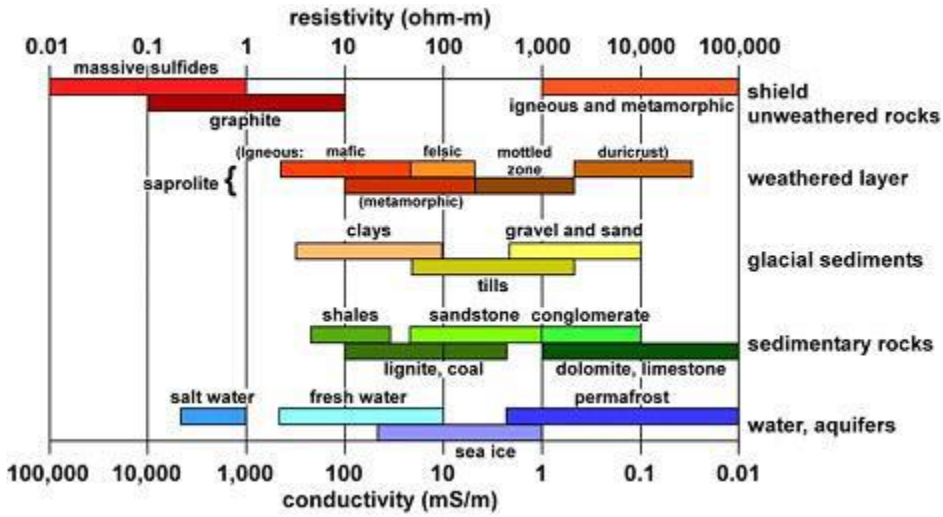

Figure 3. General resistivity/conductivity classification of earth materials (Palacky, 1988)

Figure 3 shows that there are several different classifications for each resistivity span. For instance the resistivity span of unweathered igneous and metamorphic rock covers the resistivity span of duricrust and sedimentary rock such as dolomite and limestone. The resistivity of clays is lower than the resistivity of gravel and sands. The figure also shows that salt water is more conductive than fresh water.

3.2 Vertical electrical sounding

Resistivity measurements of the ground are carried out by transmitting a current (I) between two separate electrodes in direct contact with the ground. The potential (U) is then measured between two intermediate electrodes (Schlumberger, 1920). A schematic view of how direct current resistivity measurements can be carried out is seen in Figure 4.

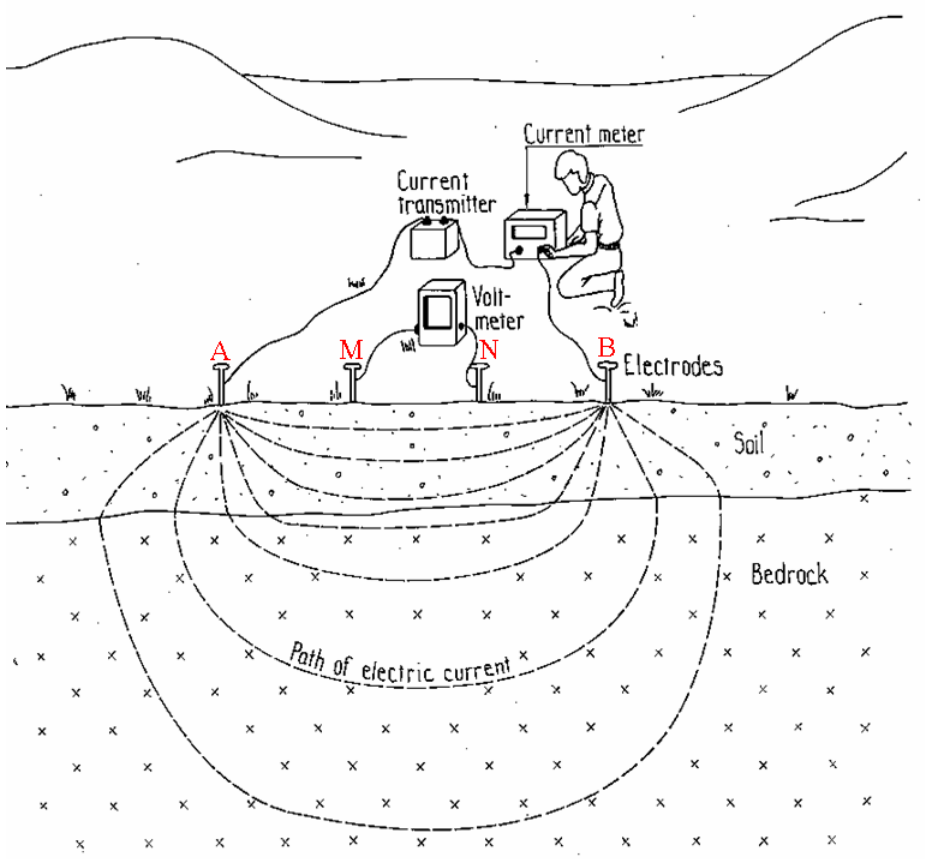

Figure 4. Principle set-up for direct current resistivity measurement (adapted from (Robinson & Coruh, 1988))

After measuring the current and voltage, the resistance can be calculated by the use of Ohm's law:

$$R = \frac{U}{I}$$

Where R is the resistance in Ohms, U is the voltage in Volts and I is the current in Amperes.

In order to calculate the material parameter resistivity (ρ_a), which is the inverse of electrical conductivity, a geometrical factor (K) is needed. The geometrical factor depends on the arrangement of the electrodes and varies depending on the individual distances between the electrodes, also known as the electrode

configuration (Schlumberger, 1920). A schematic view of the distances that make up the geometrical configuration of the electrodes can be seen in Figure 5.

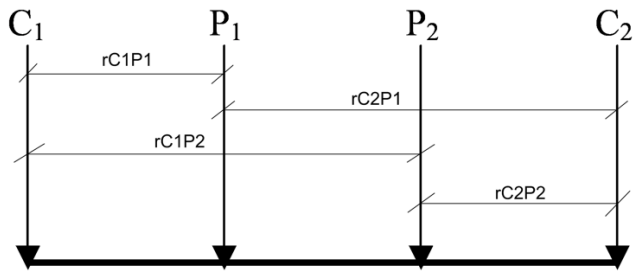

Figure 5. Schematic electrode arrangement with two current electrodes (C1 and C2) and two potential electrodes (P1 and P2), also showing the distances needed for calculation of the geometrical factor (K).

With knowledge of the geometries in figure 5, the geometrical factor can be calculated as:

$$K = 2\pi\left[\frac{1}{rC1P1} - \frac{1}{rC2P1} - \frac{1}{rC1P2} + \frac{1}{rC2P2}\right]^{-1}$$

The apparent resistivity (ρ_a) in Ωm can now be calculated by:

$$\rho_a = K \cdot \frac{U}{I} = (K \cdot R)$$

The apparent resistivity is the response of the measured geological formations. In order to obtain the true resistivity of the actual geological formations, a model, similar to that of the measured geological formations, must be formed using inversion routines (Menke, 1989).

The Vertical Electrical Sounding (VES) technique measures the apparent resistivity assuming that the physical properties of subsurface are layered and horizontally homogenous. Therefore VES measures the vertical change in resistivity value. The change can be related to the variation of the lithology or groundwater content.

VES is widely used in groundwater exploration not only in Mozambique but also in different African countries (De Beer & Blume, 1985; Ismail et al., 2005; Meyer & De Beer, 1980; Okereke et al 1998; Soltau & Anderson, 2006).

3.3 Electrical resistivity tomography

Electrical resistivity tomography (ERT) can be described as an automated way of measuring resistivity of the ground with a lateral change (Dahlin, 1993) producing two-dimensional models. The method has ability to measure the potential between several electrodes in the same setup and uses more electrodes compared to VES.

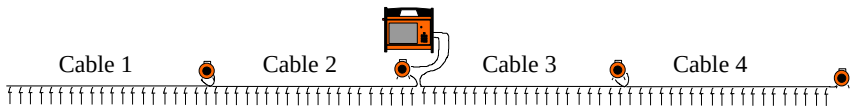

Figure 6. Positioning of electrodes and cables with intervals of 5 meters between the electrode take-outs. The system will have a total length of 400 meters when all four cables are connected. (Modified from Dahlin (1993))

The measurements are made by a resistivity instrument connected to an electrode selector. The electrode selector is connected to the cables (100 m each, see Figure 6). A profile of more than 400 m can be covered by applying the roll-along technique where the first cable is moved to the end of the fourth cable and the instrument is moved 100 m. The multiple-gradient array was used in this survey. This array has the advantage of good resolution and a fast process of measurements with a multi-channel instrument (Dahlin & Zhou, 2006; Owen et al., 2006).

3.4 Induced polarization

The phenomenon of induced polarization has been known since the beginning of the 20th century and uses the same electrode setup as resistivity (Reynolds, 1987). When a current is transmitted through the ground it will take a short period of time for it to reach its maximum chargeability. When the current is terminated the ground will return to its initial state after a short period of time. The decay of the charge in conductive geological material will take more time compared to non-conductive material (Reynolds, 1987). In this case, the chargeability is studied using the time domain induced polarization (Loke et al., 2003).

The measured chargeability can be normalized by dividing the chargeability by the resistivity. The normalized IP results are useful for characterizing lithological and geochemical variability (Slater & Lesmes, 2002) of the groundwater.

When the normalized IP parameters are used, it is assumed that the formation conductivity is mainly the result of ionic conduction in the porous media. This assumption is valid for metal free soils (Slater & Lesmes, 2002).

3.5 Magnetic resonance sounding

The magnetic resonance sounding (MRS) method in groundwater exploration was developed as early as the 1960s. However only in the 1980s the equipment was effectively designed and put into operation for surface geophysical exploration (Hertrich, 2008). The physical property used in MRS applications is the spin of the nuclei under investigation, i.e. hydrogen protons of water molecules. This is done by exciting the hydrogen protons resulting in an angular momentum, without physical rotation, and an associated magnetic moment.

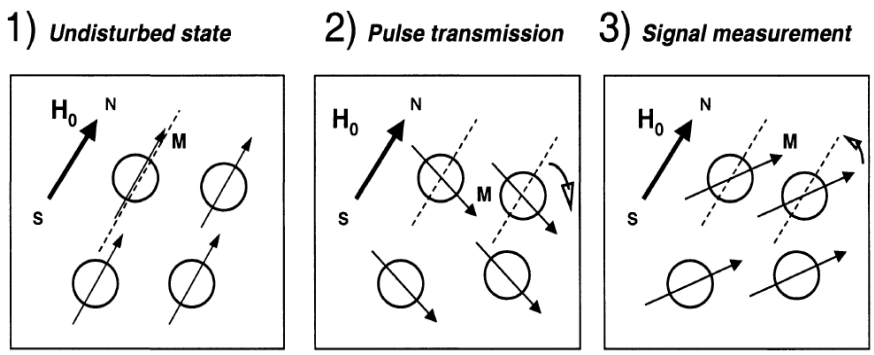

Figure 7. Three different phases of a magnetic resonance measurements (Legchenko et al., 2002)

The spin system is perturbed by a pulse in the transmitter coil (Figure 7) and emits after pulse cutoff the response signal from the subsurface (Hertrich, 2008). Here the Earth's magnetic field is the static field, leading to a Larmor frequency of some 1.2-2.5 kHz. The secondary field perturbing the spin system is given by the electromagnetic fields of large surface loops.

The response signal is also recorded in a surface loop, usually of the same dimension. In conventional depth soundings, measurements are realized with transmitter and receiver being the same loop, the coincident configuration (Chongo et al., 2011; Hertrich, 2008). From a single recording, the curve characteristics,

initial amplitude and decay constant of the transient curve are derived as well as the phase shift. The decay signal obtained after switching off the excitation pulse is very sensitive because it has a low amplitude, in the order of tens of nano Volt (nV) (Plata & Rubio, 2002). The decay signal is easily disturbed by (1) presence of anthropogenic noise in the area, (2) ambient noise from natural sources and (3) a small signal of the earth´s magnetic field that easily drowns in noise.

The two main MRS output data types are free water content (Φ_{MRS}) and decay time constant (T_d). The free water content is usually related to effective porosity, specific yield and specific storage and T_d is correlated empirically with hydraulic conductivity (Lubczynski & Roy, 2003; Plata & Rubio, 2002).

3.6 Borehole geophysics

Geophysical borehole logging is a more or less continuous profile measurement in a borehole by lowering a probe that reads the signal of the "ground sounding" downwards (Darling, 2005). The objective of geophysical borehole logging is to obtain additional information to the information obtained by conventional drilling, sampling, and testing.

Strictly speaking borehole logging is an alternative supplement to the analysis of the drill cores and cuttings. Cuttings, extracted from drilling, are one of the largest sources of subsurface sampling. However the reconstruction of the lithological sequence from cuttings is imprecise due to the problem of exactly associating a depth with any given sample. It also demands skilled personnel to determine the lithology and weathering from the small cutting samples.

The applied geophysical borehole logging operation in this study consists of conductivity (inverse of resistivity) and magnetic susceptibility measurements. The data are acquired at two points placed 52 and 84 cm from the bottom of the sonde and labeled as short conductivity (SCON) and long conductivity (LCON) respectively. The SCON gives information in the vicinity of the borehole and LCON penetrates deeper into the formation (see also 4.4.2).

An additional sensor that measures the natural gamma radiation in the vicinity of the borehole was used. Natural gamma logging is a passive logging technique where the natural gamma-ray intensity of the formation is measured along the borehole. The gamma photons are mainly produced by decay of naturally occurring potassium (40K), uranium (238U) and thorium (232Th). The radioactivity is measured in counts per seconds (cps).

3.7 State of art of geophysics in Mozambique

There is a lack of information about historical geophysical methods used in Mozambique for groundwater exploration. Many research results are kept in the form of internal reports and very little has been published in international journals.

The oldest report about geophysical research was done by the Portuguese government. In 1962 they created the hydrological brigade composed of three different groups: hydrogeological exploration group, geophysical exploration group and drilling group, in order to start the pioneer work for groundwater exploration. The brigade produced the first hydrogeological maps at a scale of 1:250,000 and 1:50,000. The geophysical method used during the exploration was VES (Mendes, 1966) which used the Schlumberger configuration. These maps were the base of the actual existing 1:1,000,000 hydrogeological map produced in 1988. VES was the main technique used on this map production with Schlumberger and Wenner configuration (Ferro & Bouman, 1987). The equipment used comprises an ABEM terrameter SAS 300B and the data were interpreted by using curve matching and the software GEOELEK. The application of resistivity for coastal aquifer exploration was studied in 1990 and the collected data were interpreted with Symphony software (Vieira & Chandra, 1990). In 1991, resistivity equipment, ABEM SAS 3000C with a booster, was used in Nampula province to study the occurrence of groundwater in Nacala district (Leal, 1992).

Although the geoelectric method is the most used, other methods are being used. Bireque et al. (1993) conducted an electro-magnetic study in Cabo Delgado province by using Geonics EM 34-3 equipment. Most recently, Daudi et al. (2014) studied groundwater contamination (saline intrusion) by means of a frequency domain electro-magnetic profiling method in Beira city. They made 3600 measurements in 600 stations using Geonic EM 34 equipment to produce a profile which indicated the saline intrusion patterns both horizontal and vertically.

4. Case studies

The use of combined hydrogeophysics methods to improve the understanding of hydrogeology problems is an appropriate approach in area with lack of reference data. Information such as borehole geological logging, an up-dated hydrogeological map, hydraulic parameters of the aquifers and water quality are examples of such reference data that can be used for a better understanding of hydrogeology of certain area. This approach was used to solve two hydrogeological problems in Mozambique aiming to understand: 1) the surface-groundwater interaction and 2) lack of groundwater flow to newly drilled wells.

Case Study 1: The Urema Lake, situated in central part of Mozambique, has the problem that the amount of water decreases considerably during the dry season (Beilfuss et al., 2007). A hydrogeophysical survey was carried out around the lake aiming to locate the recharge zone of the Urema Lake and to understand a possible interaction between surface water and groundwater. Steinbruch (2010) pointed out that contact zone between igneous rock and alluvium sediment is presumably the recharge zone. Beilfuss et al. (2007) suggested that groundwater sustains the lake during the dry season however the possible contact between surface and groundwater was not clear. Therefore ERT in combination with MRS was used to study the possibility of interaction between surface water and groundwater in the flood plain of Urema Lake.

Case Study 2: In Nampula province (Figure 1), a high failure rate when drilling new water supply wells in two districts (Rapale and Mongicual) has been reported (Salomon, 2010). VES was the geophysical method used to access the potential of places selected by the community. The selection made by community did not follow any scientific approach and many boreholes came out with low or no yield. The combination of hydrogeophysical surveys with ERT and MRS (in Rapale district) and with ERT and IP (in Mongicual district) were used to analyze and understand the reason for these failures.

Case Study 3: Also in Nampula province, borehole logging in combination with slug testing was used to improve the interpretation of the results obtained by other hydrogeophysical methods used in case study 2.

4.1 Data acquisition and processing

The ERT measurements were carried out with an ABEM Lund Imaging system, consisting of a Terrameter SAS4000 (paper 1, 2 and 3) or LS (paper 4 and Chirindja et al., 2017b), an Electrode Selector ES10-64C, electrode cables and stainless steel electrodes. An electrode spacing of 5 m was used with a total electrode layout of 400 m giving a depth penetration of around 75 m. Inverse numerical modelling (inversion) was used to produce models of vertical cross sections through the ground, employing Res2dinv (ver.3.58.14) with the robust (L1-norm) inversion constraint (Loke et al., 2003). The computer softwares Erigraph 2 and EriViz were used for visualizing the models. The results are presented as resistivity and normalized chargeability (only measured in Mongicual district). For visualization, the results are plotted on a diagram of distance along the profile versus depth.

The MRS measurements were carried out with the Numis-Plus from Iris Instruments using a 100 × 100 m coil with a maximum penetration depth of 100 m. The measured data were analyzed based on the least square solution with regularization with a smooth inversion using Samovar 11.3 software (Legchenko & Shushakov, 1998). The results are presented as free-water content (Φf) and decay time (T2*; T1) plotted versus depth.

The borehole logging was performed by means of a dual induction logging probe. The probe measures electrical conductivity of the rock formation, magnetic susceptibility, and natural gamma radiation in the vicinity of the borehole. Electric conductivity and magnetic susceptibility are acquired at two measurement points in the receiver coil. These points are labeled as short conductivity (SCON) and long conductivity (LCON) respectively. The difference between the two is the penetration depth into the rock formation, i.e., the SCON gives information in the vicinity of the borehole and LCON penetrates deeper into the formation. Slug tests were performed by introduction of a known volume of water to the well and measuring the change in head. The obtained data were evaluated using Aqtesolv software. The software calculated the hydraulic conductivity using Bouwer & Rice (1976) and Cooper et al (1967) solutions.

4.2 Case study 1: Geophysical study in Urema Graben basin

4.2.1 Introduction

Gorongosa National Park (GNP) is situated at 19ºS and 34ºW, within the Sofala province (Figure 1) in the central part of Mozambique. The park is located within the southern-most extension of the East African Rift System (EARS), the Urema Rift, and covers an area of approximately 3770 km^2 (Beilfuss et al., 2007). The park protects a vast ecosystem of floodplains, grasslands and woodlands. During the dry season the evapotranspiration is higher than the precipitation (Steinbruch, 2010). As a consequence all the streams dry out and the Urema Lake is the only source of water for the wildlife. The lake flood area is steadily reducing year after year (Beilfuss et al., 2007).

Authorities want to understand the causes in order to maintain sound management and decision-making processes about water resources in the Gorongosa region (Beilfuss et al., 2007). As there are no documented boreholes in the area, the hydrogeological setting was based on the study carried out by Owen (2004) which was only descriptive. Owen (2004) consider the Urema Lake as a window of an open aquifer however, the spatial variation and depth of the aquifer is unknown. Therefore, a survey based on a combination of ERT and MRS methods could improve the understanding of the geohydrology of the floodplain. Additional information that could help the interpretation of the geophysical results was obtained from grain size analyses and dilution tests.

4.2.2 Basin margin: groundwater recharge zone

Geophysics was used to give the first overview of the hydrogeological conditions. The ERT method was chosen because of the expected basement depth, and Quaternary sediments that fill the basin were expected to be easily distinguished by the method. The regional and local geology and geomorphology are described in paper 1, Stenberg (2011) and by Arvidsson (2010).

Measurements were done on the western side of the park aiming to identify the zone of recharge to a water-table in contact with the Urema Lake. Three ERT lines were conducted along the Nhandungue River. The first line is situated in the contact zone between hard rock and the alluvial sediments, the second line is in the middle of the Nhandungue River and the third one in the Urema rift valley.

Sediments were sampled at each profile for grain size classification. The soil samples were collected at a depth of ~15 - 30 cm (Stenberg, 2011) for the alluvial sand and collected at a depth of ~3.65 m in the floodplain by auguring. The dilution test was performed using 500 g of normal table salt dissolved in 20 l of water. The solution was poured into the stream to mix with the water and then electrical conductivity of the water was measured at a distance of 10 m downstream, approximately every second. The readings were taken until the conductivity stabilized.

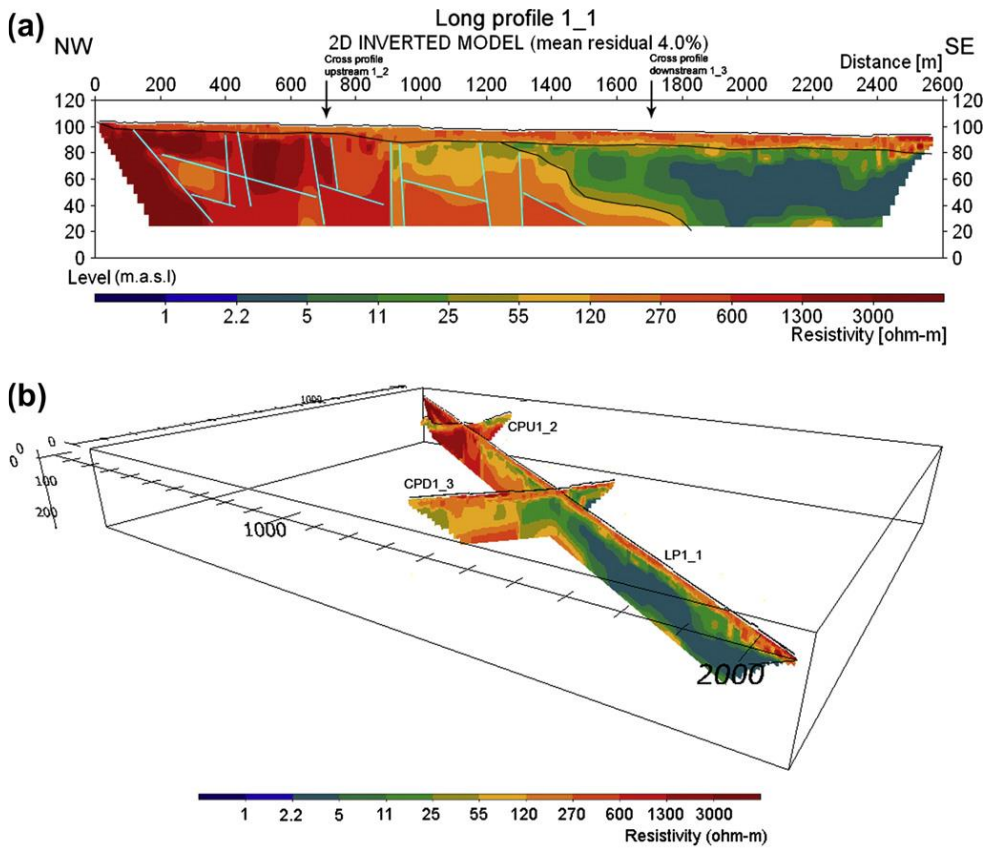

Figure 8. Resistivity model showing the igneous and sedimentary rock contact zone (black line) and interpreted faults (blue lines). (b) Three-dimensional model of Area 1 showing profiles LP1_1, CPU1_2 and CPU1_3. (Arvidsson et al., 2011).

Figure 8 is an example of inverted ERT models in 2D and 3D view of the transition zone between the igneous and sedimentary rocks. With only a 1 : 250 000 geological map (GTK, 2006) available for this area was possible to interpret the

high resistive formation in the NW as basement and interpret the low resistive formation in the SE as alluvial sand. The results of sieving and hydrometer analysis match well with the resistivity of saturated alluvial sand. Unfortunately the sand samples reflects only 30 cm below the surface. Additional borehole geological logging data would have been valuable as ground truth. Numerous minor vertically oriented heterogeneities can be distinguished in the basement (Figure 8a) and are marked by vertical lines, which are interpreted with some degree of uncertainty as fractures and faults.

The dilution test results show that river flow declines strongly downstream from the basement/sediments contact zone due to change in surface discharge. This suggests that this is a groundwater recharge zone and that the groundwater in these zones is flowing towards the Urema Lake.

4.2.3 The interaction between surface and groundwater

In the Urema floodplain the ERT method was combined with MRS to describe the possible interaction between surface water and groundwater. The MRS method was selected because it detects directly the free water molecule and the inverted results can be presented in terms of block models. The blocks indicate different layers with different water content. The relationship of the measured parameter and the hydraulic properties are discussed in section 3.5.

MRS Measurements were made at the start of three short ERT profiles located in the middle of floodplain. Four long ERT profiles with length varying from 4,500 to 6,000 m were measured in Urema flood plain. Two long profiles are located in the middle of floodplain and two at borders of the floodplain.

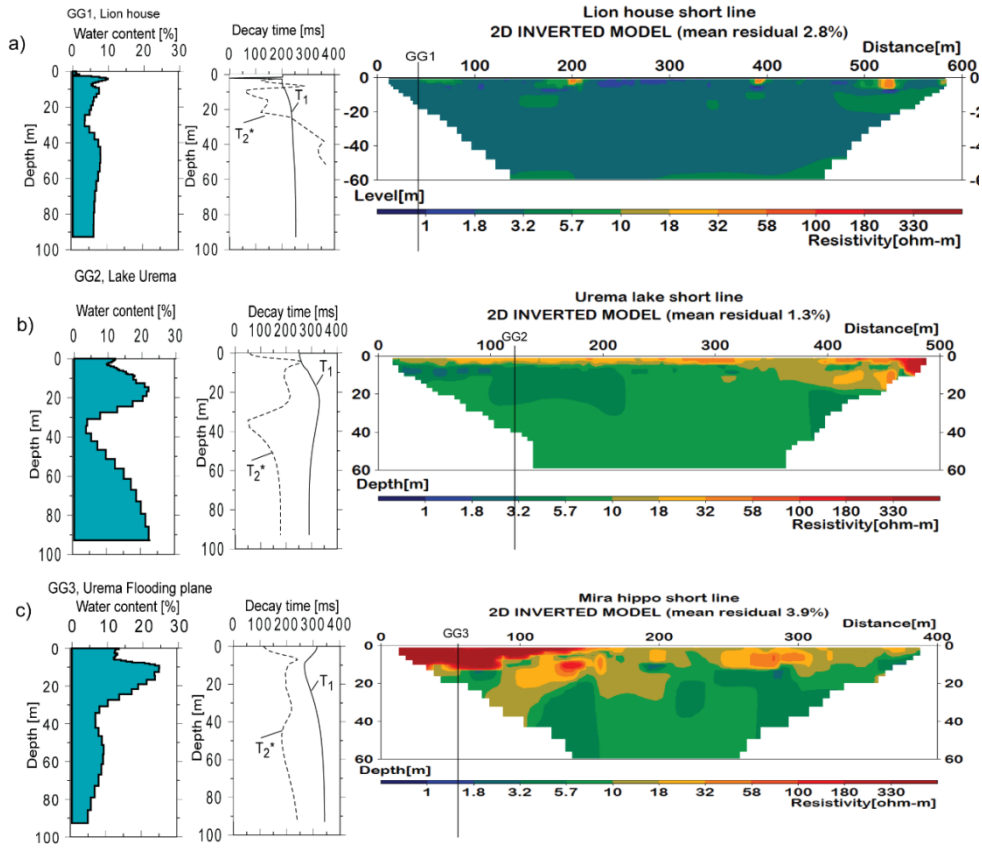

Figure 9. MRS at point GG1, GG2 and GG 3 showing the water content, water content inversion fit, decay time and its position at the short ERT lines. The black line indicate the position of MRS (Chirindja et al., 2016a)

Figure 9 shows the results of combined ERT and MRS. The combined interpretation of the inverted models indicate that where the free water content is low (less than 5%), the resistivity is also low (Figure 9.a) and when the water content is high (higher than 22%) the resistivity is also relatively high (Figure 9.c). In general four layers were identified: i. One layer with low resistivity and low free water content and interpreted as clay layer, ii. Two layers with intermediate values of both water content and resistivity interpreted as mix of clay and sand and iii. The layer with high value of water content and resistivity interpreted as sand. The auguring made at each site confirmed this interpretation. The maximum augured borehole depth is 3.65 m, so the verification is only for the top part of the formation.

.

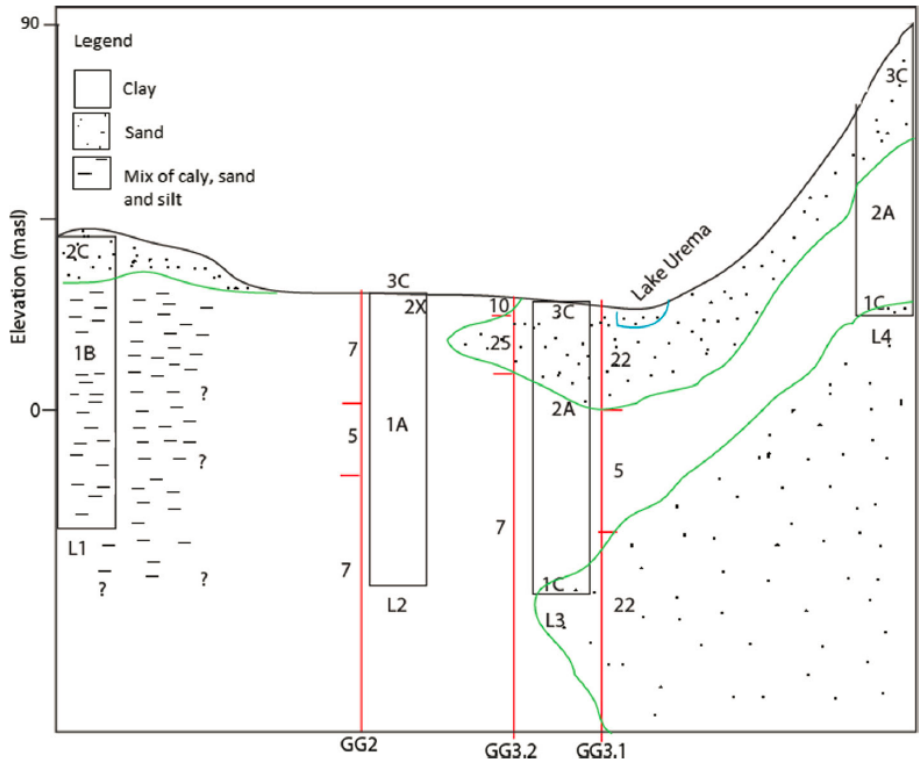

Figure 10. Obtained conceptual model of the Urema floodplain. No horizontal scale. GG2, GG3.1 and GG3.2 are the names of MRS measurement sites and L1, L2, L3 and L4 are the position of ERT profiles (Chirindja et al., 2016a)

The hydrogeological situation in the Urema floodplain is presented in the Figure 10. The model is a result of correlation between the interpreted ERT profiles and MRS. The floodplain is composed by two sand layers interpreted as aquifers (1C and 3C in Figure 10) separated by clay layers labeled as 1A and 2A interpreted as confining layers and one layer composed by a mixture of sand and clay labeled as 1B and interpreted as aquitard. The thickness of the lower and confined aquifer (1C) was not detected due to limitation of the method however, both ERT and MRS have detected a sandy layer below a clay layer. The confining layers (1A and 2A) is composed by clay and it is 30-40 m thick. The lateral separation of 1A and 1B between profile L1 and L2 (Figure 10) is not clear however, they have different hydrogeological properties. Additional information is needed to improve the understanding of the hydrogeology of Urema Lake.

The location and elevation of the upper aquifer (3C) suggest that the Urema Lake is a part of the upper aquifer. Also, it is likely that 3C is linked to the Pungue River (Figure 2). Both lower aquifer and possibly the Pungue River recharge the upper aquifer during the dry season when all other rivers are dry (Chirindja et al., 2016a).

4.3 Case study 2: Geophysical study in Nampula basement complex

4.3.1 Introduction

The Millennium challenge account granted funds to drill 600 boreholes for water supply in Cabo Delgado and Nampula provinces in Mozambique (Salomon, 2010). A committee was created to represent each community selected by the drilling project to have a water well. One of the duties of the committee was to indicate three preferred (by the community) places to drill a well. One VES was performed in each preferred site and ranked as potential 1, 2 and 3. Then if the potential site 1 is unsuccessful, potential site 2 was drilled. If the water supply failed in all 3 potential sites, then the water well committee chose 3 new sites to perform resistivity measurements again.

When the drilled borehole had a yield higher than 900 l/h it was considered successful and equipped to be a water supply well. Below that value, if the community is small then a yield of 600 l/h is accepted. Below the yield of 600 l/h, the borehole was considered as unsuccessful and filled with cement. In order to achieve the 600 successful boreholes, many unsuccessful boreholes were drilled. An overall failure rate of 25% was reported (Salomon, 2010). The failure rate was even higher in consolidated rock areas in Nampula province (about 35%).

Each borehole has a report with information about the drilling operation, lithological logging, water quality and pumping test results. This information was expected to be used during the interpretation of the collected geophysical data. However, the quality of borehole reports is often bad, being incomplete with obvious errors. There is also an apparent copy-and-paste of results between different borehole reports. The information from the reports was of poor quality and did not help as much as expected in the interpretation of geophysical data.

The reason why the VES partially failed to successfully indicate potential sites to drill a successful borehole was the main objective of the study. Combined ERT and MRS were performed at the same location where previous VES were measured in an attempt to understand the reasons for failure. As the combination of these two methods worked well in Urema flood plain, it was hoped to have useful results in consolidated rock area. However MRS did not work due to local conditions. The reasons will be discussed in the section 5.1.3. In total 21 boreholes were investigated (Figure 11) with cross profiles of 400 m with some exceptions. The profiles cross each other in the vicinity of the water well.

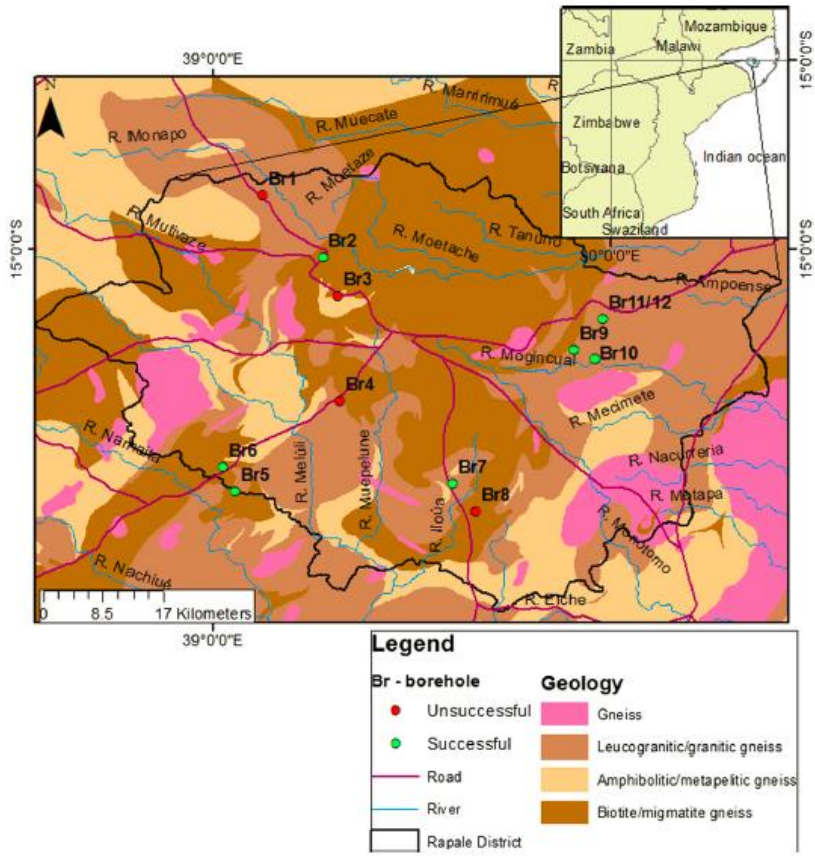

Figure 11. Geology of the study area in Nampula province and the location of surveyed successful in green and unsuccessful boreholes in red (Chirindja et al., 2017a)

The study area is located in Nampula province and covered by the Mesoproterozoic granite and gneiss of the Nampula complex (Andersson & Björkström, 2014; Enkel & Sjöstrand, 2013). These rocks are weathered and the groundwater is controlled by the thickness of the weathered layer and fracture zones in the rock with distinguishable resistivity properties (Acworth, 2001).

4.3.2 Causes of insufficient water supply from new boreholes

An advantage of ERT compared with VES is that the lateral variation of the resistivity along the profile can be visualized in 2 or 3 dimensions whereas VES gives only 1D variation. As result, with ERT the geological structures such as fault and fracture zones can be detected. However small geological structures cannot be resolved by the method but can be observed indirectly by lateral variation of

resistivity. Layers of fresh rock will have higher resistivity values than the fractured and weathered rock layers. The interpretation was based on this principle.

The lithological description of each borehole in the drilling report was problematic. Some descriptions were not useful for the interpretation due to a probable mix-up of the reports. The descriptions were based on the cuttings and was made by non-professionals. However the ERT models are presented and compared to the lithological descriptions.

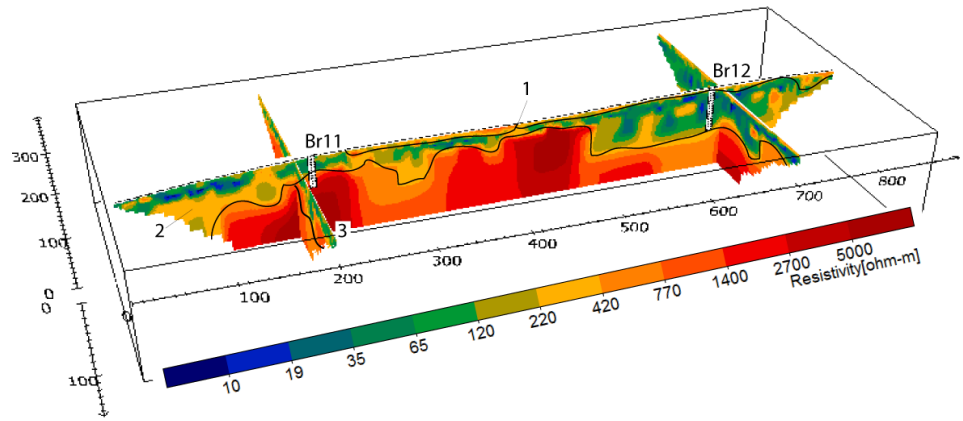

Figure 12. Inverted ERT block model of Naholoco EP1 community showing an unsuccessful (Br11) and a successful (Br12) borehole (Chirindja et al., 2017a).

Two drilled boreholes (Br11 and Br12. See location of the boreholes in Figure 11) with 500 m separation had opposite results. Br11 was unsuccessful while Br12 was successful. The resistivity variation in the inverted ERT models presented in Figure 12 was divided into three different geophysical layers. Layer 1 with high resistivity was interpreted as unconsolidated sand (intensively weathered and leached layer), layer 2 with low resistivity was interpreted as weathered to semi-weathered rock and a high resistivity layer 3 was interpreted as fresh rock.

The productivity of the borehole has been linked to the thickness of layer 2. Where the layer is thick as in Br12 the borehole is likely to be successful. One other factor controlling the potential for success is the resistivity values of layer 3. Where the layer 3 has resistivity value higher than 1400 Ωm the rock is fresh as in Br11 and the borehole was unsuccessful.

The interpretation of ERT results was not conclusive due to lack of reference data which imply that the interpretation of VES is also expected to be difficult. This situation explains the reason of high failure rate in area with complex geology and no additional information available or reliable.

The example given in Figure 12 clearly shows that ERT would have been beneficial if it was the main method used. Moreover, geological criteria and a scientific approach in the site selection process would have increased the chance to select better potential sites to drill. In this context, conceptual geological and hydrogeological models should be used by the community when deciding where to do the geophysical survey.

4.3.3 Mapping areas with problems of salinity in groundwater

In Mongicual district the groundwater was considered as salty in some drilled boreholes and not suitable for human consumption. Mapping the contrasting sediments derived from either weathering of gneiss or derived from coastal sand dunes would help to map areas with problems of salinity in the groundwater. The combination of ERT and IP measurements was expected to give such a contrast. An advantage of this approach is that the ABEM Terrameter LS measures both resistivity and IP simultaneously.

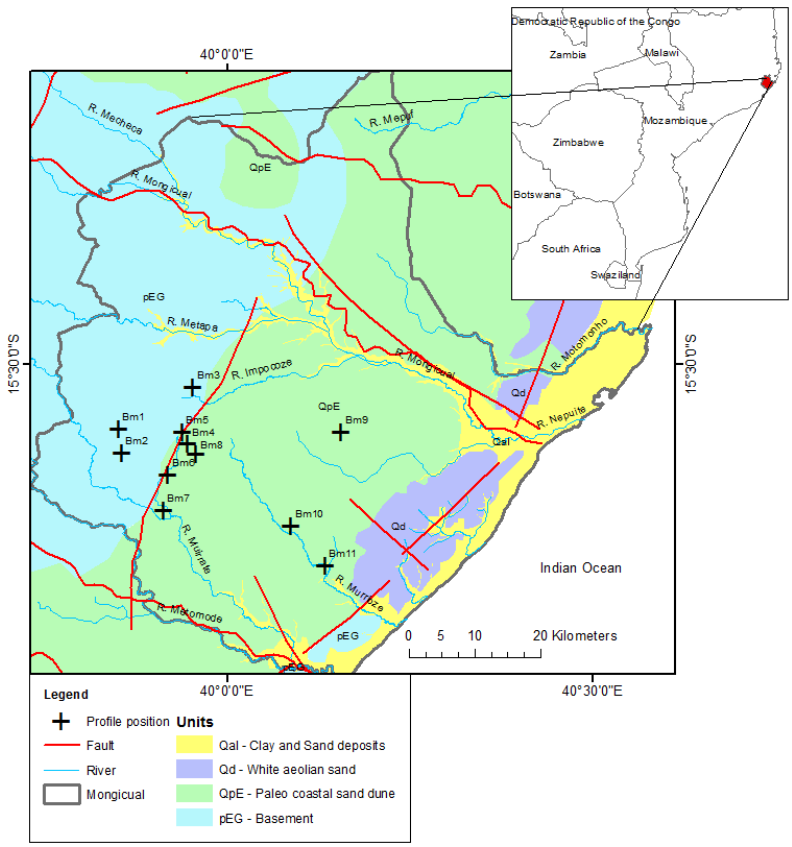

Figure 13 Geological map of Mongicual district and the location of the research sites

The location of the study area and position of the profiles can be seen in

Figure 13. The study area is a small and shallow basin separating two major and deeper basins one to the north and the other to the south. In the north the basin is called East African marginal Rovuma basin and in the south it is the Mozambique basin. The basement is covered by a weathered layer and aeolian sediments of different ages described by Salman and Abdula (1995).

Some of the obtained results of IP were too noisy with high residual errors, but in profiles where the mean residual error was less than 3%, the resultant models were considered acceptable (Chirindja et al., 2016b). The inverted IP models were presented as normalized chargeability (

Figure 14).

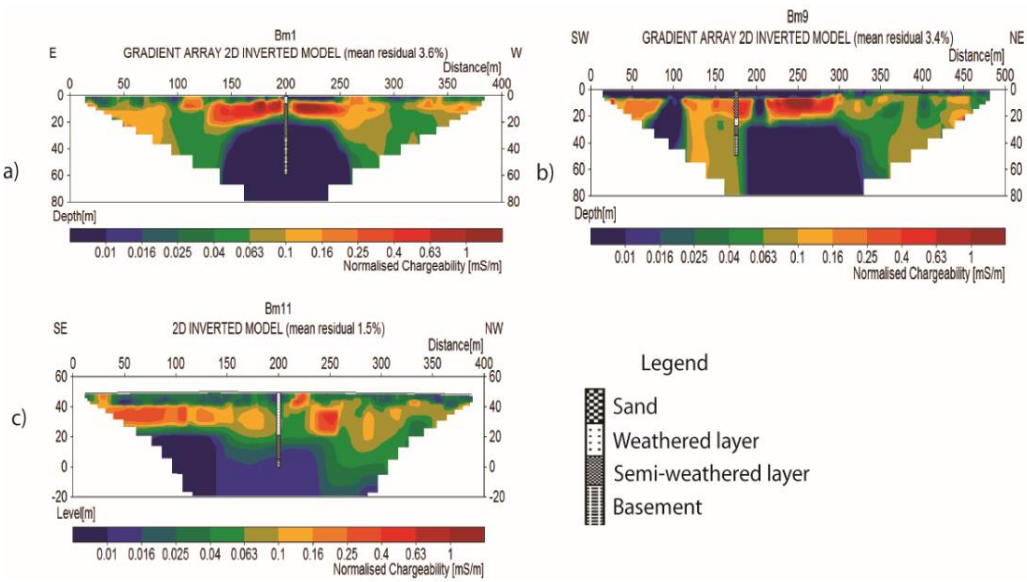

Figure 14. Inverted IP models showing the normalized chargeability: a) Bm1, b) Bm9 and c) Bm11.

The resultant models agreed with the local geology (presented along the borehole in Figure 14): where the normalized chargeability was high, the red sand paleo dunes were affected by oxidation of iron, while the normalized chargeability value was low in white sand dunes, without oxidized iron. The presence of paleo dunes on top of the weathered layer can affect the mineralization of the groundwater (Chirindja et al., 2016b). Although both IP and ERT have detected paleo dune formation on top of the weathered layer there are no more evidence of this setting. The weathered layer can be a continuation of paleo dune formation but due to lack of information, that cannot be clarified.

4.4 Case study 3: Borehole logging and slug testing

4.4.1 Introduction

The change in resistivity value was the basis for differentiating the lithological layers throughout the interpretation. However, not all the models gave expected results: unsuccessful borehole in layers with high resistivity values and successful wells in layer with low resistivity values. There are a few successful boreholes in unexpected locations and unsuccessful boreholes in sites identified as having a good potential for drilling. On the other hand, the IP results were noisy and only few of them could be used. A borehole logging method was applied to improve the understanding of the hydrogeology and to get down-hole information in the borehole aiming to detect fractures and the groundwater contributing layers. Also, some inverted ERT models in Rapale and Mongicual districts indicated that the drilling stopped in a fractured rock but the geological logging report indicated that the drilling stopped in a fresh rock. Therefore, the borehole logging results were expected to clarify whether or not the drilling stopped in fresh rock. For borehole logging the pump is removed, and therefore it was opportune to also conduct slug tests to estimate hydraulic properties of the aquifer.

4.4.2 Borehole logging

The Robertson Geologging LTD (2017) dual induction logging probe was used for this study. The logging sensors measure the electrical conductivity, magnetic susceptibility and natural gamma. Two geophysical logging runs were conducted at each borehole and the mean value was recorded. All logging started at a depth between 2 to 3 m therefore, the geological interpretation were done from this point. The maximum resistivity reading was set to 2000 Ωm due to limitation of the logging instrument. For each surveyed borehole the resistivity measured with the ERT method was extracted and plotted together with resistivity (converted from measured conductivity) from borehole logging.

The drawback is the presence of casing centralizers that are metallic and caused peaks for both conductivity and magnetic susceptibility. This noise made

interpretation of the results difficult. The natural gamma is not affected by the metal therefore those measurements were not affected by the metallic centralizers.

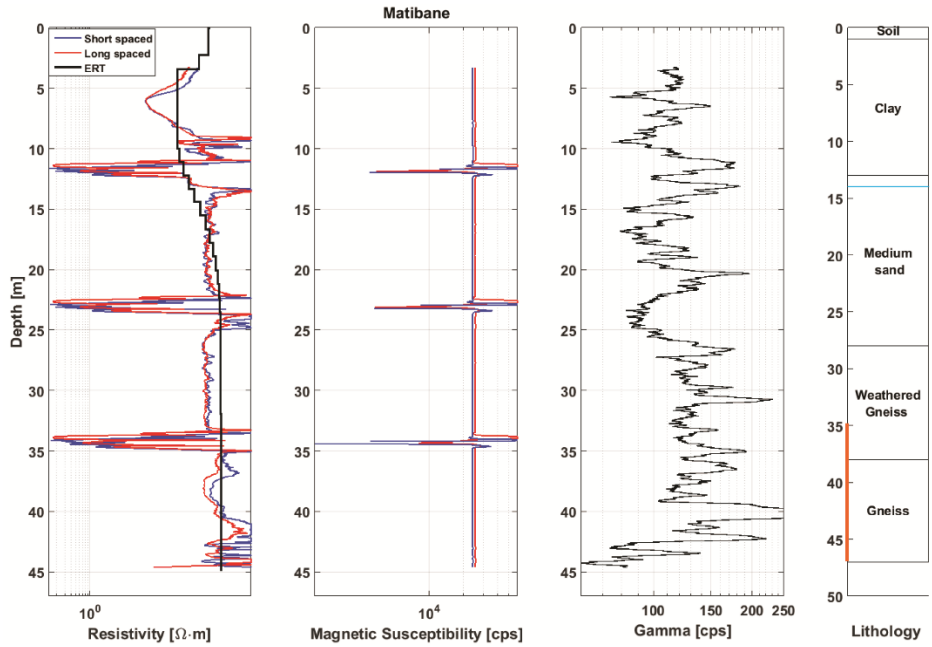

Figure 15. Borehole results and lithological description at Matibane borehole (labeled as Br10 in Figure 11). The black line indicates the resistivity measured by ERT method. The orange color indicates the screened section in the borehole and the blue line in the lithology profile indicates the groundwater level (Chirindja et al., 2017b).

Figure 15 shows the peaks caused by metallic centralizers in the resistivity and magnetic susceptibility. The resistivity measured between the peaks is in line with the variation of resistivity measured by ERT method. The magnetic susceptibility did not show any variation between the peaks. Although it shows the location of metallic centralizes it is not suggested to be included in the borehole logging as the resistivity already detected the peaks.

It would be ideal to run borehole logging before installing casing in the borehole (Olsson, 2016). However, when it is done after the casing installation, the resultant borehole logging is useful for inspection of well completion including how the centralizers were positioned in the well.

The logged natural gamma was not affected by the presence of metallic centralizers. The observed natural gamma peak may be caused by lithological variation, which could be associated with narrow but possibly hydraulically conductive fractures in the contact zone between the lithological units. Slug testing

Slug testing is a rapid hydraulic testing method performed in a borehole to estimate hydraulic conductivity (K). The obtained result is usually accepted for the surrounding formation close to the well and not for the entire geological formation (Hallerbäck, 2016; Vermeulen & van Tonder, 2004). For the ten selected sites, six to ten slug tests were conducted, giving in total 68 tests. Each test was evaluated using Aqtesolv software giving in total 136 evaluations. The K and T were calculated by the Bouwer and Rice (1976) and Cooper et al.,(1967) method. Both results of K and T were plotted together with aquifer thickness. The aquifer thickness was estimated from the ERT profiles.

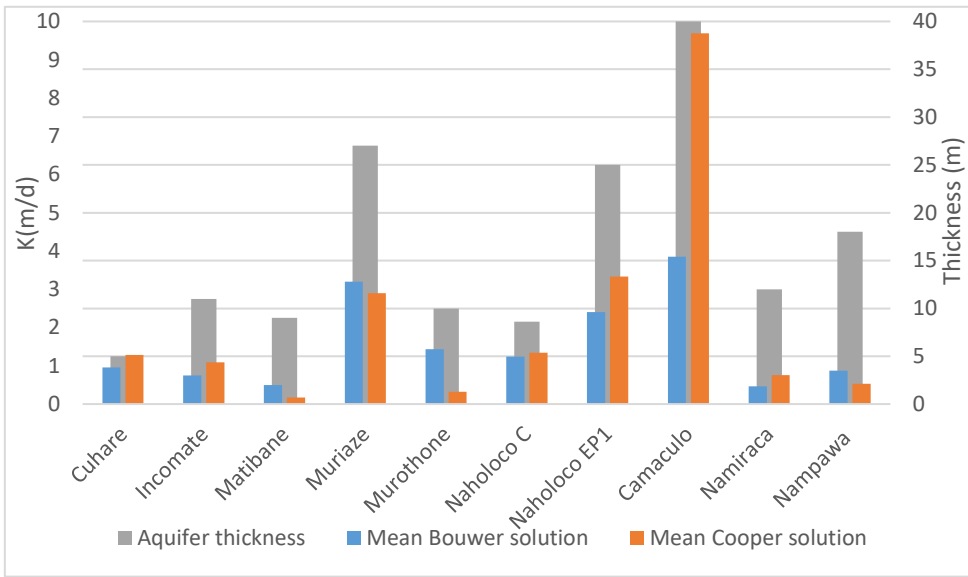

Figure 16. Hydraulic conductivity results based on Bouwer and Rice and Cooper et al. solutions and thickness of the aquifer (Chirindja et al., 2017b). The names of the borehole are labeled in Figure 11 as Br2, Br5, Br6, Br7, Br10, Br11 and Br12 respectively for Cuhare B, Murothone, Incomate, Muriaze, Matibane, Naholoco C and Naholoco EP1 and labeled in Figure 13 as Bm1, Bm 5 and Bm7 respectively for Camaculo, Nampawa and Namiraca.

The K values presented in Figure 16 shows that the Camaculo borehole (in Mongicual district) gave the highest value of K both by the Bouwer & Rice and Cooper et al. methods. The borehole Matibane (Rapale district) gave the lowest value for both methods. Where the weathered layer and fractured layer are thick, generally the K value is also high for both solutions. However this rule doesn't apply in Namiraca and Nampawa boreholes (Figure 16) because aeolian sand was deposited on top of the weathered basement. The aeolian sediments are paleo dunes that were oxidized and the fine sediments were leached and deposited in layer 2.

The deposited fine sediments and leached solution may have lowered the hydraulic conductivity of the aquifer.

5. Discussion

5.1 Hydrogeophysics as a tool for groundwater exploration

As more than 50% of the population in Mozambique live in rural areas (with scattered houses), groundwater is the main water supply. About 1/3 of the country is covered by Quaternary sediments constituting porous and permeable aquifers. The Quaternary sediments are mainly alluvial, dunes or of marine origin. About 2/3 of the country is covered by hard rock. Significant aquifers in hard rocks develop within the weathered and fractured bedrock and have limited yield.

As seen in section 3.7, the VES method is widely used in Mozambique for groundwater exploration due to the contrast between a saturated layer and the surrounding rocks (Acworth, 2001). This contrast is well exploited by VES in unconsolidated sediments with homogeneous horizontal layers (Daudi et al., 2014). However in hard rock areas, the use of VES is limited due to lateral variation in the thickness of the weathered layer and complexity of the fracture behavior.

Different geophysical methods are presented, often in combination, as alternative tools for hydrogeophysical studies as compared to VES. The discussion is focused on the methods used in this study.

5.1.1 Applicability and limitation of ERT method

The presented case studies have shown that ERT need less reference data for interpretation compared to VES. Based only in visual interpretation of ERT, different geophysical layers were identified because different earth materials responded in different ways when the electrical current was injected. Geological structures, such as major faults and fractures, were identified in the recharge zone but not small fractures occurring in weathered rocks. As the weathering profiles give distinct resistivity values for each layer (Acworth, 2001; Kumar et al., 2016), the resulting ERT models give indication of a potential zone to drill a water well. Also, the resulting geophysical model can be used to predict the groundwater flow (Clair et al., 2015). Misinterpretation of some geophysical layers is usually caused

by the presence of some artifact, the influence of water quality and local variation of rock composition.

In favorable conditions and with sufficiently moist ground, three people are needed for both ERT and VES data collection. In a typical field-day it may be possible to measure two pairs of VES with orthogonal spread directions, an approach that is recommended to get information about the lateral variability. If both sounding curves are similar the VES approach is probably adequate, and if not, the results should not be used or used only with great care. A maximum current electrode separation of 100-200 m is assumed. Two ERT sections with 5 m take-out separation and a total spread of 400 m can often comfortably be measured in a field-day, allowing for transport to and from the site. The VES produces very little information in relation to the man-power consumption compared to ERT. Unfortunately there is no information about the costs of a VES campaign but it is far cheaper than an ERT campaign.

The use of VES for investigating the potential locations to site boreholes in geologically complex areas has proven to be inappropriate. The inverted ERT models show the lateral variation of the geological material that is considered as homogenous by the VES method. However ERT also has some limitations. The first limitation is that ERT does not detect small fractures and fissures. Therefore the presence of fractures and fissures was interpreted by the reduction in the resistivity value of the high resistive layer. If well documented data of previous drilling projects in the same area is available, it would improve the interpretation of VES results and unsuccessful well drillings could be avoided.

The second limitation is illustrated in Figure 17. In Figure 17a, ERT suggested a good potential borehole, but it was an unsuccessful borehole. In Figures 17b and c, ERT indicated no potential for drilling a well, but VES gave good indications and the drillings were successful.

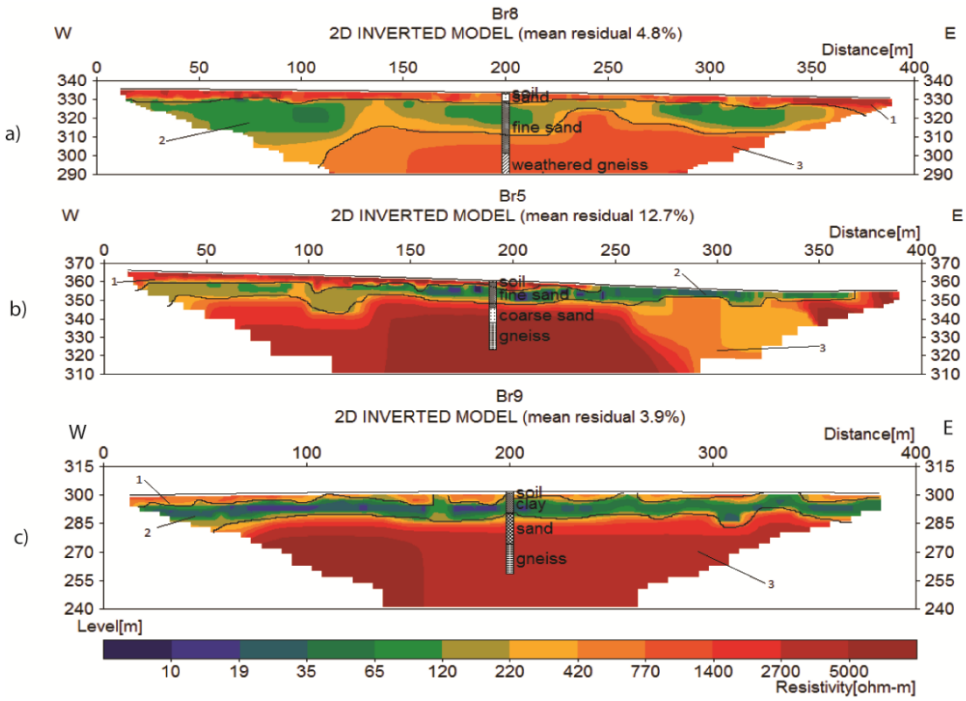

Figure 17. Example of the inverted ERT model contradicting with the expected result after drilling. The drilled borehole is located in the center of the profile (Chirindja et al., 2017a).

In Figure 17.a the resistivity value expected for fresh rock was not reached. It was interpreted by ERT as a potential site to drill borehole. However the drilling result was unsuccessful. In Figure 17.b and 17.c the resistivity value for fresh rock was detected close to surface and the layer 2 was not developed enough to be considered as target to drill. But, after drilling, for both cases, the boreholes were considered as successful. However the yield in both boreholes is about 600l/h. One plausible explanation for success at the boreholes at Figure 17.b and 17.c is that the drilling could have hit fractures.

5.1.2 Applicability and limitation of MRS method

The MRS is a non-invasive method that gives an indication of aquifer properties (Lubczynski & Roy, 2003). The MRS method appears to work well in unconsolidated sediments in Urema floodplain as discussed in section 4.2.3. Possible interpretation of hydraulic properties from MRS results was not verified due to lack of reference information.

The results of MRS in areas with hard rock were noisy and not useful due to low signal level. The noise sources that can reduce the signal detection were described in section 3.5 as anthropogenic, natural and caused by variation in the earth´s magnetic field.

The major anthropogenic sources of noise are power lines. As the communities are growing, powerlines are directed to these communities. As a consequence, the use of MRS is affected negatively.

The natural noise sources include minerals with magnetic properties. Minerals such as pyrite and chalco-pyrite are common in gneiss in the form of veinlets. These minerals are important factors in determining relaxation rates and surface relaxivity (Keating & Knight, 2010). The decay time is strongly affected by relaxation rates and surface relaxivity.

The earth magnetic field is small close to the equator and also in the north part of Mozambique. Therefore the magnetic field will give a weaker signal of the water molecules. The measured magnetic field caused by solar radiation in the study area induces a signal of around 5000 nV in the MRS coil. This value is by far higher than the one measured by the instrument related to the hydrogen molecules.

5.1.3 Applicability and limitation of IP method

Induced polarization data were only evaluated for the Mongicual area, where it was expected that water with high salinity could be encountered. For some boreholes, layers containing groundwater with high electrical conductivity were detected as high normalized chargeability layers with the IP method. Dissolution of metallic minerals was the main reason identified as source of the electrical conductivity of the water. Therefore the IP method may be useful in this specific areas due to presence of disseminated metallic minerals in the sand dunes in this area. It is also applicable in areas with solid rocks rich in metallic minerals where it is also expected that ERT will get a good contrasts.

The limitation of the IP method in this study is the poor data quality due to high levels of noise. The IP measurements require good ground contact of the electrodes, which was not always achieved.

5.1.4 Applicability and limitation of borehole logging method

Borehole geophysics is a down-hole method that gives the variation of the lithology in a drilled borehole (Karasaki et al., 2000). With this method, a wide range of sensors measuring different properties can be used. The obtained information can

help the interpretation of ERT results. However additional information such as geological borehole logging may increase the confidence of resulting models.

The drawback to borehole logging in this study is the possible presence of metal objects in the borehole. Such objects can be either the casing, the centralizers or material used to back fill the borehole. In all these cases the borehole geophysical logging will not perform well due to signal attenuation, except the natural gamma measurement that is not influenced by metals. Another drawback is that the borehole logging was not performed in unsuccessful boreholes because they were backfilled.

5.1.5 Integrating different hydrogeophysical methods

The lack of additional information that could help the interpretation of the inverted geophysical models was the main issue in this study. Therefore combing two or more methods will help the interpretation as each geophysical method will measure a different ground property or measure the same property in different ways.

The combination of ERT and MRS methods worked well in the unconsolidated sedimentary areas. The recharge area was well mapped with this combination. Also both spatial and depth variation of sand and clay layers in the flood plain of Urema lake were described despite the absence of background information. Therefore it is suggested to use this combination in similar geological conditions. Depending on the geological setting and depth of investigation, TEM could also have been used as a complementary method. The integration of ERT and IP methods is dependent on the local geology. If the soil material is not chargeable, then the IP will not give a significant response. On the other hand, the measurement of IP is often more time consuming because of the need for good electrode ground contact. If however the available equipment measures both resistivity and chargeability and site conditions allow the combination, it can add valuable information.

One way of overcoming the lack of reference data is the calibration of the geophysical models by using the existing water wells in the villages or communities. The calibration by the existing boreholes can be combined with the geophysical logging preferably in boreholes with non-metallic casing. Another method that may be of great use is slug testing as it gives general information about the hydraulic properties of the aquifer close to the well.

After drilling, the borehole logging should also be performed before casing is installed. The advantage of this approach is that the characteristics of the aquifer can be related to other areas with the same geological condition. The logging should also be considered as a tool to verify the well installation and positioning of centralizers).

5.2 Inadequate reference information

The geophysical results are ambiguous and thus reference data are needed for interpretation. The optimal reference data are detailed geological maps, hydrogeological maps, a drilling documentation, borehole geophysical data and hydrogeological tests like slug tests. The geological map gives a description of the rock types and their mineral composition. Hydrogeological maps give information about the potential for groundwater occurrence and quality. The quality of the groundwater will have an influence on the measured geophysical data. The lithological description in a borehole together with a geological map will give an overview of the local variety of rock types and sediments. In absence of such information, the interpretation of geophysical data becomes unreliable and possibly inconsistent.

In Mozambique the basic information used for the interpretation is available from geological and hydrogeological maps. The existing geological maps are at the scale of 1:1 000 000 and 1:250 000. The only available hydrogeological map of Mozambique was produced in 1988 at scale of 1:1 000 000. There is also additional information in the form of reports, but many times such reports are missing or are unreliable. Hydrogeological projects have been done in the entire country after 1988, however most of the project reports are in the form of unpublished reports and little is published as scientific work. The consequence is that for new research projects this information is not available and then there is repetition of work that could be avoided.

Different geophysical methods measure different physical properties which are related to different geological properties. Therefore the combination of two or more methods may help each other in the interpretation. This approach is useful when no reference data is available. However, the result of such interpreted geophysical data is not totally valid. It has some degree of uncertainty which means that results of this approach should be used with caution.

5.3 Field work limitations in Mozambique

A critical issue for field work in Mozambique is the optimum period of the year for good measurements. During the beginning of the wet season (from October to December) the measurements are difficult because of high temperatures. When it is hot, the surface soil is completely dry and it is difficult to get good ground contact for electrodes. As a consequence, low signal/noise ration readings are frequent. Pouring water or wet clay at the electrodes is necessary but time consuming to improve the ground contact. During the end of the wet season (January to March) it rains constantly and the field work is almost impossible due to bad road conditions. The beginning of dry season (April to July) is the optimum period for field work in Mozambique because the ground is still moist with water, the temperature is mild and there is no rain. The moist ground gives a good ground contact. At the end of the dry season (between July and October) the ground is dry and the temperatures start to increase, and therefore this period can be considered as fairly good for field work. But watering the electrodes and working early in the morning and late afternoon is advisable, rather than working in the middle part of the day.

For borehole logging and slug testing the main issue is the time used to collect the data. The local population frequently uses the wells because they do not have tanks to store water. Therefore, the time taken for the measurements should be as brief as possible to ensure that the population can continue to draw water from the well as needed. When the boreholes are opened and the pumps lifted out, it often turns out that some parts of the pumps are old and worn and malfunctioning. In the process of re-installing the pumps, new parts are needed. Therefore, it is advisable to have a set of essential spare parts.

6. Conclusions and future work

In this thesis the main focus has been on the understanding of hydrogeological conditions in area with little background information by use of geophysical investigation. Applying the ERT method in different geological environments has proven that this method is versatile. The ERT method gave a good contrast between sand and clay and also a good contrast between unweathered rock and weathered layers. More detailed interpretation is hampered by lack of reference data. Therefore a combination of two geophysical methods was the approach used to improve the interpretation of ERT results.

The combination of the ERT and MRS methods works well in unconsolidated sediments. However in this study the applicability of MRS was not fully explored. The relationship between the free water content and effective porosity of the aquifer and the relationship between decay time and hydraulic conductivity estimated by other methods was not studied due to lack of information.

IP results presented as normalized chargeability give a good contrast between clay and sand layers and between clay layers and unweathered rock in Mongicual district. Clay gives a high value of normalized chargeability whereas in sand layers and unweathered hard rock the value is low. The high value of normalized chargeability found in sand layers in this study are attributed to a content of heavy metal minerals. The electrical conductivity of groundwater increases when these minerals are dissolved.

Borehole loggings together with ERT results have shown that the lithological descriptions in the drilling reports are sometimes inconsistent. The inconsistence may be caused by the mix of site information or copy and paste of the description from different reports. As a consequence of this inconsistency, it is expected that even some VES presented in the borehole drilling report are presumably wrong. Future geophysical survey projects for groundwater exploration would benefit from starting with a calibration of ERT measurements and geophysical logging in the existing boreholes.

The logged data and calibration models should be kept in an organized way so that they can be used in future projects. The lithological descriptions of the drilled boreholes should be made under supervision of well-trained people to avoid waste of important information. Such information should be kept in a national archive for drilling reports and geophysical data.

This survey has shown that even with little background information, the combination of geophysical methods can help in detecting a recharge zone and the possible interconnection between two aquifers in the Urema floodplain. The study also improved the understanding of interaction between surface and groundwater in the Urema floodplain. However, it failed to demonstrate a possible connection between the Urema Lake and Pungue River. Therefore, further studies are needed to confirm this possibility. Such connection is vital for the management of the national park as it will regulate the land use priorities upstream of the park.

The results of slug testing indicated that when the weathered and fractured layers are well developed, the hydraulic conductivity is high. This observation is not applicable when the weathered profile is covered by paleo coastal sand dunes. Therefore ERT method can be useful to indicate the geometry of the hydraulic conductivity variation in the aquifer which is helpful to maximize the groundwater abstraction.

Combining hydrogeophysical methods and other non-geophysical methods has proven to be useful when no other information is available. This effort has increased the knowledge of hydrogeological situation in different parts of Mozambique.

6.1 Future work

It is recommended to continue this approach of combining geophysical methods but with more control on how they can be interpreted together and thereby overcome the lack of background data. This control may reduce the degree of uncertainties.

Some other possible topics for future work are:

1. Extension of the study to the volcanic terrains and sedimentary basins.
2. The inverted ERT and IP models presented in this study did not take into consideration the groundwater level. It may be possible to assess the improvement of the inverted model quality by constraining the inversion with groundwater level information.
3. Assessment of groundwater quality influence in the measured resistivity to improve the interpretation of inverted ERT and IP models.
4. The economic implication in shifting from traditional VES to ERT or other method used in this study as the method for groundwater investigation was not considered in this study. It is recommended to assess the economic implication of the survey as a whole and its outcomes.

5. Evaluation of hydraulic properties of the aquifers in the Urema flood plain and relating them to aquifer properties obtained from the MRS method.
6. Confirmation of a possible connection between Urema Lake and Pungue River by using other methods such as hydrochemical and isotopic investigations.

7. References

Acworth, I. (2001). The electrical image method compared with resistivity sounding and electromagnetic profiling for investigation in areas of complex geology: A case study from groundwater investigation in a weathered crystalline rock environment. *Exploration Geophysics, 32*(2), 119-128.

Afonso, R. S. (1978). *A geologia de Moçambique* Mozambique: National Directorate of Geology

Andersson, B., & Björkström, T. (2014). *Geophysical Investigation in Nampula province, Mozambique - Rural water point installation program - part 2.* Master thesis, Engineering Geology, Lund University, Sweden. (LUTVDG/(TVTG-5133)/1-85/(2014))

Andrade, C. (1929). *Esboço geológico da Província de Moçambique. Imp. Nac. Lisboa, Carta anexa na esc. 1:5 000 000* (I. G. S. o. S. Africa Ed.). South Africa.

Arvidsson, K. (2010). *Geophysical and hydrogeological survey in a part of the Nhandungue River valley, Gorongosa National Park, Mozambique.* Master thesis, Department of Earth and Ecosystem Science, Lund University, Sweden. (256)

Arvidsson, K., Stenberg, L., Chirindja, F., Dahlin, T., Owen, R., & Steinbruch, F. (2011). A hydrogeological study of the Nhandugue River, Mozambique–a major groundwater recharge zone. *Physics and Chemistry of the Earth, Parts A/B/C, 36*(14), 789-797.

Beilfuss, R., Owen, R., & Steinbruch, F. (2007). Long-term plan for hydrological research: adaptive management of water resources at Gorongosa National Park. *Report Prepared for Gorongosa Research Center, Gorongosa National Park*.

Bireque, A., Magaia, L., & Mendes, E. (1993). *Pesquisa electromagnética dos aquíferos de calcários, Relatório interno*. Mozambique: National Directorate of Water.

Bouwer, H., & Rice, R. (1976). A slug test for determining hydraulic conductivity of unconfined aquifers with completely or partially penetrating wells. *Water Resources Research, 12*(3), 423-428.

Briggs, P. (2007). *Mozambique* (Sixth Edition ed.). USA: Bradt Travel Guides.

Chirindja, F., Dahlin, T., Perttu, N., Steinbruch, F., & Owen, R. (2016a). Combined electrical resistivity tomography and magnetic resonance sounding investigation of the surface-water/groundwater interaction in the Urema Graben, Mozambique. *Hydrogeology Journal, 24*(6), 1583-1592.

Chirindja, F., Dahlin, T., Steinbruch, F., & Juizo, D. (2016b). Reconstructing the formation of a costal aquifer in Nampula province, Mozambique from ERT and IP methods for water prospection. Published: Environmental Earth Sciences Journal, 76:36, DOI 10.1007/s12665-016-6364-0.

Chirindja, F., Dahlin, T., & Juizo, D. (2017a). Improving the groundwater-well siting approach in consolidated rock in Nampula Province, Mozambique. *Hydrogeology Journal*, 1-13.

Chirindja, F., Rosberg, J.-E., & Dahlin, T. (2017b). Borehole Logging and Slug Tests for Evaluating the Applicability of Electrical Resistivity Tomography for Groundwater Exploration in Nampula Complex, Mozambique. *Water, 9*(2), 95.

Chongo, M., Wibroe, Staal-Thomsen, K., Moses, M., Nyambe, I., Larsen, F., & Bauer-Gottwein, P. (2011). The use of time domain electromagnetic method and continuous vertical electrical sounding to map groundwater salinity in the barotse sub-basin, Zambia. *Physics and Chemistry of the Earth, 36*, 798-805.

Clair, J. S., Moon, S., Holbrook, W., Perron, J., Riebe, C., Martel, S., . . . Singha, K. (2015). Geophysical imaging reveals topographic stress control of bedrock weathering. *Science, 350*(6260), 534-538.

Cooper, H. H., Bredehoeft, J. D., & Papadopulos, I. S. (1967). Response of a finite-diameter well to an instantaneous charge of water. *Water Resources Research, 3*(1), 263-269.

Dahlin, T. (1993). *On the Automation of 2D Resistivity Surveying for Enginnering and Environmental Applications*: Department of Engineering Geology, Lund Institute of Technology, Lund University.

Dahlin, T., & Zhou, B. (2006). Multiple-gradient array measurements for multichannel 2D resistivity imaging. *Near Surface Geophysics, 4*(2), 113-123.

Darling, T. (2005). *Well logging and formation evaluation*. United States of America: Elsevier.

Daudi, E., Ramalho, E., Fernandes, J., Batista, M., Quental, L., Dias, R., & Manhiça, V. (2014). *Geofísica aplicada à gestão da água subterrânea e ao ordenamento do território da cidade da beira*. Paper presented at the 12CGPLP, Mozambique.

De Beer, J., & Blume, J. (1985). Geophysical and Hydrogeological Investigations of the Ground-Water Resources Of Western Hereroland, South West Africa/Namibia. *Verhandelinge van die Geologiese Vereniging van Suid-Afrika, 88*(483-493).

Enkel, O., & Sjöstrand, E. (2013). *Geophysical investigation of a rural water point installation program in Nampula Rapale district, Nampula provinve, Mozambique - a minor field study.* Master thesis, Department of measurement technology and industrial electrical engineering, Lund University, Sweden. (LUTVDG/(TVTG-5128)/1-109/2013)

Ferro, B., & Bouman, D. (1987). *Explanatory notes of the hydrogeological map of Mozambique, scale 1:1,000,000. Project of the hydrogeological map of Mozambique*. Mozambique: National Directorate of Water Affairs.

GTK. (2006). *Map explanation* (G. Consortium Ed. mineral resources management capacity building project ed. Vol. 2). Mozambique: National Directorate of Geology.

Hallerbäck, S. (2016). *Water well investigation in Nampula province - Slug tests in weathered crystalline rocks.* BSc thesis, Engineering Geology, Lund University, Sweden. (ISRN: LUTVDG/(TVTG-5146)/1-72/(2016))

Hertrich, M. (2008). Imaging of groundwater with nuclear magnetic resonance. *Progress in Nuclear Magnetic Resonance Spectroscopy, 53*(4), 227-248.

Holmes, A. (1951). *The sequence of Pre-Cambrian orogenic belts in South and Central Africa. Report of the XVIII Session IGC*. Great Britain.

Hubbard, S. S., & Rubin, Y. (2005). Introduction to hydrogeophysics *Hydrogeophysics* (pp. 3-21): Springer.

Ismail, A., Anderson, N., & Rogers, J. (2005). Hydrogeophysical investigation at Luxor, Southern Egypt. *Journal of Environmental and Engineering Geophysics, 10*(35-49).

Karasaki, K., Freifeld, B., Cohen, A., Grossenbacher, K., Cook, P., & Vasco, D. (2000). A multidisciplinary fractured rock characterization study at Raymond field site, Raymond, CA. *Journal of Hydrology, 236*(1), 17-34.

Keating, K., & Knight, R. (2010). A laboratory study of the effect of Fe (II)-bearing minerals on nuclear magnetic resonance (NMR) relaxation measurements. *Geophysics, 75*(3), F71-F82.

Kellett, R. L., Anscombe, J. R., Bauman, P. D., Hankin, P., & Engelbrecht, L. (2001). Geophysical mapping of groundwater potential in a rural water supply project; Malawi, Africa. *Proceedings - Symposium on the Application of Geophysics to Engineering and Environmental Problems (SAGEEP), 2001*.

Kirsch, R., & Yaramanci, U. (2009). Geoelectrical methods *Groundwater Geophysics* (pp. 85-117): Springer.

Kumar, D., Mondal, S., Nandan, M., Harini, P., Sekhar, B. S., & Sen, M. K. (2016). Two-dimensional electrical resistivity tomography (ERT) and time-domain-induced polarization (TDIP) study in hard rock for groundwater investigation: a case study at Choutuppal Telangana, India. *Arabian Journal of Geosciences, 9*(5), 1-15.

Lächelt, R. (2004). *Geology and Mineral Resources of Mozambique* (D. J. Winterbach Ed.). Mozambique.

Leal, A. d. S. (1992). MODELO DOS MAPAS HIDROGEOLÓGICOS DA CPRM. *Águas Subterrâneas*.

Legchenko, A., Baltassar, J., Beauce, A., & Bernard, J. (2002). Nuclear magnetic resonance as a geophysical tool for hygrogeologists. *Journal of Applied Geophysics, 50*, 21-46.

Legchenko, A., & Shushakov, O. (1998). Inversion of surface NMR data. *Geophysics, 63*, 75-84.

Linde, N., Chen, J., Kowalsky, M. B., & Hubbard, S. (2006). Hydrogeophysical parameter estimation approaches for field scale characterization *Applied Hydrogeophysics* (pp. 9-44): Springer.

Loke, M. H., Acworth, I., & Dahlin, T. (2003). A comparison of smooth and blocky inversion methods in 2D electrical imaging surveys. *Exploration Geophysics, 34*(3), 182-187.

Lubczynski, M., & Roy, J. (2003). Hydrogeological interpretation and potential of the new magnetic resonance sounding (MRS) method. *Journal of Hydrology, 283*(1), 19-40.

MacDonald, A., & Calow, R. (2009). Developing groundwater for secure rural water supplies in Africa. *Desalination, 248*(1), 546-556.

MacDonald, B., H C B ´E ´O Dochartaigh and R G Taylor. (2012). Quantitative maps of groundwater resources in Africa. *ENVIRONMENTAL RESEARCH LETTERS*. doi:Res. Lett. 7 024009

Mendes, V. (1966). Recherches Hidrologiques dans la Plateau de Cajueiros, Porto Amélia, Moçambique. *Diplome d´ Ingénieur Geophysicien, Institut de Pyisique du Globe*, 99.

Menke, W. (1989). *Geophysical data analysis: discrete inversion theory - First edition*. Volume 45, Academic press, 289 pages, ISBN: 97800124909212, USA.

Meyer, R., & De Beer, J. (1980). Geophysical Study of The Cape Flats Aquifer. *Verhandelinge van die Geologiese Vereniging van Suid-Afrika, 84*, 107-114.

Møller, I., Søndergaard, V. H., & Jørgensen, F. (2009). Geophysical methods and data administration in Danish groundwater mapping. *Geological Survey of Denmark and Greenland Bulletin, 17*, 41-44.

Moyce, W., Mangeya, P., Owen, R., & Love, D. (2006). Alluvial aquifers in the Mzingwane Catchment: their distribution, properties, current usage and potential expansion. *Physics and Chemistry of the Earth, Parts A/B/C, 31*(15), 988-994.

Muiuane, E. (1999). *Hydrogeophysicis of tropical Africa - Recent advances and perspectives*. Uppsala, Sweden.

Okereke, C., Esu, E., & Edet, A. (1998). Determination of potential groundwater sites using geological and geophysical techniques in the Cross River State, southeastern Nigeria. *Journal of African Earth Sciences, 27*(149-163).

Olsson, E. (2016). *Water well investigation in Nampula province, Mozambique - a minor field study*. Master thesis, Engineering Geology, Lund University, Sweden. (LUTVDG/(TVTG-5147)/1-87/(2016))

Owen, R. (2004). *GM SAFMA Hydrogeology condition and trend report. The Millenium Ecosystem Assessment (MA)*. Zimbabwe.

Owen, R., Gwavava, O., & Gwaze, P. (2006). Multi-electrode resistivity survey for groundwater exploration in the Harare greenstone belt, Zimbabwe. *Hydrogeology Journal, 14*(1-2), 244-252.

Palacky, G. (1988). Resistivity characteristics of geologic targets. *SEG, 1*, 53-129.

Plata, J., & Rubio, F. (2002). MRS experiments in a noisy area of a detrital aquifer in the south of Spain. *Journal of Applied Geophysics, 50*(1), 83-94.

Reynolds, J. M. (1987). The role of surface geophysics in the assessment of regional groundwater potential in Northern Nigeria. *Engineering Geology Special Publication, 4*, 185-190.

Robertson Geologging LTD (2017). http://www.geologging.com/slimhole-logging/about-slimhole-logging/. (Accessed on 17th of august 2018).

Robinson, E., & Coruh, C. (1988). *Basic exploration geophysics*. United States: Somerset, NJ (US); John Wiley and Sons, Inc.

Salman, G., & Abdula, I. (1995). Development of the Mozambique and Ruvuma sedimentary basins, offshore Mozambique. *Sedimentary Geology, 96*(1), 7-41.

Salomon. (2010). *Design Report No. 1 for 150 Water Points - Cabo Delgado and Nampula Rural Water Point Installation Program Mozambique*. Maputo: Cowater International Inc. and Salomon Lda.

Schlumberger, C. (1920). Etude sur la prospection electrique du sous-sol, Paris, Gauthier-Villars, 94p.

Sharma, P. V. (1997). *Environmental and engineering geophysics*: Cambridge university press.

Slater, L. D., & Lesmes, D. (2002). IP interpretation in environmental investigations. *Geophysics, 67*(1), 77-88.

Soltau, L., & Anderson, N. (2006). An integrated geophysical survey of groundwater resources, Mamre area, Western Cape Province. *South African Journal of Geology, 109*, 433-438.

Srivastava, P. K., & Bhattacharya, A. K. (2006). Groundwater assessment through an integrated approach using remote sensing, GIS and resistivity techniques: a case study from a hard rock terrain. *International Journal of Remote Sensing, 27*(20), 4599-4620.

Steinbruch, F. (2010). Geology and geomorphology of the Urema Graben with emphasis on the evolution of Lake Urema. J*ournal of African Earth Sciences, 58*(2), 272-284.

Stenberg L (2011) Geophysical and Hydrogeological survey in a part of the Nhandungue River valley, Gorongosa National Park, Mozambique – Area 1 and 2. Master thesis, 46 pp. Department of Earth and Ecosystem Sciences, Division of Geology, Lund University, Sweden.

Vermeulen, P., & van Tonder, G. (2004). *Slug tests in fractured rock formations: value, pitfalls and misinterpretations.* Paper presented at the Water Resources of Arid Areas: Proceedings of the International Conference on Water Resources of Arid and Semi-Arid Regions of Africa, Gaborone, Botswana, 3-6 August 2004.

Vieira, F., & Chandra, N. (1990). case study of geophysical prospecting for groundwater in coastal Mozambique -Un exemple de prospection geophysicque pour l'eau souterraine au Mozambique. Publication Occasionnelle *International Center for Training and Exchanges in the Geosciences, 20*(426).

Paper I

Physics and Chemistry of the Earth 36 (2011) 789–797

Contents lists available at SciVerse ScienceDirect

Physics and Chemistry of the Earth

journal homepage: www.elsevier.com/locate/pce

A hydrogeological study of the Nhandugue River, Mozambique – A major groundwater recharge zone

K. Arvidsson [a], L. Stenberg [a], F. Chirindja [b], T. Dahlin [c,*], R. Owen [d], F. Steinbruch [e]

[a] Dept. of Earth and Ecosystem Sciences, Lund University, Sölvegatan 12, SE-22362 Lund, Sweden
[b] Geology Dept., Eduardo Mondlane University, Maputo, Mozambique
[c] Engineering Geology, Lund University, Box 118, SE-22100 Lund, Sweden
[d] Geology Dept., University of Zimbabwe, Harare, Zimbabwe
[e] Scientific Services, Gorongosa National Park, Sofala, Mozambique

ARTICLE INFO

Article history:
Available online 12 August 2011

Keywords:
Gorongosa National Park
Groundwater recharge zone
Hydrogeology
Resistivity
Urema Rift

ABSTRACT

The Nhandugue River flows over the western margin of the Urema Rift, the southernmost extension of the East African Rift System, and marks the north-western border of Gorongosa National Park, Mozambique. It constitutes one of the major indispensable water resources for the ecosystem that the park protects. Our study focused on the hydrogeological conditions at the western rift margin by resistivity measurements, soil sampling and discharge measurements. The resistivity results suggest that the area is heavily faulted and constitutes a major groundwater recharge zone. East of the rift margin the resistivity indicate that solid gneiss is fractured and weathered, and is overlain by sandstone and alluvial sediments. The top 10–15 m of the alluvial sequence is interpreted as sand. The sand layer extends back to the rift margin thus also covering the gneiss. The sandstone outcrops a few kilometers from the rift margin and dips towards east/south-east. Further into the rift valley, the sand is underlain by lenses of silt and clay on top of sand mixed with finer matter. In the lower end of the investigated area the lenses of silt and clay appears as a more or less continuous layer between the two sand units. The topmost alluvial sand constitutes an unconfined aquifer under which the solid gneiss forms a hydraulic boundary and the fractured gneiss an unconfined aquifer. The sandstone is an unconfined aquifer in the west, becoming semi-confined down dip. The lenses of silt and clay forms an aquitard and the underlying sand mixed with finer matter a semi-confined aquifer. The surface runoff decreases downstream and it is therefore concluded that surface water infiltrates as recharge to the aquifers and moves as groundwater in an east/south-eastward direction.

1. Introduction

1.1. Location of the area

Gorongosa National Park (GNP) is situated at 19°S and 34°W, within the Sofala province in the central part of Mozambique (Fig. 1). The park is located within the southernmost extension of the East African Rift System (EARS), the Urema Rift, and covers an area of approximately 3770 km^2. The park protects a vast ecosystem of floodplains, grasslands and woodlands.

1.2. Geology and geomorphology

The rift valley floor constitutes the lowest part of the park and it is filled with mainly Quaternary alluvial sediments, in west resting on top the Sena Formation (Fig. 2; Lächelt, 2004). East of the rift margin the Sena Formation and also the Lupata Group are outcropping north respectively south of the Nhandugue River. The Sena Formation consists of massive conglomeratic arcosic sandstones and the Lupata Group comprises red conglomeratic sandstones and phonolitic lava (Tinley, 1977; Lächelt, 2004; National Directorate of Geology, 2006). In general coarse alluvial sediments, like gravel and sand, have formed alluvial fans on the sides while finer sediments have been deposited further out on the valley floor (Tinley, 1977; Chirindja and Hellman, 2009). Sets of NNE–SSW and NNW–SSE orientated faults and fracture zones on both sides of the Urema Rift (Tinley, 1977) are responsible for the system of half-grabens that constitute the 40 km wide rift valley. On the eastern side the valley is defined by the Cheringoma Platform and on the western side it is bounded by the Báruè Platform (Fig. 2). Rising west of the Báruè Platform is the Gorongosa Mountain.

1.3. Climate and drainage

For the function of the ecosystem water resources are indispensable. Several rivers are flowing into the park and merges in

* Corresponding author. Tel.: +46 46 222 96 58; fax: +46 46 222 91 27.
E-mail address: torleif.dahlin@tg.lth.se (T. Dahlin).

1474-7065/$ - see front matter © 2011 Elsevier Ltd. All rights reserved.
doi:10.1016/j.pce.2011.07.036

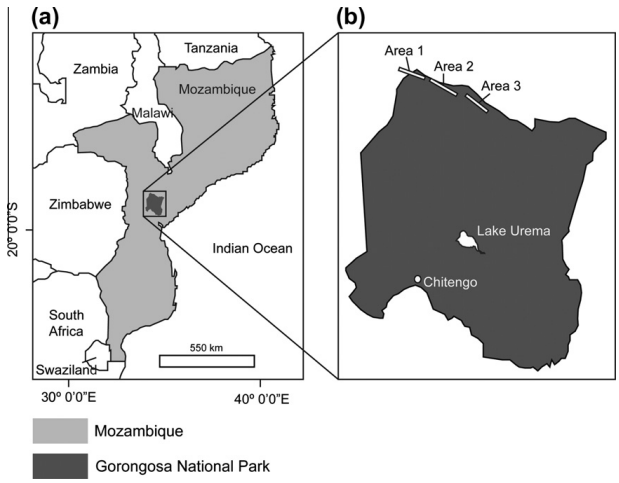

Fig. 1. (a) Map showing the location of Gorongosa National Park in Mozambique, where the study was conducted. (b) Close up on Gorongosa National Park and the location of the three areas in the north of the park.

Lake Urema (LU) in the central part of the park. The lake is a reservoir lake impounded by alluvial fans (Böhme et al., 2006) and due to annual variations in precipitation and evapotranspiration the naturally shallow LU is typified by expansions and withdrawals of its shorelines. The annual amount of precipitation and evapotranspiration varies between the different morphological units and it is only on the Gorongosa Mountain the annual water balance is positive. From here water drains through perennial streams and probably much of the water is recharging groundwater storages along the rift margin. The Nhandugue River is a seasonal sand river which rises from outside the park and crosses the park boundary in the north-western corner (Tinley, 1977). Seasonal means the river has a surface flow that reaches LU only during the rainy seasons. Instead water might be flowing in the sediments from the rift margin and reach LU as groundwater. It was decided to pay special attention to the area where the Nhandugue River flows from the basement gneisses across the western fault margin and onto the rift valley floor sedimentary fill. Field work was conducted in July to August 2009, during the dry season, and data were collected from three areas (Areas 1–3) along the north-western border of GNP (Fig. 1).

1.4. Aim of the research

LU is vital for GNP and park authorities want to predict the effects of changes in different environmental factors in order to maintain sound management and decision-making processes about water resources in the Gorongosa region (Beilfuss et al., 2007). To obtain this information, Gorongosa Research Center in 2007 prepared *Long-term plan for hydrological research: adaptive management of water resources at Gorongosa National Park* (Beilfuss et al., 2007). A result of this plan was a multi-resistivity survey started in 2007, with the aim of obtaining two-dimensional images of the subsurface across the Urema Rift. An initial survey was conducted in 2008 in the downstream area of LU (Chirindja and Hellman, 2009). Evaluation of the results suggested need for further surveys, with additional resistivity profiles. Also it was recommended that reference data is collected in connection to the new resistivity measurements, in order to improve the reliability of the interpretation of the profiles. This study focuses on the western margin of the Urema Rift since it has been anticipated that this area is a potential major groundwater recharge zone to the deeper rift valley floor sediments. The aim is to develop a geological and hydrogeological model for the area in order to understand the infiltration and recharge possibilities for surface water and groundwater.

2. Methods

In order to produce two-dimensional images of the subsurface of the Nhandugue River valley 4-channel multi-electrode gradient array CVES roll-along measurements (Dahlin, 2001) were conducted. An ABEM Lund Imaging System was used, consisting of a Terrameter SAS4000, an Electrode Selector ES10-64C, electrode cables, stainless steel electrodes, etc (ABEM, 2009). An electrode spacing of 5 m was used with a total electrode layout of 400 m, giving a depth penetration around 75 m. Inverse numerical modelling (inversion) was used to produce models of vertical cross sections through the ground, employing Res2dinv (ver.3.58.14) with the robust (L1-norm) inversion constrain (Loke et al., 2003).The computer software Erigraph 2 and EriViz were used for visualizing the models.

In total, resistivity data were collected along nine profiles, three within each of the three study areas (Fig. 3). Due to the high discharge in the rainy seasons and low discharge in the dry seasons the Nhandugue River valley can be divided into three morphological units; (i) a dry-season channel (permanently filled with water), (ii) a wet-season channel (filled with water during rainy seasons) and, (iii) the river flanks. For all three areas a long profile (LP) was placed along the dry-season channel. Each long profile was then crossed by one upstream perpendicular cross profile (CPU) and one downstream perpendicular cross profile (CPD), stretching from the river flanks across the wet-season channel and the dry-season channel.

For geological ground truthing soil samples, from a depth of ~15–30 cm, were collected at locations along the resistivity

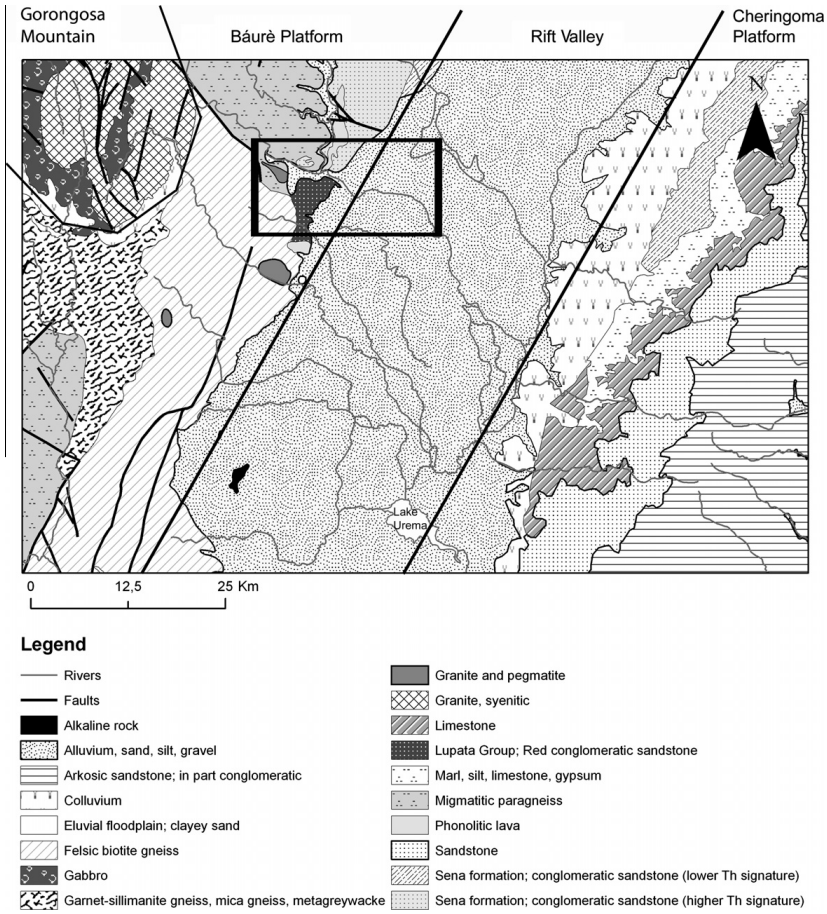

Fig. 2. Geological map of the Urema Rift based on geological data from National Directorate of Geology (2006). The studied area is marked by a black rectangle. Marked are also the four geomorphological units (from left) Gorongosa Mountain, Báruè Platform, Rift Valley and Cheringoma Platform.

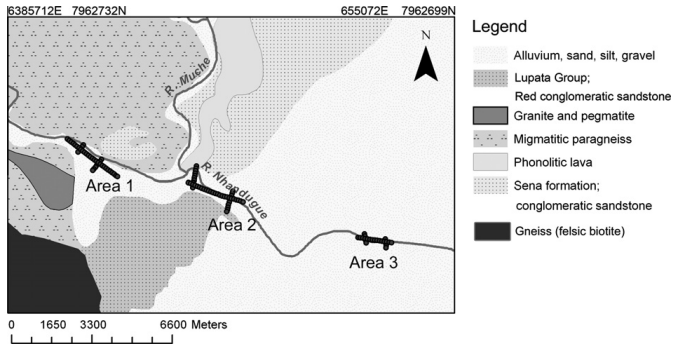

Fig. 3. Location of resistivity profiles in Areas 1–3.

profiles (Fig. 4). In total 21 soil samples were collected for grain size analyses, including sieving and hydrometer analysis. To determine if the soil was permeable enough for water to infiltrate the grain size data were used to calculate the hydraulic conductivity (k). For samples with a uniformity coefficient (C_u) < 5 (after Bowen, 1986) values of k were calculated with Hazen's formula, as defined by Chapuis (2004):

$$k = 1.16 \times d_{10}^2 \quad (1)$$

where d_{10} is Hazen's effective grain size in mm, relative to which 10% of the sample is finer.

To estimate the downstream change in surface discharge (Q) dilution tests were conducted. Tests were conducted on 14th of August 2009 at three locations, one in each area (Fig. 4). In order to get reliable data, sections where the river flowed in one single channel were preferably chosen. For Area 1 this was not possible and measurements were instead conducted in one main channel plus in a smaller channel. The results were then added together. For the tests 500 g of normal table salt (mainly NaCl) was dissolved in 20 L of water and the electrical conductivity (EC) of the solution was measured using an HQ40d Dual-Input Multi-parameter Meter Configurator. By using "EC-masses" ($M \times EC_1$) instead of NaCl-masses it was avoided to have to dry and weigh the salt and to determine the specific relationship between salt and electrical conductivity (Merkel and Steinbruch, 2008). The solution was poured into the stream so that it mixed with the water. At the same time continuous measurements (approximately every second) of the EC was started

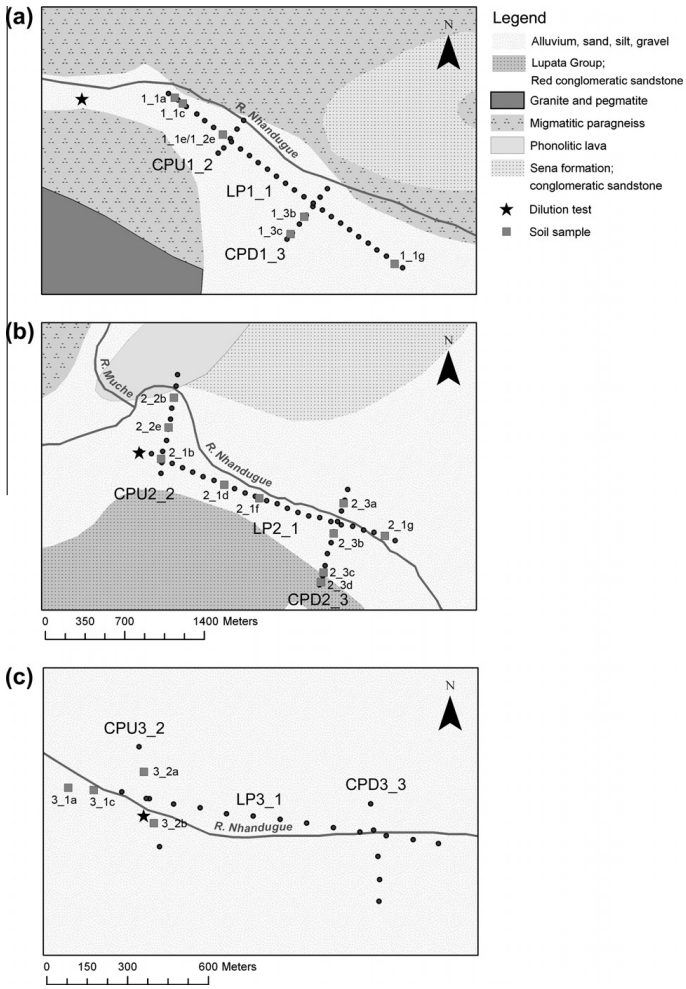

Fig. 4. Close up of Areas 1–3 with locations of soil samples and discharge measurement points marked.

10 m downstream of the injection point. Readings were taken until the conductivity stabilized. Q was then calculated in L/s using Eq. (2), modified from Merkel and Steinbruch (2008):

$$Q = \frac{M \times EC_1}{\int EC} \quad (2)$$

where EC is the electrical conductivity downstream of injection point (μS/cm), M is the amount of water used (L) and EC_1 is the electrical conductivity of the tracer solution (μS).

3. Results

Four main resistivity units are identified for Area 1 (Fig. 5a and b). A top unit with medium to high resistivity (120–1300 Ω m) can be seen in LP1_1. The thickness of the unit varies between 5 m and 15 m. At the edges of CPU1_2, i.e. on the river flanks, this top unit is overlain by two other units, a low resistivity (5–55 Ω m) unit in turn overlain by a medium resistivity (120 Ω m) unit. From the start of LP1_1 and up to 900 m east of the starting point a unit with high resistivity (600–3000 Ω m) is underlying the topmost unit extending to the bottom of the section. Numerous minor vertically oriented heterogeneities can be distinguished in this unit and are marked by vertical lines in Fig. 5a. From 900 m and up to 1500 m another unit, with a medium resistivity (120–600 Ω m), is present. Towards south-east this unit wedges in under a fourth unit of low resistivity (2.2–25 Ω m) that starts at 1300 m. This fourth unit is present in the last ~1300 m of the profile (from 1500 to 2600 m) and has an average thickness of ~60 m.

For Area 2 four resistivity units are identified in the resistivity profiles (Fig. 6a and b). The top unit varies in thickness between ~5 m and 10 m and the resistivity ranges from high to medium (330–1400 Ω m, 37–160 Ω m). The second unit has low resistivity (8.8–37 Ω m) and is discontinuous and varies in thickness between 5 m and 10 m. The third unit is ~15–45 m thick and has a medium resistivity (18–160 Ω m). This unit thickens towards south-east. The bottommost unit stretches all the way to the bottom of the model section, and is thus at least ~15-50 m thick and has low resistivity (2.1–18 Ω m). The unit is found at increasingly larger depths towards south-east. Numerous minor vertical oriented heterogeneities can be distinguished in LP2_1, marked by vertical lines in Fig. 6a.

In the resistivity profiles from Area 3 three resistivity units are clearly identified and a fourth unit is indicated to be present below the third unit (Fig. 7a and b). The top unit is continuously ~5–10 m thick and has medium to high resistivity (37–1400 Ω m). The second unit is somewhat discontinuous with a thickness of ~5–10 m, with a low resistivity (1–18 Ω m). The third unit has a thickness of ~45–50 m and the resistivity is low to medium (18–77 Ω m). The bottom layer is low resistive (<18 Ω m).

From the grain size analyses, the main part of the soil samples from Area 1 are classified as medium and medium to coarse sand (Table 1). One sample (1_1c) is classified as sandy gravel. For Area 2 samples 2_1f and 2_2e are classified as medium sand and samples 2_3b and 2_3d as fine and medium to coarse sand respectively (Table 1). Sample 2_1b and 2_3c are classified as gravelly sand and sandy gravel. Two samples from Area 2 (2_1g and 2_3a) are classified as silty sand and clayey silty sand. Samples 3_1a, 3_1c and 3_2b from Area 3 consist of coarse, medium to coarse and medium sand respectively (Table 1). Two samples from Area 2 (2_1d and 2_2b) and one sample from Area 3 (3_1a) have high organic content (>6%) and grain size analyses could not be performed. The

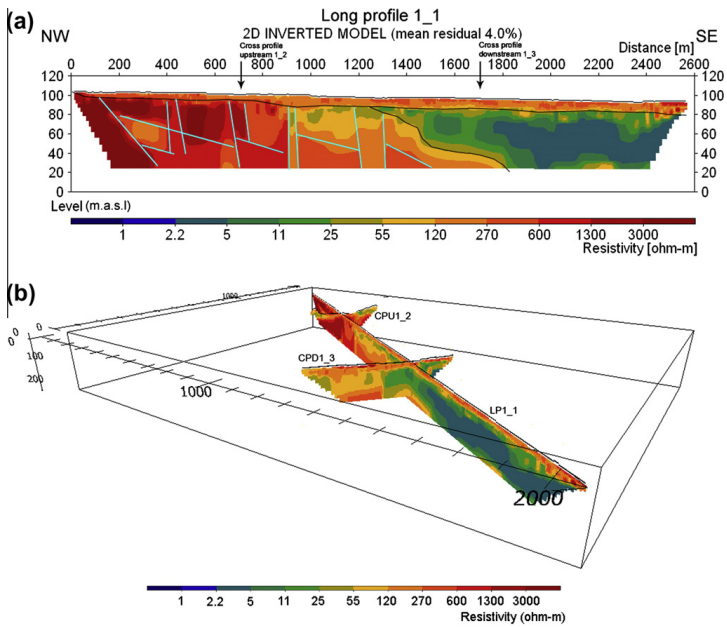

Fig. 5. (a) Resistivity model for profile LP1_1 from Area 1. It shows a thin top unit (orange) and the three units below, 0 to ~900 m (red), ~900 to ~1500 m (orange) and ~1500–2600 m (blue/green), respectively. The blue lines indicate faults. (b) Three-dimensional model of Area 1 showing profiles LP1_1, CPU1_2 and CPU1_3. (For interpretation of the references to color in this figure legend, the reader is referred to the web version of this article.)

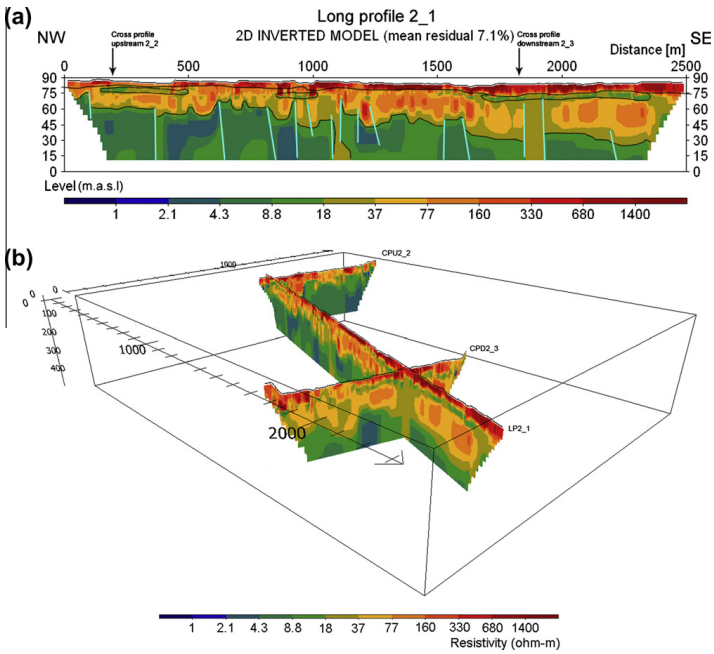

Fig. 6. (a) Resistivity model for profile LP2_1 from Area 2. Four different units can be identified (red, green, orange and blue/green). The blue lines indicate faults. (b) Three-dimensional model of Area 2 showing profiles LP2_1, CPU2_2 and CPU2_3. (For interpretation of the references to color in this figure legend, the reader is referred to the web version of this article.)

hydraulic conductivity in Area 1 ranges from 0.37×10^{-3} to 7.4×10^{-3} m/s. For Area 2 the values range between 0.38×10^{-3} and 2.45×10^{-3} m/s and in Area 3 it ranges from 0.46×10^{-3} m/s to 1.18×10^{-3}.

Just upstream of Area 1, the discharge (Q) was calculated to be 475.74 L/s for the main channel and 88.79 L/s for the small channel. Together they give a total discharge of 564.53 L/s. For measurements just upstream of Area 2 and in Area 3, Q was calculated to 214 L/s and 74 L/s, respectively.

4. Discussion

Fig. 8 is a schematic block model of the interpreted geology. The topmost 10–15 m in all resistivity profiles are highly resistive (Figs. 5–7). This unit is interpreted as alluvial sand, changing from very dry sand at the surface into more moist sand further down. This was visually confirmed during the field work and from the grain size analyses. Below the sand, a highly resistive unit stretches from the start of LP1_1 and up to 900 m (Fig. 5a and b). This unit probably consists of gneiss which is mainly solid, but with fractures indicated by vertical lines in the profiles. The middle section (900–1500 m) in LP1_1 with medium resistivity probably also consist of gneiss, but here it appears to be more fractured and weathered, possibly caused by the presence of water. The vertical and oblique boundary between the sections in LP1_1 probably represents faults in a north-west/south-east direction and in a north/south direction. Vertical heterogeneities are also present in the profiles from Areas 2 and 3, probably indicating fault zones. The faults are most likely minor normal faults that formed simultaneously with the larger faults along the rift margin.

The last section of LP1_1 has low resistivity and most likely consists of saturated sandstone. This is suggested by the presence of outcrops of Sena and Lupata sandstones a few kilometers east of the rift margin. The sandstone in the last section of LP1_1 is most likely also present further downstream, indicated by the bottom-most low resistivity unit in LP2_1 and the low resistivity values in the bottom of LP3_1. Indicated by a dipping of the upper boundary of this unit in the resistivity data the sandstone seems to dip towards east/south-east.

In Areas 2 and 3 a medium resistivity unit is indicated on top of the dipping sandstone. This unit most likely consists of saturated sand mixed with finer material. In LP2_1 and LP3_1 it is indicated that the unit thickens in a downstream direction, which is confirmed by the cross profiles. CPU2_2 shows that the layer is only ~5–10 m thick upstream, while it increases to a thickness of ~40–50 m downstream according to CPU2_3, CPU3_2 and CPU3_3. The sand has most likely been transported from the rift margin and into the rift valley and as the water velocity has decreased the material has been deposited. The thickening of the unit in a downstream direction is probably formed by deposition of material first in lower areas. Between the thickening sand unit and the topmost alluvial sand, low resistive lenses interpreted as lenses of silt and clay are present. In the lower end of the investigated area these lenses appear as a more or less continuous layer.

The calculated values on hydraulic conductivity are 0.37×10^{-3}–7.4×10^{-3} m/s for Area 1, 0.38×10^{-3}–2.45×10^{-3} m/s for Area 2, and 0.46×10^{-3}–1.18×10^{-3} m/s for Area 3.

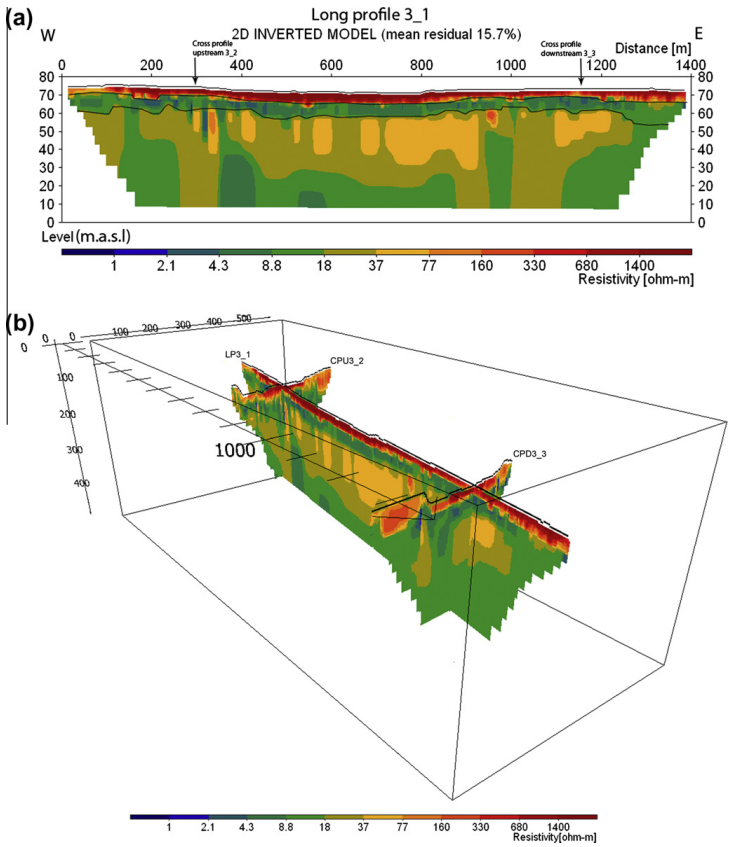

Fig. 7. (a) Resistivity model for the long profile in Area 3. Three different layers can be identified (red, blue/green and orange) and a fourth underlying layer is indicated in the bottom (green). (b) Three-dimensional model of Area 3 showing profiles LP3_1, CPU3_2 and CPU3_3. (For interpretation of the references to color in this figure legend, the reader is referred to the web version of this article.)

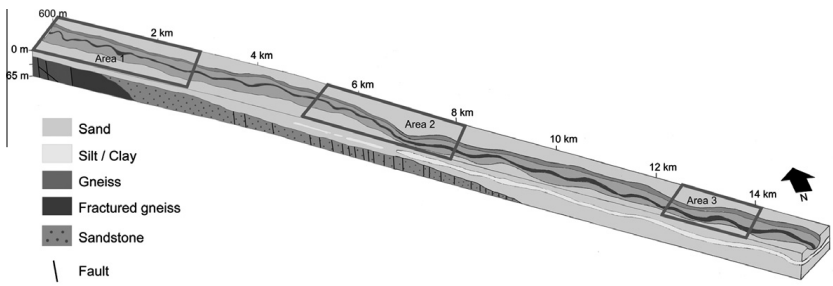

Fig. 8. Schematic block model of the geology in Areas 1–3. Areas 1–3 are marked by black rectangles; Area 1 to the left, Area 2 in the middle and Area 3 to the right. All scales and the extent and location of the different morphological units, i.e. the dry-season channel, wet-season channel and the river flanks, are somewhat approximate. Six different units can be distinguished; (i) a topmost layer of sand, (ii) a unit of solid gneiss, (iii) a unit of fractured gneiss, (iv) a unit of faulted sandstone, (v) a unit of silt and clay and (vi) a unit of sand, mixed with some finer material.

Table 1
Distribution of grain sizes and classification of analyzed soil samples from Areas 1–3.

Sample	Fraction (%)				Classification
	Gravel	Sand	Silt	Clay	
1_1a	0.94	98.91	0.15	0.00	Sand (medium to coarse)
1_1c	52.89	47.11	0.00	0.00	Sandy gravel
1_1e/1_2e	5.51	94.39	0.10	0.00	Sand (medium to coarse)
1_1g	1.48	97.63	0.89	0.00	Sand (medium)
1_3b	1.84	97.47	0.70	0.00	Sand (medium to coarse)
1_3c	6.17	93.19	0.64	0.00	Sand (medium to coarse)
2_1b	28.37	71.24	0.39	0.00	Gravelly sand
2_1f	0.09	99.51	0.40	0.00	Sand (medium)
2_1g	0.19	77.48	13.80	8.53	Silty sand
2_2e	0.00	86.27	6.49	7.24	Sand (fine)
2_3a	0.15	68.84	20.42	10.59	Clayey silty sand
2_3b	1.39	93.35	5.26	0.00	Sand (medium)
2_3c	49.56	47.98	2.47	0.00	Sandy gravel
2_3d	6.23	87.49	6.29	0.00	Sand (medium to coarse)
3_1a	15.31	84.45	0.23	0.00	Sand (coarse)
3_1c	9.17	89.93	0.91	0.00	Sand (medium to coarse)
3_2b	10.72	88.78	0.50	0.00	Sand (medium)

Hence, the values seem to decrease downstream, indicating the material becoming finer further out from the rift margin. The soil samples are on the contrary showing that fine grained material is present in Area 2 but not in Area 3. However, the samples containing fine grained material were less sorted, and as the method used for calculation of hydraulic conductivity states that the uniformity coefficient (C_u) for the sediments has to be <5, values could not be calculated for these samples. Also it is just the maximum values that are decreasing while the lower values are about the same. Hence, the hydraulic conductivity values are somewhat misleading in terms of being related to distance from the rift margin. In this case the location of the samples within the river valley is most likely more important for the sorting of the material and the variation in hydraulic conductivity than the distance from the rift margin. Considering the location of the samples the finer material is located on the river flanks whereas the more sorted materials appear in the closer vicinity of the dry-season channel. This distribution most likely reflects changes in the location of the dry- and wet-season channel and annual variations in discharge.

From the hydraulic conductivity values it is concluded that the topmost alluvial sand is relatively permeable and forms an aquifer. A direct contact between the aquifer and the atmosphere makes it unconfined. Below this aquifer the solid gneiss forms a hydraulic boundary in the west and the fractured gneiss constitutes an unconfined fracture aquifer. Further out from the rift margin the discontinuous layer of finer sediments below the alluvial sand forms an aquiclude through which there is a possibility for leakage in a downward direction. The third unit of alluvial sediments are most likely relatively permeable, hence forming an aquifer. Because of the aquiclude of finer sediments this aquifer is semi-confined. The sandstone unit shows very low resistivities, indicating high porosity and water-saturated conditions. Several small water filled-fracture zones are also most likely present due to heavy faulting. It therefore forms an unconfined aquifer in the west becoming semi-confined down dip where it is overlain by the aquiclude. An east/south-eastward flow direction of the river together with the gentle dip of the sandstone layer is indicating a hydraulic groundwater gradient towards the rift valley floor. This direction is also indicated by the hydraulic boundary in the west and the gently east/south-east sloping ground surface.

The surface discharge for Area 1 has been calculated to ~564 L/s. A true discharge value cannot be given for the main channel in Area 1, due to two major peaks in conductivity instead of one. Still, when comparing the value to the calculated values for Areas 2 and 3 it appears reasonable. In order to get more reliable data it is recommended to repeat and to do continuous measurements, which was not possible in this study due to time limitation. Going about 6 km downstream to the measuring point in Area 2 the water discharge is decreasing to ~214 L/s, and another 7 km downstream, at the measuring point in Area 3, the discharge has decreased to ~74 L/s. Hence, there is a loss in surface water downstream. The river is seasonal and has a wet-season and a dry-season channel. The dry-season channel, in which the discharge measurements were conducted, is meandering within the wider and straighter wet-season channel. Just upstream of Area 1 the river is flowing on bedrock and by the heterogeneity of the surface the dry-season channel is divided into a larger main channel and a couple of smaller channels. Within Area 1 the bedrock becomes overlain by alluvial sediments and the river bed and bank material from there on consists of mainly sandy sediments. The interpreted stratigraphy of the area suggests it is possible for water to infiltrate from the surface to deeper layers. It is therefore suggested that this lost surface water is in parts evapotranspirated and in parts infiltrating downwards, forming groundwater in the lowermost layers.

5. Conclusion

From the resistivity data it can be concluded that east of the rift margin the solid gneiss is fractured and weathered, and overlain by sandstone and Quaternary sediments deposited by alluvial processes. The alluvial sediments are relatively permeable and infiltration of water is possible. The decrease in surface water discharge in the downstream direction is partly attributed to surface water infiltrating into the ground and being transported as groundwater in an east/south-eastward direction, which would confirm that the rift margin is a likely groundwater recharge zone. The east/south-eastward hydraulic gradient further suggests groundwater is flowing towards, and feeds LU.

Acknowledgements

This paper is based on field and laboratory work conducted as part of the M.Sc. theses by K. Arvidsson and L. Stenberg (Arvidsson, 2010; Stenberg, 2010). Research was supervised and enabled by the SIDA-SAREC funded research cooperation between Lund University, Eduardo Mondlane University and GNP. The organization of logistics in the GNP was supported by the Gorongosa Restoration Project and Eduardo Mondlane University in Maputo. USAID funded equipment and staff time in the park. The cost of the field work in Mozambique was supported by two Minor Field Study scholarships from SIDA.

References

ABEM, 2009. Instruction Manual Terrameter SAS 4000/SAS 1000. ABEM Instrument AB, Sundbyberg.
Arvidsson, K., 2010. Geophysical and hydrogeological survey in a part of the Nhandugue river valley, Gorongosa National Park, Mozambique – area 2 and 3. M.Sc. thesis, Department of Earth and Ecosystem Sciences, Lund University, Lund.
Beilfuss, R., Owen, R., Steinbruch, F., 2007. Long-term plan for hydrological research: adaptive management of water resources at Gorongosa National Park. Report Prepared for Gorongosa Research Center, Gorongosa National Park.
Böhme, B., Steinbruch, F., Gloaguen, R., Heilmeier, H., Merkel, B., 2006. Geomorphology, hydrology and ecology of Lake Urema, central Mozambique. J. Phys. Chem. Earth 31, 745–752.
Bowen, R., 1986. Groundwater, second ed. Elsevier Applied Science Publishers, London.
Chapuis, R.P., 2004. Predicting the saturated hydraulic conductivity of sand and gravel using effective diameter and void ratio. Can. Geotech. J. 41, 787–795.
Chirindja, F., Hellman, K., 2009. Geophysical investigation in a part of Gorongosa National Park in Mozamique – a minor field study. M.Sc. thesis, Department of Engineering Geology, Lund University, Lund.

Dahlin, T., 2001. The development of DC resistivity imaging techniques. Comput. Geosci. 27, 1019–1029.
Lächelt, S., 2004. The Geology and Mineral Resources of Mozambique. National Directorate of Geology, Maputo.
Loke, M.H., Acworth, I., Dahlin, T., 2003. A comparison of smooth and blocky inversion methods in 2-D electrical imaging surveys. Explor. Geophys. 34 (3), 182–187.
Merkel, B.J., Steinbruch, F., 2008. Characterization of a Pleistocene thermal spring in Mozambique. Hydrol. J. 16, 1655–1668.
National Directorate of Geology, 2006. Geological Map of Gorongosa, Mozambique. Scale 1:250 000.
Stenberg, L., 2010. Geophysical and hydrogeological survey in a part of the Nhandugue river valley, Gorongosa National Park, Mozambique – area 1 and 2. M.Sc. thesis, Department of Earth and Ecosystem Sciences, Lund University, Lund.
Tinley, K.L., 1977. Framework of the Gorongosa eco system. Ph.D. thesis, Faculty of Science, University of Pretoria, Pretoria.

Paper II

Hydrogeol J (2016) 24:1583–1592
DOI 10.1007/s10040-016-1422-y

REPORT

Combined electrical resistivity tomography and magnetic resonance sounding investigation of the surface-water/groundwater interaction in the Urema Graben, Mozambique

F. J. Chirindja[1] · T. Dahlin[2] · N. Perttu[3] · F. Steinbruch[4] · R. Owen[5]

Received: 1 June 2015 / Accepted: 18 April 2016 / Published online: 5 May 2016

Abstract This study focusses on the hydrogeology of Urema Graben, especially possible interactions between surface water and groundwater around Lake Urema, in Gorongosa National Park (GNP). Lake Urema is the only permanent water source for wildlife inside GNP, and there are concerns that it will disappear due to interferences in surface-water/groundwater interactions as a result of changes in the hydraulic environment. As the lake is the only permanent water source, this would be a disaster for the ecosystem of the park. The subsurface geology in Urema Graben was investigated by 20 km of electrical resistivity tomography (ERT) and three magnetic resonance sounding (MRS) surveys. The average depth penetration was 60 and 100 m, respectively. The location of the ERT lines was decided based on general rift morphology and therefore orientated perpendicular to Urema Graben, from the transitional areas of the margins of the Barue platform in the west to the Cheringoma plateau escarpments in the east. ERT and MRS both indicate a second aquifer, where Urema Lake is a window of the first upper semi-confined aquifer, while the lower aquifer is confined by a clay layer 30–40 m thick. The location and depth of this aquifer suggest that it is probably linked to the Pungwe River which could be a main source of recharge during the dry season. If a dam or any other infrastructure is constructed in Pungwe River upstream of GNP, the groundwater level will decrease which could lead to drying out of Urema Lake.

Keywords Electrical resistivity tomography · Magnetic resonance sounding · Unconsolidated sediments · Groundwater flow · Mozambique

✉ F. J. Chirindja
farisse.chirindja@uem.mz

[1] Geology Dept, Eduardo Mondlane University, Maputo, Mozambique

[2] Engineering Geology, Lund University, Lund, Sweden

[3] Exploration geophysics, Luleå University of Technology, Luleå, Sweden

[4] Indian Institute of Technology Madras, Chennai, India

[5] University of Zimbabwe, Harare, Zimbabwe

Introduction

Gorongosa National Park (GNP) in Mozambique is under rehabilitation. The understanding of hydrogeological conditions is a key factor for better management (Beilfuss et al. 2007) because key ecosystems, particularly the mega-fauna, are strongly dependent on the perennial water of Lake Urema. The lake is considered a perennial groundwater-dependent ecosystem (GDE; Beilfuss et al. 2007) linked to groundwater discharges. The Urema Graben with its floodplains is host to many ecosystems supporting a rich biodiversity with a huge carrying capacity for large herbivores.

The sustainability of Lake Urema is sensitive to changes in surface-water/groundwater interactions that may change the prevailing hydraulic gradients; to climate variability leading to reduced recharge to the groundwater systems; and to removal of vegetation cover in the upstream areas, either by climate change or by anthropogenic pressures, leading to increased sedimentation and siltation in the floodplain. Understanding the hydraulics of the Lake Urema GDE is key to the sustainability of these ecosystems.

In the tropical climate in central Mozambique, the rainfall is strongly seasonal. On an annual basis, the evapotranspiration exceeds rainfall by 500–1,000 mm, causing a water deficit during the dry season, and resulting in the drying out of many small lakes and rivers (Beilfuss et al. 2007). An

exception is the Lake Urema located in the terminal end of the Urema Graben, the southernmost extent in the East African Rift in Mozambique (Fig. 1). Lake Urema receives surface run-off from seasonal sources and has only a single outflow known as Urema River. Part of the contribution to the inflow to the lake originates from groundwater (Owen 2004); however, the groundwater inflow into the lake is small in the dry season (McCartney and Owen 2007). Isotope hydrology studies have shown that Lake Urema is maintained by water generated during the wet season. The flat planar graben valley floor has restricted outflow, and as a result forms a waterlogged area (Steinbruch and Weise 2014a). This zone stores water during the wet season, both as surface-water storage in shallow depressions and in a shallow sandy surficial aquifer. It releases this water through exfiltration and evaporation during the dry season, thus providing moisture for the formation of local dry-season rainfall as well as discharging groundwater into Lake Urema (Steinbruch and Weise 2014a, b). The hydraulic mechanisms of this surface-water/groundwater system have not been clearly identified.

A recent study by Arvidsson et al. (2011) measured river flow in the Nhandugue River as it flowed from the basement gneiss on the Barwe platform onto the sedimentary strata in the Urema graben. It was found that surface flow diminished from 564 to 74 L/s across this boundary, clearly signalling the rift margins as a major groundwater recharge zone. Rift valley margin sediments are comprised of coarse clastic materials such as conglomerates that are very permeable and form favourable groundwater recharge zones (e.g. Leeder and Gawthorpe 1987). Other streams discharging across the rift

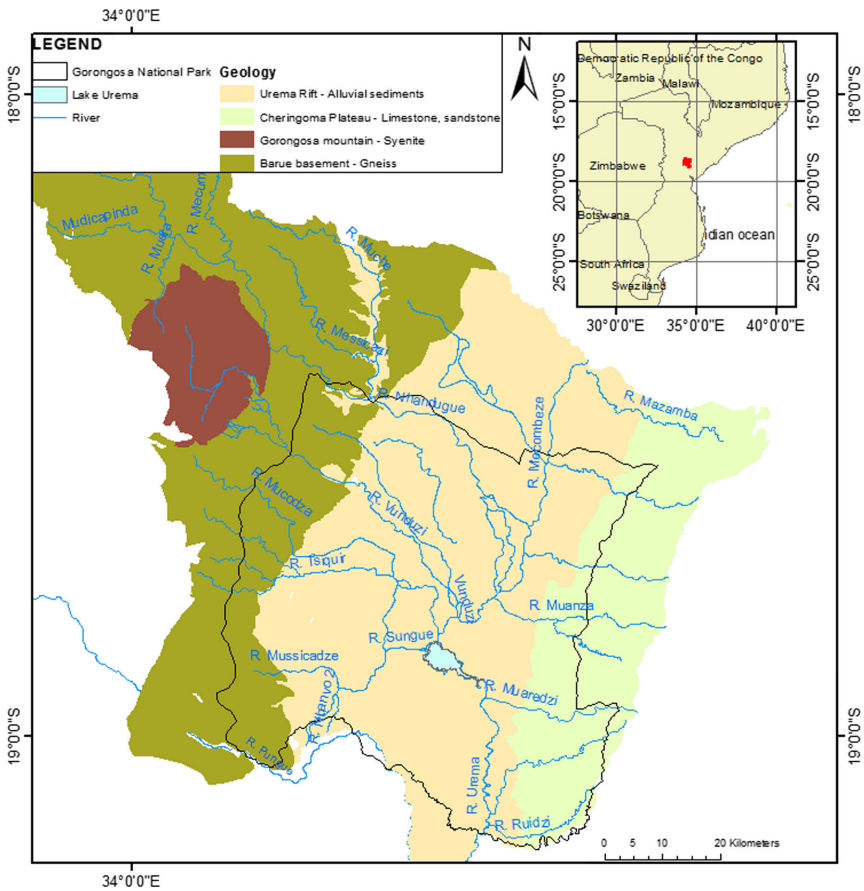

Fig. 1 Stratigraphical units of the Urema Catchment (from Steinbruch 2010)

margin from the Barwe platform such as the Vunduzi, show a major decrease in stream valley size, suggesting reduction in stream flow, presumed to be due to groundwater recharge into the coarse clastic wedge at the rift margin. However, the significance of this finding for the recharge of Lake Urema has not been established, and there is no information on the hydrogeological link between the rift margin and the valley floor beneath Urema Lake.

A promising approach is offered by geophysical methods used in hydrogeological studies. These methods provide spatially distributed models of physical properties in regions that are difficult to sample using conventional hydrogeological borehole methods (Linde et al. 2006). Many physical properties are indirectly sensitive to the amount of water in the ground; however, some geological constituents (e.g. water and clay) have sometimes similar or overlapping physical properties. It is therefore recommended to use more than one method to acquire a more unique signature of different geological units (Garambois et al. 2002). This research tests a combination of magnetic resonance sounding (MRS) with electrical resistivity tomography (ERT) methods extending the length of the electric lines by applying the roll-along technique (Dahlin 2001). The aim is to investigate the hydrogeological conditions in the graben floor and the mechanism of groundwater–lake recharge. Auguring and field observation yielded additional surface and near-surface data to support the findings from the geophysical survey. This method was successfully used for the characterization of aquifers in the Vientiane Basin in Laos (Perttu et al. 2011) and for interpretation of evapo-transpiration measurements in Bénin (Descloitres et al. 2011).

Study area

This work was carried out in the Urema Graben, inside the GNP in Sofala province, situated in the central part of Mozambique. The Urema Graben is located in the southernmost extent of the East African Rift system. The Urema catchment covers an area of approximately 9,300 km^2 that includes three major landscape units: the Rift Valley floor, the Gorongosa Mountain massif and the Cheringoma escarpment (Fig. 1; Beilfuss et al. 2007).

There are many seasonal rivers from Gorongosa Mountains feeding the Urema Lake. The main rivers feeding the lake are the Vunduzi, Mucodza, Sungue, Nhandugue and Mecumbedzi. The rivers Vunduzi, Mucoza and Nhandugue join Mecumbedzi River before it reaches the lake, while the Sungue River goes straight to the lake (Fig. 1). The Urema River is the only out flow of the lake and it is a tributary of the Pungue River. The main Pungue River, which is also the name of the catchment, drains directly to the Indian Ocean.

The local geology consists of four major parts: the Barue basement, the Gorongosa Mountain, the Urema Rift Valley and the Cheringoma Plateau forming the Urema catchment (Steinbruch 2010; Fig. 1). The Barue basement consists of granitic Precambrian rocks, and the Cheringoma Plateau consists of limestone and sandstone of Sena formation. Alluvial sediments cover the Urema Rift floor. The W–E cross section of the Urema Rift Valley is about 60 km and has a modest elevation variation between 14 and 70 m above sea level. The rift floor is almost flat with slopes below 1°, thus forming a water retention area. The sediments consist of heavy montmorillonite-rich clays and leached sands with different grain sizes with coarser sediments along the flanks. The mean grain size generally decreases when moving from the edges of the Urema Rift Valley towards the centre; however, along the major drainages within the Graben there appear to be channels with coarser sediments (Steinbruch 2010). There also exists a Precambrian gneiss inlier in a tectonic window of the rift floor (Steinbruch 2010) and a thermal spring, Nhambita hot spring, occurring along the western rift border with a water temperature above 40 °C (DNA 1987; Steinbruch and Merkel 2008).

Böhme (2005) collected five sediment cores in the bottom of the Urema Lake. The thickness of cores ranges from 0.17 to 0.28 m and four different layers were described: a layer rich in organics, pure sand layer, medium sandy clay layer and pure clay. The identified particle sizes of the sediments were used for the interpretation of the geophysical data presented here. Böhme (2005) also measured the electrical conductivity of the lake water, which can serve as reference to understanding the geophysical data. The reported conductivity values of 2.6–17.5 mS/m for freshwater would correspond to an estimated soil's resistivity of 58–320 ohm-m, and thus indicate the presence of freshwater in the subsurface.

Methods

The study was carried out in the dry seasons in July 2009 and August 2012, where ERT with multi-electrode equipment (Dahlin 2001) was used to obtain an overview of the geology. ERT data were produced and analysed for coherent features such as layered sedimentary formations and discontinuities. MRS was conducted in 2012 in order to partially overcome the difficulties with data interpretation because of the lack of hydrogeological reference data in the form of borehole log archives. Sample site locations are shown in Fig. 2.

Electrical resistivity tomography

The resistivity data were collected using a version of the ABEM Lund Imaging System based on Terrameter SAS 4000 in 2009, using multiple-gradient array (Dahlin and Zhou 2006). A 400-m-long electrode spread of 81

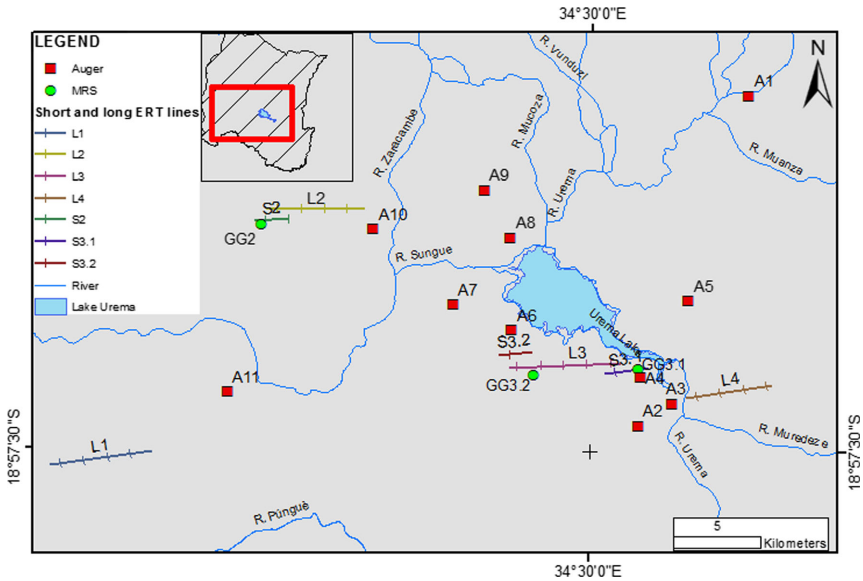

Fig. 2 Location of four long resistivity lines (*L1–L4*), three short resistivity lines (*S2*, *S3.1*, *S3.2*), three MRS sites (*GG2*, *GG3.1*, *GG3.2*) and 11 soil-auguring positions (*A1–A11*)

electrodes at 5-m separation was used for the measurements, and a roll-along technique was employed to extend the lines (Dahlin 2001). An ABEM Terrameter LS was used for the ERT data acquired in 2012. The length of the four ERT lines varied from 4,500 m in Muaredze up to 6,000 m in the power line clearing. The maximum depth of penetration of all profiles was around 75 m and was referenced in relation to mean seawater level.

The true resistivity was estimated through inverse numerical modelling (inversion). The software Res2dinv was used to generate a finite element model of a hypothetical vertical cross section through the ground and adjust the resistivity of each model cell until the apparent resistivity of the model response matched the data measured in the field (Loke et al. 2003). The difference between model response and measured data forms the mean residual which provides a measure of how well the model is fitted to the data. In this study the inversion was made using a robust constrain (L1-norm) because it performs better in handling noise in the data as well as strong resistivity contrasts compared to the otherwise used least-squares constrain (L2-norm; Loke et al. 2003).

The identified layers are labelled as 1, 2 and 3 from bottom to top. Each layer has indication of corresponding resistivity ranges as follows—X: less than 1 ohm-m; A: 1–10 ohm-m; B: 10–32 ohm-m; and C: above 32 ohm-m (derived from Palacky 1989 combining types of sediments and groundwater).

Magnetic resonance sounding

MRS is based on the principle of nuclear magnetic resonance. It indirectly measures the water content and the mean pore size, which in turn is related to the permeability of the ground (Shirov et al. 1991; Legchenko and Valla 2002). The instrument produces, by the steady increase of the current in the coil, scans of the MRS signal beginning at the soil surface to the limit of penetration in the subsurface.

The MRS measurements were carried out with the Numis-Plus Iris instruments using a 100 × 100 m coil with a maximum penetration depth of 100 m. Three sites were surveyed and analysed based on the least square solution with regularization with a smooth inversion using Samovar 11.3 software (Legchenko and Shushakov 1998). The result from an MRS is presented as free-water content (Φ_f) and decay time (T_2*; T_1) plotted versus depth. Free-water content is interpreted as non-adhesive water in voids per total rock volume and corresponds roughly to the effective porosity or the portion of water that is released under gravity or in the presence of a hydraulic head gradient (Lubczynski and Roy 2005). The decay time indicates connectedness of the pore space or how extractable groundwater is, and represents rock permeability (Lubczynski and Roy 2005). The MRS signal and penetration depth are highly influenced by the resistivity of the ground (Perttu et al. 2011); thus, it is necessary to have a geoelectrical model for each site for correct interpretation of the data.

Soil auguring and indicator of vegetation

A regular hand auger with T-handle and 1-m extensions was used to drill small-diameter holes ranging from 0.83 to 4.0 m depth. The technique worked well to the uppermost groundwater-bearing formations below which further penetration was impossible because of collapsing formations. The drilling was conducted at 11 locations surrounding Lake Urema.

The vegetation was also used as ground truth. The expected vegetation in a flood plain and its variation due to water content gives an indication of grain size of the surface soil and saturation of the ground (Van Wyk and Van Wyk 1997). The variation of the vegetation only gives surface information not the information in the subsurface. Green grass is an indication of soil moisture, and dry grass is an indication of water content below the wilting point; forest landscape typically is an indication of presence of groundwater but at greater depth. Short grass is an indication of temporary water logged areas. Ana tree (*Faedherbia albida*) together with elephant grass (*Pennisetum thunbergii*) are indications of the fringes of margins of floodplains, while the Lala palm (*Hyphaene coriacea*) occurs in dry areas or in well-drained areas.

Results

From the total W–E width of the Urema Graben, four subsections, each of 4.5–6 km length, were measured with ERT and produced four resistivity cross sections. L2 and L3 are in the valley floor, whereas L1 and L4 are at the west and east flank, respectively (Fig. 1). The location of L1 was selected to detect the change in the West flank from basement to rift-filling sediments known from the geological map and boreholes located in the national park's sanctuary (Steinbruch 2010). The L1 line crosses two seasonal rivers and the riverbeds are characterized by fine materials such as fine sand and clay (Steinbruch 2010) and L2 is part of the current floodplain, which was suspected to be a part of an ancient lake because of the presence of many abandoned river channels. L3 is perpendicular to the lake outflow and was chosen to study the variation of sediments at the transition between the floodplain and ancient Pungue River fan, while L4 was chosen to identify structural or geological features that may control the Urema out flow (Tinley 1977).

MRS was carried out at three sites considered as hydrologically relevant based on the ERT results. Also additional short ERT transects were carried out together with the MRS survey in order to link both datasets with each other to obtain more complete hydrogeological images of the sites.

Resistivity results

Figure 3 presents all four lines surveyed in the study area with Fig. 3a showing L1 which is characterized by a forest landscape and lies between 32 meters above sea level (masl) in the western part and 38 masl, with a lowest point of 31.73 masl. The profile shows two horizontal resistivity layers (1C and 2A) of the inverted section of L1. 1B has a thickness of at least 45–60 m and occurs from the surface at 36 masl to the maximum depth penetration of −28 meters below sea level (mbsl) and 2C is a discontinuous layer with a thickness varying from 10 to 15 m and occurs from the surface to 17 masl.

L2 is situated in the flood plain of the Urema Lake and stretches for approximately 5 km in a W–E direction laying between 21 masl at the beginning of the line to 26 masl at the end. The surface consists of clay covered with short green grass in the distance interval of 0–1,000, 1,500–1,700, 2, 300–4,300 m and tall dry grass from 1,500 m to the endpoint. Three horizontal layers can be identified in the inverted section (Fig. 3b). Layer 1A is 40–60 m thick, occurs in parts from the surface at 21 masl to the maximum penetration of the method but is covered by layers 2X and 3C from 1,100 m to the end of the profile. The layer 2X also occurs in parts in the surface but in some spots is covered by layer 3C (Fig. 3b). The thickness of layer 2X is 5–15 m, which corresponds to a maximum depth of 4 masl. The top and discontinuous layer 3C has a thickness of 2–5 m and appears in pockets and L3 in Fig. 3c has three layers 1C, 2A and 3C.

The results of L3 are illustrated in Fig. 3c. The profiles lie between elevations of 18 masl at the beginning of the line to 23 masl at the end. The surface is occupied by dense vegetation with Lala palm trees, Ana trees and elephant grass. The typical soils supporting such vegetation have a relatively high resistivity. Small streams and wetlands are present in the first 1,000 m. After 2,500 m, the grass becomes dry and dry forest vegetation changes into predominately Lala palm trees, which are abundant from this point up to the endpoint at 4,900 m. The vegetation beyond the endpoint is different, with Ana trees typical around the edges of floodplains and without grass. Three horizontal layers can be identified in the inverted section of L3 (Fig. 3c). The layer 1C was detected at depth of −39 mbsl and due to depth limitation the thickness of this layer in unknown. The layer 2A is 35–60 m thick and it can be observed in the surface from 900–1,000 m and from 1,700–1,800 m of the profile L3 (Fig 3c). The separation of 2A and 3C varies at depth, from 21 to 13 masl; 3C has a thickness varying from 3 to 10 m.

L4 (Fig. 3d) is parallel to the Muaredze River and it extends 4,400 m along the line (see Fig. 3), at an elevation that increases from 19 masl at the beginning of the line up to 89 masl at the end. The line starts at the eastern margin of the Urema River near the park's ranger station and goes along a mud road from W–E. The vegetation along this transect consists of

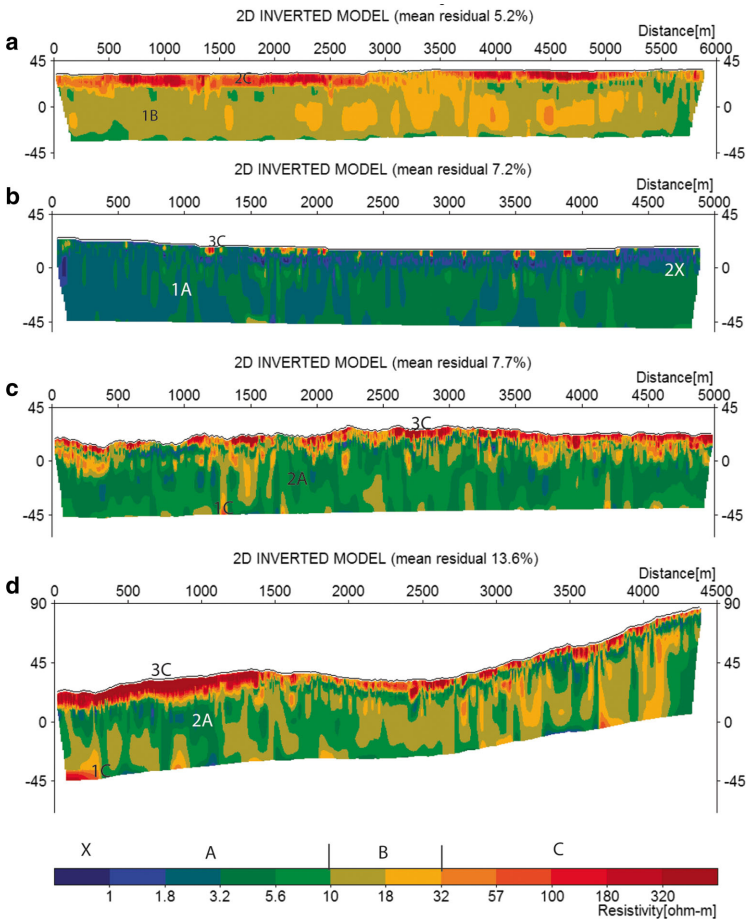

Fig. 3 Four ERT lines showing the length and resistivity values: **a** Line L1, **b** Line L2, **c** Line L3, **d** Line L4. Resistivity values—*X*: less than 1 ohm-m, *A*: 1 ≤10 ohm-m, *B*: 10 ≤32 ohm-m and *C*: 32–320 ohm-m

dense forest. Some depressions were observed at 1,400, 1,500 and 2,900 m, and a dried pond was crossed from 3,600 to 3, 700 m (Fig. 3d). Three horizontal resistivity layers are identified. At the bottom occurs a thick layer 1C which is at depth of −45 mbsl and its thickness is unknown due to the limitation of the methods. 2B is a layer, with a thickness that varies from 45 to 60 m, that is covered by 3C, which covers all the surface and has a thickness that thins from the beginning of the profile to the end.

MRS results

Figure 4 shows the results of the MRS at three different sites, indicated in Fig. 2. The fitting error (mean residual) ranges from 1.3 to 3.9 nV and thus suggests an acceptable quality of the inversion results. The free-water contents and decay times vary for each investigated site, indicating the presence of a diverse lithology across the Urema Graben floor.

The GG2 MRS measurement was made at the beginning of line L2 (Fig. 4a) with an elevation of 21 masl. Three evident layers can be identified from MRS. A shallow layer reaching from 2–3 m depth to 10 m depth with a free-water content of 7–10 %. The second layer from 10 m depth to about 30 m depth, has a free-water content of about 5 %. The layer below 30 m depth has a lower water content of about 7 %. No big variation was observed in decay time T_1 except from 2 to 3 m depth, which is in line with the variation observed in water content. MRS measurement GG3.1 (Fig. 4b), located at the end of line L3 (Fig. 2) with an elevation of 30 masl, is similar to the findings from the ERT of L3. It also shows three distinct

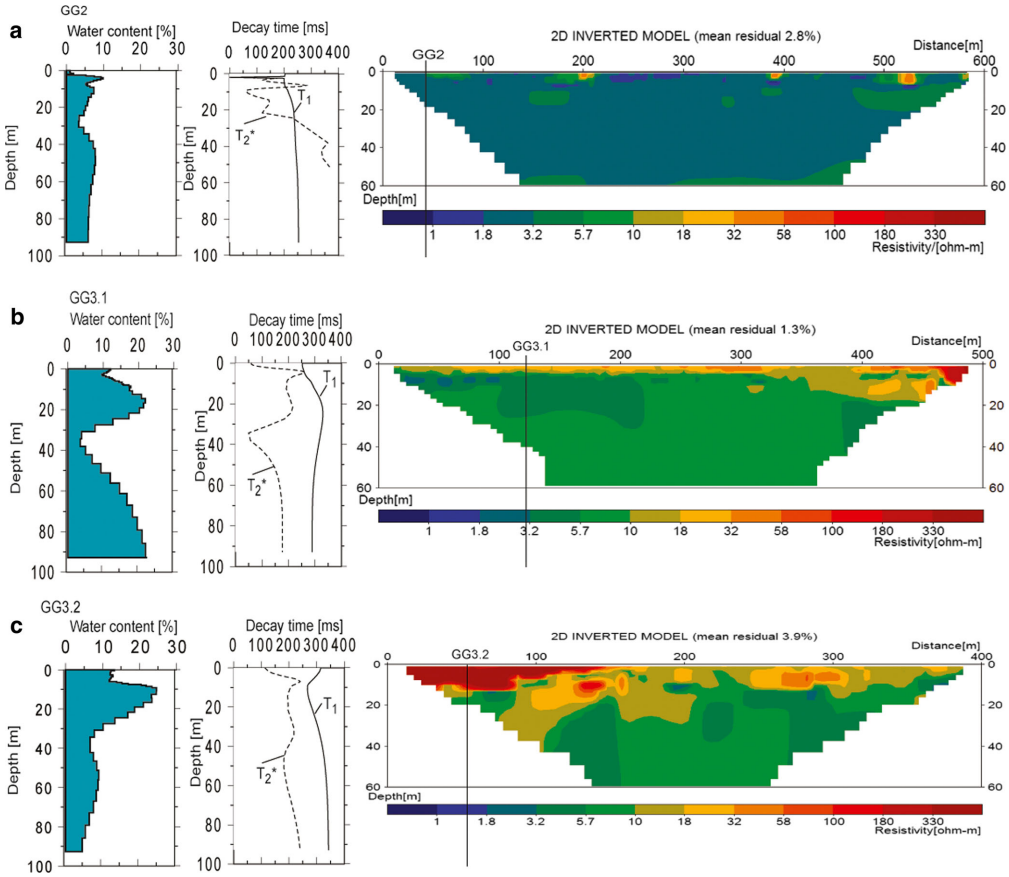

Fig. 4 MRS at points **a** GG2, **b** GG3.1 and **c** GG3.2 showing the water content, water content inversion fit, decay time and its position at the short ERT lines S2, S3.1 and S3.2, respectively (locations indicated in Fig. 2). It should be noted that the T_2* values vary greatly, but are more reliable for higher water content

layers: a shallow surface layer with a water content reaching 22 % with a thickness of 30 m; a second layer stretching from 30 to 40 m depth with less than 5 % of mobile water; and a third layer from 40 m depth with water contents which increase steeply by depth from 5 to 22 %. The decay time T_1 increases from 250 to 350 ms at 15 m depth and then decreases again to 250 ms; T_2* is similar to water content variation. The third sounding was made in the floodplain at the beginning of L3 (CG3.2, Fig. 4c). Four layers were identified with MRS. The topmost layer reaches from 0 to 8 m depth (10–18 masl) with a water content of 10–15 %. The second layer from 10 masl to −12 mbsl depth, has a water content of around 25 %. This layer is followed by the third layer stretching from −12 to −45 mbsl depth with a water content of almost 5 % (Fig. 4c). The water content increases below −57 mbsl depth downward to about 10 % forming the fourth layer. The decay time T_1 reduces from 325 to 250 ms at 10 m depth (20 masl) and increases again to 325 ms; T_2* is similar to water contend variation.

Results from augers

For the ground truth, 11 augurings were carried out in different locations on the Urema floodplain in August 2012. The equipment used is a regular hand auger with T-handle and extensions of 1 m each. The technique works well before reaching the groundwater level, but below that, sandy horizons collapse and prevent further penetration. The common characteristic of

the floodplain is the first 25 cm of clay. The sand layer, where it was found, follows this thin clay layer.

Table 1 summarises the results of auguring in 11 sites along the floodplain where the depth penetration varies from 0.83 to 4 m. The water table was measured when it was stable and it varies from the surface to 3.19 mbs. In the middle of the flood plain, all the auger holes indicate clay as the main sediment type at shallow depth.

Discussion

The study was limited to a transect crossing the Urema floodplain, inside the conservation park, by means of four profiles and three MRS. Additionally the Urema floodplain lies in the southernmost part of the East African rift system. An interpreted conceptual model is presented in Fig. 5. The following can be inferred about the geology, depositional environment and hydrogeology.

Geological interpretation

The coarse sediments, which have high resistivity values, are present in the study area with high free-water content (22 %) and labeled as layers 1C and 3C. The coarse sediments layer has resistivity values typical of coarse to medium sand. The value of 32 ohm-m was also observed in other studies (Arvidsson et al. 2011; Descloitres et al. 2011; Perttu et al. 2011) for sand saturated with groundwater.

The fine sediments have low free-water content and resistivity values below 10 ohm-m. Sediments with this range of resistivity values were described by Arvidsson et al. (2011) as clay. This thick layer has been identified as clay in L2, L2 and L4. Auguring has detected a clay layer at the surface with less than 2 m thickness, which was not detected by MRS. A mixed layer observed only at L1 is interpreted as a mixing of fine sand, silt and sand, having an intermediate value of resistivity.

Depositional environment

The depositional processes in the study area are closely linked to rifting activities and deformation during Tertiary times (Fonseca et al. 2014). The Mesozoic rifting is linked to the breakup of the ancient supercontinent Gondwana, culminating with extrusion of sheets of basaltic lava. The Cretaceous to recent sediment layers overlie this basaltic basement. The epicentral location of micro-earthquakes in central Mozambique delineate a NNE–SSW linear pattern which was described by Fonseca et al. (2014) as a normal fault with a strike of N31E, which would be active (Lächelt 2004).

These tectonic activities are in line with the sequential deposition of coarse sediment after a faulting event or uplifting, with fine sediments deposited when the gradient has dissipated. It may also explain the variation observed between L1 and L2 that suggests a fault. As consequence of a possible fault, coarse sediments (3C) were deposited on top of layer 1A at L2 (Fig. 3b). The deposition indicates a change in gradient upstream.

Hydrogeological implication of the geological results at Urema floodplain

The correlation of the ERT profiles and MRS (Fig. 5) are believed to give an indication of four hydrogeological units at Urema floodplain. The first confined aquifer labeled as 1C has high water content (22 %), which is an indication of high permeability. The thickness of this layer is unknown because of the limitation of depth penetration of both ERT and MRS. The second hydrogeological unit is an aquitard labeled as 1A and 2A with low free-water content (5–10 %), indicating low permeability. This layer confines the aquifer 1C and partially

Table 1 Characteristics of 11 boreholes augured around Urema floodplain

Augered borehole name	Surface elevation (masl)	Borehole bottom elevation (masl)	Borehole depth (mbs)	Water-table depth (mbs)
A1	16	13.67	2.33	2.06
A2	19	18.17	0.83	0.83
A3	16	13.37	2.63	1.63
A4	15	12.3	2.7	2.03
A5	15	13.22	1.78	-
A6	11	7	4	-
A7	11	9	2	-
A8	14	12.06	1.94	1.84
A9	17	13.35	3.65	3.19
A10	19	15.35	3.65	-
A11	20	18.32	1.68	1.33

Elevation is given as masl and depth is given as mbs

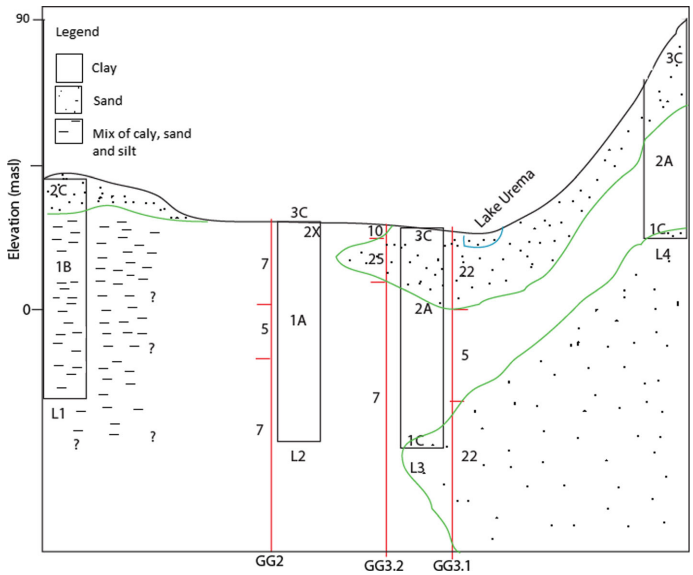

Fig. 5 Conceptual model of the Urema floodplain. No horizontal scale. *GG2*, *GG3.1* and *GG3.2* are the names of MRS measurement sites and *L1*, *L2*, *L3* and *L4* are the position of ERT profiles

the aquifer 3C. The third unit is the aquitard labeled as 1B. The extension and the thickness of this layer was not found due to limitation in depth of the ERT method. The fourth hydrogeological unit 2C is a semi-confined-to-confined aquifer. The variation in groundwater levels observed during the auguring is an indication of semiconfinement. The lake Urema is a part of this aquifer and may act as a recharge/discharge area for the semi-confined aquifer, depending on the seasonal variation in surface-water levels.

Uncertainties

L1 crossed the boundary fence of the sanctuary but there is no indication in the results of disturbances of this electrified fence. Due to dense forest, lines L1 and L3 were not completely straight, which leads to errors in the inverted model sections (Dahlin and Zhou 2006), but these are judged to be insignificant in relation to the resistivity variation. The levelling of all long ERT lines was done after the resistivity measurements and it is possible that some mismatches in positioning might have occurred.

The lack of reference data from drilling documentation and hydraulic tests is a problem, and a few boreholes in suitable locations would reduce the uncertainties for the interpretation of both resistivity and MRS results. Furthermore, both geophysical methods as configured in this study suffer from limited depth penetration and the decreasing of resolution with depth. MRS has, however, fairly good depth information for the study presented here.

Conclusions

Combined ERT and MRS geophysical investigations at Urema flood plain have been performed. Additionally auguring and vegetation description was performed to help the interpretation of geophysical data. As a result, four hydrogeological unites were identified. The thickness of the confined aquifer 1C was not determined in this study. The lateral separation of 1A and 1B between lines L1 and L2 is unknown. The change in lithology suggests a fault that also explains the deposition of layer 3C at L2 due to change in gradient.

The major finding of this study is the indication of the second aquifer (1C) identified by both ERT and MRS. The lake Urema is a window of the first upper semi-confined aquifer (3C), while the lower aquifer (1C) is confined by a clay layer 30–40 m thick. The location and depth of this semi-confined permeable aquifer suggest that it is possibly linked to the Pungwe River (downstream). If that is true, then the Pungwe River could be a main source of recharge during the dry season. This is an important finding because if a dam or any other infrastructure is constructed upstream of GNP in this river, the groundwater level will decrease which is likely to lead to drying out of Urema Lake. As the lake is the only permanent water source, this would be a disaster to the ecosystem of the park.

The depth penetration, geological borehole logging, and reference bibliography were the main limitations of the study; therefore, a deep borehole to confirm the presence of a

confined layer would help to protect the wildlife in the case the lakes dries out, because this confined aquifer would be an option for water supply.

Acknowledgements The research was jointly funded by the Swedish Agency for Research Cooperation with Developing countries (SIDA-SAREC) and Minor Field Studies Scholarships (MFS). We thank Gorongosa National Park (GNP) and Eduardo Mondlane University for logistic support. Kristofer Hellman, Erik Sjöstand and Oskar Enkel were instrumental in carrying out ERT surveying, with the help of GNP staff. We also thank the associate editor John Gates, the reviewer Broder Merkel and an anonymous reviewer for constructive criticism, which improved the quality of the paper substantially.

References

Arvidsson A, Stenberg L, Chirindja F, Dahlin T, Owen R, Steinbruch F (2011) A hydrogeological study of the Nhandugue River, Mozambique: a major groundwater recharge zone. Phys Chem Earth 36:789–797

Beilfuss R, Steinbruch F, Owen R (2007) Long-term plan for hydrological research: adaptive management of water resources at Gorongosa National Park. Internal report, Gorongosa National Park, Mozambique, 26 pp

Böhme B (2005) Geo-ecology of Lake Urema/Central Mozambique, vol 14. Freiberg Online Geology, 112 pp. www.geo.tufreiberg.de/fog/FOG_Vol_14.pdf. Accessed April 2016

Dahlin T (2001) The development of electrical imaging techniques. Comput Geosci 27(9):1019–1029

Dahlin T, Zhou B (2006) Multiple-gradient array measurements for multichannel 2D resistivity imaging. Near Surface Geophys 4:113–123

Descloitres M, Séguis L, Legchenko A, Wubda M, Guyot A, Cohard JM (2011) The contribution of MRS and resistivity methods to the interpretation of actual evapo-transpiration measurements: a case study in metamorphic context in north Bénin. Near Surface Geophys 9:187–200

DNA (1987) Hydrogeological map of Mozambique, scale 1:1,000,000 and explanatory text. National Directorate for Water Affairs, Maputo, Mozambique

Fonseca F, Chamussa J, Domingues A, Helffrich G, Antunes E, van Aswegen G, Pimto L, Custódio S, Manhiça V (2014) MOZART: a seismological investigation of the East African rift in Central Mozambique. Seismol Res Lett 85(1):108–116. doi:10.1785/0220130082

Garambois S, Sénéchal P, Perroud H (2002) On the use of combined geophysical methods to assess water content and water conductivity of near-surface. Hydrol J 259:32–48

Lächelt S (2004) Geology and mineral resources of Mozambique. DGN, Maputo, Mozambique, 515 pp

Leeder MR, Gawthorpe RL (1987) Sedimentary models for extensional tilt-block/half-graben basins. In: Coward MP, Dewey JF, Hancock PL (eds) Continental extension tectonics. Geol Soc Spec Publ 28: 139–152

Legchenko AV, Shushakov OA (1998) Inversion of surface NMR data. Geophysics 63:75–84

Legchenko A, Valla P (2002) A review of the basic principles for proton magnetic resonance sounding measurements. J Appl Geophys 50(1–2):3–19

Linde N, Chen J, Kowalsky M, Hubbard S (2006) Hydrogeophysical parameter estimation approaches for field scale characterization. J Appl Hydrogeophys 71:9–44

Loke M, Acworth I, Dahlin T (2003) A comparison of smooth and blocky inversion methods in 2D electrical imaging surveys. Explor Geophys 34:182–187

Lubczynski M, Roy J (2005) MRS contribution to hydrogeological system parameterization. Near Surface Geophys 3:131–139

McCartney M, Owen R (2007) Technical note: hydrology of the Lake Urema wetland, Mozambique. Internal report, IWMI, Colombo, Sri Lanke

Owen RJ (2004) GM SAFMA hydrogeology condition and trend report: the millennium ecosystem assessment (MA). Mineral Resources Centre, University of Zimbabwe, Harare, Zimbabwe

Palacky G (1989) Resistivity characteristics of geological targets, in electromagnetic methods in applied geophysics, vol 1. Society of Exploration Geophysicists, Tulsa, OK, 55 pp

Perttu N, Wattanasen K, Phommasone K, Elming S (2011) Characterization of aquifers in Vientiane Basin, Laos, using magnetic resonance sounding and vertical electrical sounding. J Appl Geophys 73(3):207–220

Shirov M, Legchenko AV, Creer G (1991) A new direct non-invasive groundwater detection technology for Australia. Explor Geophys 22:333–338

Steinbruch F (2010) Geology and geomorphology of the Urema Graben with emphasis on the evolution of Lake Urema. J Afr Earth Sci 58(2):272–284

Steinbruch F, Merkel BM (2008) Characterization of a Pleistocene thermal spring in Mozambique. Hydrogeol J 16(8):1655–1663

Steinbruch F, Weise SM (2014a) Analysis of water stable isotopes fingerprinting to inform conservation management: Lake Urema Wetland System, Mozambique. Phys Chem Earth 72(75):13–23

Steinbruch F, Weise SM (2014b) Characterization of the rainfall of Central Mozambique based on isotopes of water. In: Raju NJ (ed) Geostatistical and geospatial approaches for the characterization of natural resources in the environment: challenges, processes and strategies. Capital, India; Springer, Heidelberg, Germany, 187 pp

Tinley K (1977) Framework of the Gorongosa ecosystem. PhD Thesis, University of Pretoria, South Africa

Van Wyk B, van Wyk P (1997) Field guide to trees of southern Africa. K4P7-GJY-05G4, Struik, Cape Town, South Africa

Paper III

Hydrogeol J
DOI 10.1007/s10040-017-1540-1

REPORT

Improving the groundwater-well siting approach in consolidated rock in Nampula Province, Mozambique

F. J. Chirindja[1,2] · **T. Dahlin**[2] · **D. Juizo**[1]

Received: 17 June 2016 / Accepted: 6 January 2017

Abstract Vertical electrical sounding was used for assessing the suitability of the drill sites in crystalline areas within a water supply project in Nampula Province in Mozambique. Many boreholes have insufficient yield (<600 L/h). Electrical resistivity tomography (ERT) was carried out over seven boreholes with sufficient yield, and five boreholes with insufficient yield, in Rapale District, in an attempt to understand the reason for the failed boreholes. Two significant hydrogeological units were identified: the altered zone (19–220 ohm-m) with disintegrated rock fragments characterized by intermediate porosity and permeability, and the fractured zone (>420 ohm-m) with low porosity and high permeability. In addition to this, there is unfractured nonpermeable intact rock with resistivity of thousands of ohm-m. The unsuccessful boreholes were drilled over a highly resistive zone corresponding to fresh crystalline rock and a narrow altered layer with lower resistivity. Successful boreholes were drilled in places where the upper layers with lower resistivity correspond to a well-developed altered layer or a well-fractured basement. There are a few exceptions with boreholes drilled in seemingly favourable locations but they were nevertheless unsuccessful boreholes for unknown reasons. Furthermore, there were boreholes drilled into very resistive zones that produced successful water wells, which may be due to narrow permeable fracture zones that are not resolved by ERT. Community involvement is proposed, in choosing between alternative borehole locations based on information acquired with a scientifically based approach, including conceptual geological models and ERT. This approach could probably lower the borehole failure rate.

Keywords Vertical electrical sounding · Electrical resistivity tomography · Groundwater exploration · Crystalline rocks · Mozambique

✉ F. J. Chirindja
farisse.chirindja@tg.lth.se

[1] Eduardo Mondlane University, Maputo, Mozambique

[2] Lund University, Lund, Sweden

Introduction

For water supply projects in rural areas, groundwater is often the main water source because it is often ready to be used without any treatment (Macdonald and Calowb 2009); however, in consolidated rock areas, the aquifers often have low hydraulic yield and dry wells occur (Kellett et al. 2004). The consequence is a waste of time and resources and projects may be repeated in areas already included in previous water supply projects instead of extending to new areas that have not benefited previously. For example, the Integrated Water Supply and Sanitation Project for Nampula and Niassa Provinces (ASNANI) and Cabo Delgado and Nampula Rural Water Point Installation (CDNRWPI) program in Mozambique are two drilling projects implemented in the same communities in Nampula province. Based on the value of the yield, a borehole is either considered to be successful if it has a yield higher than 900 L/h or unsuccessful (failed) if the yield is lower. In both programs the reported unsuccessful or failure rate was between 25 to 35% (Salomon Lda, "Design report No. 2 for 250 water points". Internal unpublished report submitted to 'Millenium Challenge Account – Mozambique and the National Directorate of Water/Rural Water Department', 2010; hereafter referred to as "Salomon Lda, unpublished report, 2010"). The failure is reportedly related to geology, i.e. in unconsolidated rock areas the drilling success is higher compared to consolidated rock areas (Clark

Published online: 03 February 2017

1985; Salomon Lda unpublished report 2010). This research will focus only in consolidated rock areas based on the result of the CDNRWPI project.

The approach used in the CDNRWPI project was that each community indicated three different sites of their preference. Regarding the location of a new well, the geophysical investigations were carried out at these three sites to indicate the most favourable location for groundwater extraction. The investigation method chosen was vertical electrical sounding (VES), which assumes only vertical variation of the resistivity in the ground.

However in fractured and weathered consolidated rock areas, the lateral variation is often so strong that VES can be expected to give insufficient or even misleading results and ambiguities (Acworth 2001; Kellett et al. 2004; Kumar et al. 2007). Electrical resistivity tomography (ERT) can help to identify geological units and variation within lithological units which are highly significant with respect to groundwater in consolidated rock areas (Owen et al. 2005; Kumar 2012). ERT has been used to investigate groundwater in consolidated rock areas by many authors. Shemang and Chaoka (2003) investigated basement aquifer in Botswana, whereas Owen et al.(2005) and Muchingami et al.(2012) have investigated the groundwater in greenstone belt areas in Zimbabwe. In addition it is recommended that the magnetic resonance sounding (MRS) method, which detects free water content in the subsurface (Legchenko and Valla 2002), is used together with ERT (Vouillamoz et al. 2007) to reduce the uncertainties.

The aim of this study is to test whether the combination of both ERT and MRS methods can identify the reason of failure of groundwater wells sited based on investigation by VES. This is done by comparing the resulting geophysical models of unsuccessful boreholes with the models of successful boreholes; furthermore, the role of community choosing a favourable site is also discussed.

Background

Geological and hydrogeological setting

Mozambique is divided into two main geological structural regions, a Phanerozoic region and a Precambrian basement. The Precambrian basement is further divided into Archean cratonic units, Archean mobile belts and Proterozoic Units (Lächelt 2004). The Proterozoic Units consist of metamorphic rocks, quartzites, schists and gneisses along with interference of eruptive rock and dolerites. The rocks underwent pervasive tectonic reworking during the late Neoproterozoic collision orogeny at ca 550 Ma, known as the pan-African orogeny (Lächelt 2004). The eruptive rocks are weakly deformed Cambrian granites and granitoids with ages ranging from 514 to 504 Ma (Macey et al. 2013). The coastal area is constituted by post-Cambrian sedimentary rocks and Quaternary alluvial sand formations (Lächelt 2004).

The study area is situated in the Nampula Complex (Lächelt 2004; Thomas et al. 2011) or Nampula Block (Macey et al. 2013). Nampula complex is composed by Mesoproterozoic rocks that are classified as Mocuba Group (ca. 1,125 Ma meta-volcanic-plutonic rock assemblage), Rapale Gneiss (ca. 1,095 Ma intrusive orthogneiss), Molócuè Group (ca. 1,090 Ma supracrustal paragneiss, metavolcanic rock assemblage) and Culicui Group (ca. 1,070 Ma intrusive granitic orthogneisses) (Macey et al. 2013).

Figure 1 shows the main rocks in Rapale district representing the Mocuba (P2NMmd), Molócuè (P2NMa) and Culicui (P2NMga) groups. P2NMmd is banded biotite gneiss and migmatitic biotite gneiss with an age of 1,095±8 Ma, P2NMa is a variety of gneisses (ultramafic, mafic, amphibolic and metapelitic gneiss with an age of 1,090±22 Ma) and P2NMga is a variety of granitic gneiss (leucogranitic, streaky augen and augen granitic gneiss) with an age of 1,074 ±26 Ma. The Marrupula Group (Monapo complex) is composed of younger gneiss with age of 507±7 Ma and locally covers the Nampula complex's rocks. The hills are outcrops of rocks that resisted the erosion process, known as inselbergs. The eroded sediments were deposited in valley and plain areas covering the basement.

The Mesoproterozoic rocks have a low potential for groundwater production yielding less than 3,000 L/h (Salomon Lda, unpublished report, 2010). The groundwater occurrence and transport is controlled by fractures, fissures and weathered zones as in all consolidated rocks. In the Rapale district, there are three subclasses of discontinuous aquifers labelled as C1, C2, and C3 (Fig. 2). In areas classified as C1 subclass, there are local aquifers in the weathered migmatite gneiss complex, where the yield will not exceed 5,000 L/h. C1 aquifers are mainly shallow, but they can reach about 40 m in depth, while C2 is similar to C1 but with less developed weathering and the thickness of aquifer reaches 20 m and the possible yield will not exceed 3,000 L/h. The subclass C3 is an aquifer with limited groundwater situated in the gneiss-complex and the expected productivity is under 1,000 L/h (Salomon Lda, unpublished report, 2010).

Weathering process

Weathering can be described as the breakdown of materials, caused by mechanical or chemical processes generated by the climate (Acworth 1987). A weathered zone can be described as a zone where rock has degraded into smaller particles such as clay, sand, gravel and stone. In tropical climates, the chemical weathering is dominant, while mechanical weathering dominates in desert and polar areas.

Figure 3 describes the subsurface of a weathered crystalline rock in tropical areas. The weathered rock can be divided into

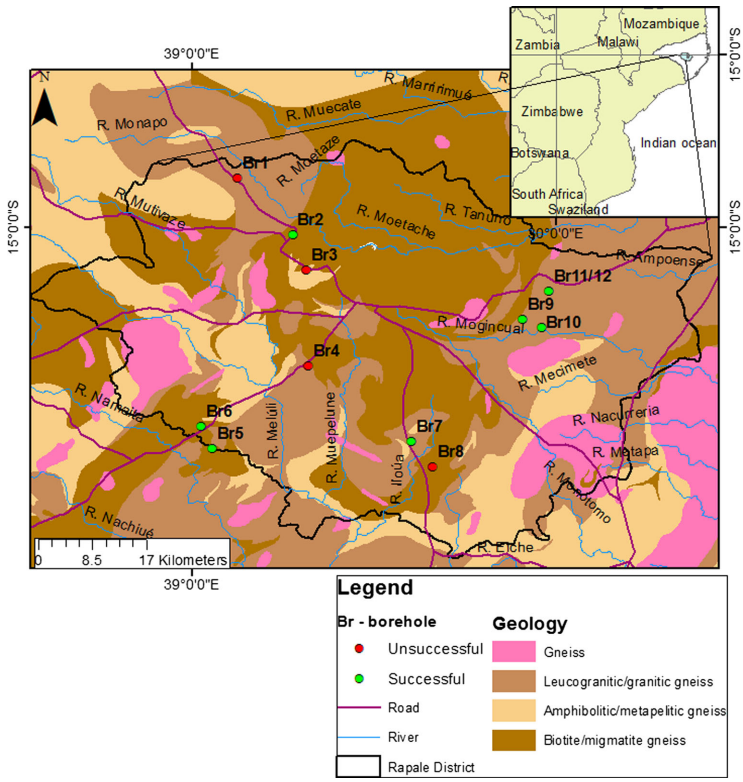

Fig. 1 Geology of Rapale District and the surveyed boreholes. *Br1* Passala, *Br2* Cuhare B, *Br3* Namitatari, *Br4* Napari, *Br5* Murothone, *Br6* Incomate Sae, *Br7* Muriaze, *Br8* Namachilo, *Br9* Matibane, *Br10* Naholoco comunidade, *Br11* Naholoco EP1, *Br12* Naholoco EP2

three different soil horizons (soil A, B and C) that vary in thickness and weathering degree, but not in order. Soil C can be subdivided in four zones (a–d). To contain aquifers, the weathered profile requires a certain areal extent and thickness, together with a sufficient permeability and thickness, to be able to yield groundwater to extraction points (Acworth 1987).

The most favourable condition for groundwater extraction can be found in zone c and d (Fig. 3), where the permeability is relatively high, together with high porosity. The most productive boreholes are those passing through at least 10 m of zone c and that intersects the fractures in zone d. Zone b could be an aquitard or a confining layer depending on its thickness and the hydraulic conductivity. Thus if the layer c is overpumped, some recharge can occur from the aquitard and from fractured zone d (Acworth 1987).

Well siting and vertical electrical sounding (VES)

For the site pre-investigation carried out prior to drilling, VES was used to identify suitable borehole sites (Salomon Lda, unpublished report, 2010). At each community a committee was created that was responsible for choosing three preferential places which were based on proximity to the community. VES was carried out at these three sites and the result used as basis for selecting which of these had the best potential to supply water. If the first option was not successful then the drillers would try the second and third option. Each borehole has a report with information of drilling rate, geological logging, casing and pumping tests. The drilling reports were used as reference material for interpretation of the ERT results and in comparison with the VES. A high number of unsuccessful boreholes are related to VES option No. 1, which is the first option of the community. It is an indication that the survey was based mainly on the community's preference, and not on geological conditions.

Figure 4 shows examples of some VES models of the pre-investigation. In general, 3–4 layers were identified with VES from which the range of 20–80 ohm-m is considered to have good conditions for drilling. Resistivity below this value was considered to be caused by saline water, while above this range it was considered as having too low a yield. Srivastava

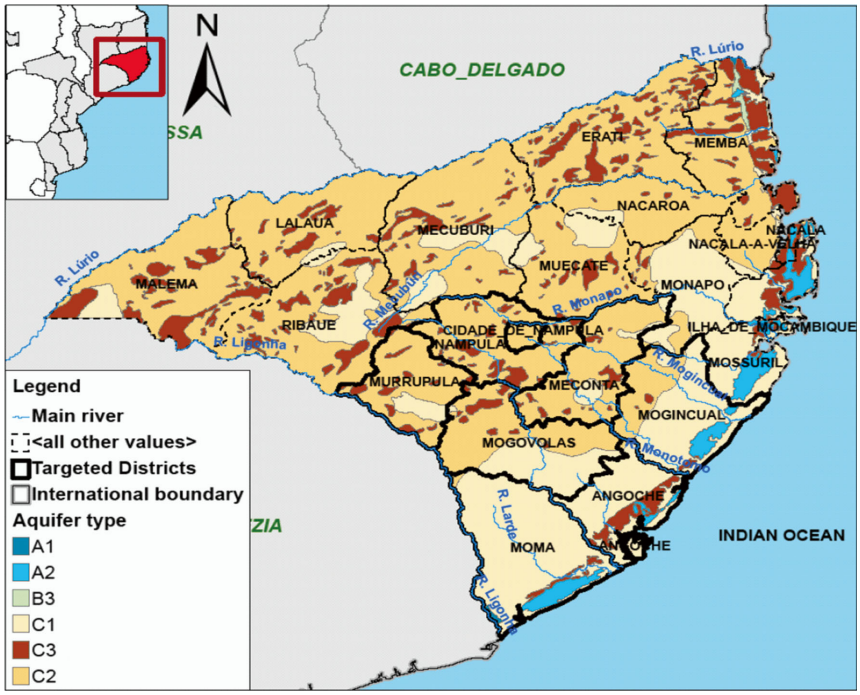

Fig. 2 Hydrogeological map of the Nampula province. Aquifer type A (*A1*, *A2* and *A3*) are continuous aquifers related to unconsolidated sediments and type C (*C1*, *C2* and *C3*) are discontinuous aquifers related to consolidated rocks. Rapale district is within the Cidade de Nampula borders (from Salomon Lda, unpublished report, 2010)

and Bhattacharya (2006) indicated a range of 100–300 ohm-m for weathered granite and a range of 300–600 ohm-m in fractured granite; in fact, Br10 (Fig. 4g) is a successful borehole with more than 80 ohm-m.

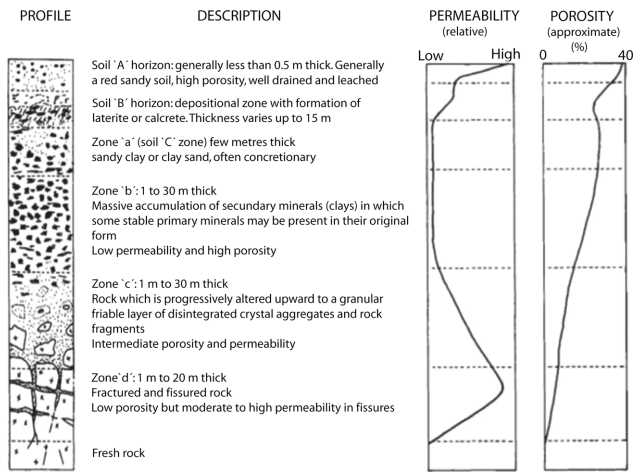

Fig. 3 A typical weathering profile describing the weathering of crystalline basement rocks (Acworth 1987)

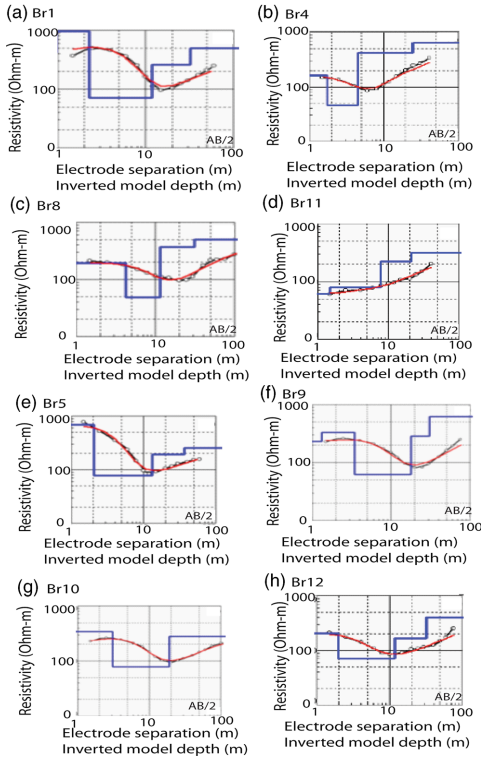

Fig. 4 Examples of VES models used to decide borehole siting (Salomon Lda, unpublished report, 2010). The *circles* indicate the measured values, the *black line* is the interpolation between the measured values, the *red line* is model response and the *blue line* is the inverted model. **a–d** VES here are unsuccessful boreholes, **e–h** VES are successful boreholes

Methodology

Borehole selection process

In total, 12 boreholes were investigated (Fig. 1). The selection of the investigation sites was based on the yield. Five unsuccessful boreholes that have a yield less than 600 L/h (Br1, Br3, Br4, Br8 and Br11), and seven successful boreholes that have a yield higher than 600 L/h (Br2, Br5, Br6, Br7, Br9, Br10 and Br12) were selected. The successful boreholes were subdivided in boreholes with high yield Br2, Br7 and Br12, intermediate yield Br5 and Br6 and low yield Br9 and Br10. Also Br12 was selected because it is located close to Br11. A profile connecting these two boreholes would give a better understating of lateral variation in resistivity between successful and unsuccessful boreholes.

Electrical resistivity tomography (ERT)

The equipment used for ERT in this survey is ABEM Lund Imaging System (Dahlin 1996). The ERT technique has proved to be versatile, fast and cost effective in delineating aquifers and mapping shallow subsurface anomalies (Kumar 2012). The information retrieved with this technique is crucial in planning for the groundwater exploration.

In total, 81 electrodes separated by 5-m spacing divided between four cables gave a spread of 400 m. Multiple gradient arrays were used throughout as they give a suitable combination of lateral and vertical resolution, and are well suited for multi-channel measuring thus making the field work time efficient (Dahlin and Zhou 2006). Data were collected by using a system based on a Terrameter SAS4000, ES10-64C switcher and 12 V battery.

A perpendicular cross with two 400-m survey lines was made close to each borehole, except in a few cases where physical restrictions limited it to one line. Additionally, a longer survey line crossing Br11 and Br12 with 900 m in length was intersected by two perpendicular survey lines, each 400 m long. All data were inverted with the Res2dinv software (Loke 1999) using robust (L1 norm type) inversion. The option for grid refinement, giving model cells with half the width of the electrode spacing, was used throughout.

Magnetic resonance sounding (MRS)

Magnetic resonance sounding (MRS) measures a magnetic resonance signal generated directly from subsurface water molecules (Legchenko and Valla 2002). The NUMIS acquisition system (IRIS instruments) was used, where the NUMIS instrument is connected to a computer, batteries and an antenna.

The decay signal obtained after switching off the excitation pulse is very sensitive because it has a low amplitude, of the order of tens of nano Volts (nV) (Plata and Rubio 2002). The decay signal is easily disturbed by (1) presence of anthropogenic noise in the area, (2) ambient noise from natural sources and (3) a small signal of the earth's magnetic field that easily drowns in noise.

Electrical power lines are the main source of the anthropogenic noise. Minerals, such as pyrite and chalco-pyrite common in granite and gneiss in forms of veinlets, are the main minerals that have magnetic properties. These minerals are important factors in determining relaxation rates and surface relaxivity (Keating and Knight 2010). Both relaxation rate and surface relaxivity will have influence on the variation of phase and frequency reducing the data quality of the decay signal.

Reference data

The reference data for interpretation of the geophysical results were based on the information collected in the

drilling reports and also the geological and lineament map. The lineament map shows the lineaments caused mainly by (1) tectonic faults, folds and fractures, (2) geomorphology features such as ridges and valleys, (3) displacement of ridge lines, scarp faces and river passages, and (4) pronounced breaks in crystalline rock masses and aligned surface depression (Sander et al. 1997; Mogaji et al. 2011). The lineaments were digitized from the geological map of the study area at a scale of 1:250,000 and classified as faults, folds and other lineaments. The drilling reports were produced for each borehole and have information about drilling rate, geological logging, water quality and pumping test results. The company that conducted the project has provided a copy of each report for this study (Salomon Lda, unpublished report, 2010).

Results and interpretation

Vertical electrical sounding survey

The pre-study in the EDNRWPI program was done basically with the VES method performed where the communities have chosen their three options. One field observation is that usually one of these three options coincides with the vicinity community leader's home. In a total of 16 unsuccessful boreholes in Rapale district, 10 are the first option of the community, 4 are the second option and 2 are the third option. Clearly the third option had given few unsuccessful boreholes.

A summary of the VES model resistivity values is presented in Table 1. The unsuccessful boreholes are marked as 'Un' and the successful as 'S'. Br1, Br6, Br9 and Br12 have 4 layers whereas others have only 3. Based on the Acworth (1987) classification (Fig. 4), layer 1 is the soil or zone a with a thickness in range of 0.63–4.53 m and resistivity value in range of 85.6–892 ohm-m. The second layer is classified as zone b with a thickness in range of 1.33–20.6 m and resistivity value in range of 48.7–951 at Br6. The third layer is classified as zone c with a thickness in range of 9.56–23.6 m and a resistivity value in range of 62.2–543 ohm-m. The fourth layer is classified as a mix of the zone d and the basement with a resistivity value in range of 81.7–478 ohm-m.

Geological lineaments results

Over the last four decades many studies have employed lineament mapping as the core of the groundwater exploration work (Sander et al. 1997) with an important role in complex geology as in this study area. The density of lineaments intersection in the area is a good indication of groundwater presence (Mogaji et al. 2011) but fractures are often covered by the weathered layer, making them hard to detect. A limitation of this approach is the scale of the map because the geology varies significantly each meter and, by using a 1:250,000 map, one cannot locate the precise lineament position in the ground which calls for follow-up by geophysics in order to pinpoint the location of the fracture zone below the weathered layer.

The resulting map of digitized lineaments is presented in the Fig. 5. The successful boreholes Br9, Br10 and Br12 are well positioned in relation to a fault with WE direction and Br 7 is close to a fold. The most favourable places to site water wells is close to the end of the lineaments (Sander et al. 1997; Owen et al. 2007) which is in line with the position of all boreholes; however, Br3 and Br4 are unsuccessful boreholes located close to the end of the lineaments.

Electrical resistivity tomography results

The ERT data were generally of good quality and the inversions resulted in good model fit with small deviations between model responses and measured data. The mean residual of all profiles ranged between 1.3 and 4.8% except in Br5 with 15.4% mean residual.

Successful boreholes surveyed

Figure 6 shows two examples out of several where low-resistivity layers match with productive wells (Br12 and Br10) and a high-resistivity layer matches with an unsuccessful well (Br11). Both sites show intermediate values of resistivity at the subsurface, followed by a low-resistivity layer and a high-resistivity layer at the bottom, respectively numbered as layers 1, 2 and 3 (Fig. 6).

The ERT model between Br11 and BR12 starts with a thin layer (1) at the surface, with intermediate resistivity values (220–770 ohm-m) to an approximate depth of about 0–5 m (Fig. 6a). Layer 2 has a low resistivity value (10–220 ohm-m) and thickness of 5–35 m (Fig. 6a), which could represent weathered to moderately weathered rock material or zone c (Fig. 3). Layer 3 has relatively a high resistivity value (>120 ohm-m) representing P2NMga lithology (Fig. 1). The lateral variation of thickness of the layer 2 explains the success at Br12 and lack of success at Br11. Figure 6b shows an ERT model of Br10 with slightly low resistivity values for layer 3 when compared with the ERT model of Fig. 6a. This layer is interpreted as weathered layer or zones c and d. As indicated by geological borehole logging, the basement was not reached. The interpretation of VES for Br10 and Br11/Br12 (Fig. 4g,d,h) indicated three resistivity layers. In Br12, the drilling stopped at depth of 35 meters where the resistivity value is 70.6 ohm-m (Fig. 4h), which is in the range of layer 2 (Fig. 6a). The VES of Br10 also

Table 1 Summary of the VES model resistivities and their corresponding thickness (Salomon Lda, unpublished report, 2010). *Un* unsuccessful; *S* successful

VES	Borehole outcome	First layer		Second layer		Third layer		Fourth layer	
		Resistivity (ohm-m)	Thickness (m)	Resistivity (ohm-m)	Thickness (m)	Resistivity (ohm-m)	Thickness (m)	Resistivity (ohm-m)	Thickness (m)
Br1	Un	417	0.96	951	1.33	71.1	9.56	261	20.3
Br2	S	892	3.48	61.2	16.5	143	18.2	–	–
Br3	Un	189	2.44	85.6	20.6	186	14.2	–	–
Br4	Un	293	1.5	138	11.4	543	19.3	–	–
Br5	S	689	2.06	77.4	11.2	192	23.6	–	–
Br6	S	114	0.63	357	1.41	38.7	19.1	81.7	12.5
Br7	S	196	4.53	55.6	13	123	16	–	–
Br8	Un	193	4.22	48.7	7.19	365	20.2	–	–
Br9	S	231	1.32	332	2.14	62.2	14.5	285	12.6
Br10	S	207	0.88	343	2.2	78.5	16	–	–
Br11	Un	205	1.98	70.6	9.85	167	20.2	–	–
Br12	S	85.6	0.76	219	1.45	90.2	18	478	24.1

indicated 3 layers and the resistivity of 78.5 ohm-m (Fig. 4g), which is out of the range indicated in Fig. 6b (220–420 ohm-m).

Unsuccessful boreholes surveyed

When the layer 2 is not well developed and the basement is close to surface, a successful borehole is very unlikely. That is shown in the Fig. 7 where the layer 2 has a thickness of 10 m at Br4 and less in Br1 (Fig. 7b). From the ERT model of Br4 (Fig. 7a) the layer 1 is discontinuous with resistivity in the range of 220–770 ohm-m and thickness 10–12 m, the layer 2 is a continuous layer with intermediate resistivity in range of 19–220 ohm-m, and layer 3 has a resistivity value higher than 770 ohm-m. Br1 (Fig. 7b) also shows 3 different layers. The layer 1 is discontinuous with resistivity in range of 220–1400 ohm-m and thickness less than 10 m, the layer 2 is a continuous layer with intermediate resistivity in the range of 19–420 ohm-m, and layer 3 has a resistivity value higher than 770 ohm-m. The description of the borehole indicates that the layer 1 is dry sand and soil, the layer 2 is composed by clay, and layer 3 is granitic fresh rock. The description of weathered granite does not match with the ERT model .

In the Br4 model, layer 2 has good conditions for siting a borehole from 0 to 100 m and from 200 to 300 m (towards the east) due to development of the weathered layer. By using the

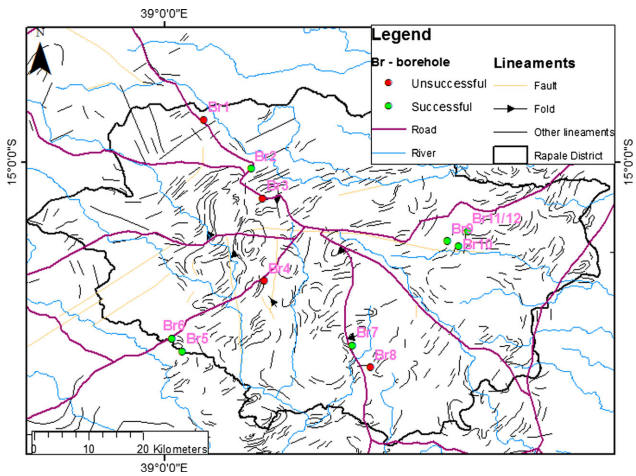

Fig. 5 Different lineaments at Rapale district and the position of both successful and unsuccessful borehole (adapted from Macey et al. 2006)

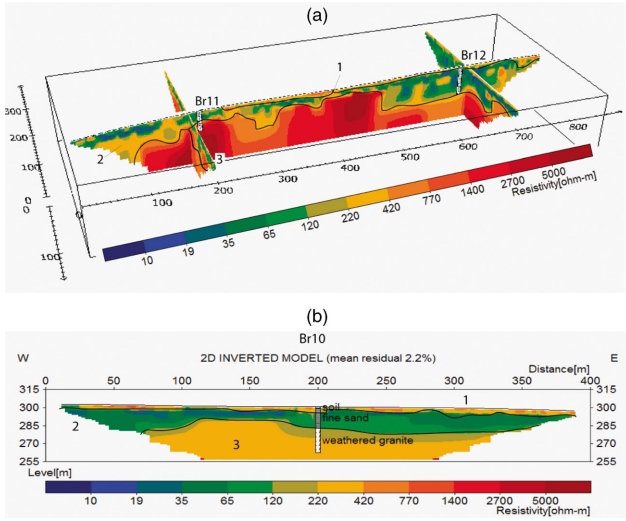

Fig. 6 ERT model of two sites at **a** Br11/Br12 and **b** BR10. The numbers *1*, *2* and *3* indicate the different geophysical layers. The length and depth scales in 6.**a** are given in meters

ERT method these areas could have been indicated as having potential to site a water well. Both VES (Fig. 4a,b) indicate that although the resistivity value is in range for a potential borehole siting, the thickness of this second layer is too thin (Table 1) to be considered as productive.

Exceptions to the expected geophysical models

Exceptions to the expected geophysical models are presented below; they display successful wells in areas where the geophysics would not lead to expectations of such wells.

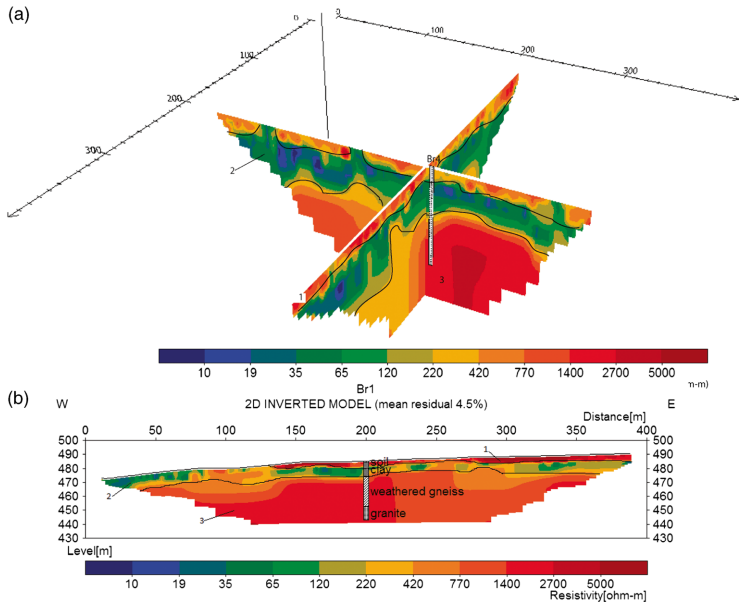

Fig. 7 ERT models of unsuccessful boreholes: **a** the model at Br4 and **b** the model at Br1

The borehole in Br8 is located in a zone with lineaments (Fig. 5) suggesting good conditions for a successful borehole but it turned out an unsuccessful one. Although the layer 2 is 20 m thick (Fig. 8a), the layer 3 has a low resistive value that is interpreted as highly fractured and therefore a potential site for drilling. The resulting models at Br5 and Br9 suggest unsuccessful boreholes due to a high resistive layer 3 and a thin layer 2 (Fig. 8b,c). In these two communities, the obtained models are similar to the unsuccessful borehole model Br4 (Fig. 7). However, they have a good yield and were considered as successful boreholes. As no lineaments were detected close to both boreholes (Fig. 5), a reasonable explanation would be that layer 3 (zone d in Fig. 2) has open fractures that increase the transmissivity. Possibly the fractures act as pathways for groundwater from surrounding zones with high porosity; however, the ERT cannot resolve relatively narrow fractures.

Magnetic resonance sounding (MRS)

MRS was performed at Br5 and Br6 (Fig. 1), where the earth magnetic field and primary porosity were small resulting in a weak signal from the water molecules. The measured magnetic field caused by solar radiation in the study area was 5,000 nV. This value is by far higher than the expected value of around 1,500 nV in this part of the world (Plata and Rubio; 2002), and it is too high to allow the measurement of good quality data over aquifers in granite and gneiss. The antenna loop was laid out in two different ways in attempts to improve the quality of measurements: square loop (100 × 100 m) and figure-of-eight loop (2 squares of 50 × 50 m each) respectively; however, the quality of data was not good enough to detect the decay signal pattern.

Geological setting for surveyed sites

Table 2 summarizes all the surveyed boreholes in terms of geology, yield and drilled depth. The geology is based on the map of Figs. 5 and 1, and the yield values were obtained from the drilling report of each borehole. The boreholes at Br1, Br3, Br4, Br8 and Br11 were dry and have no yield (less than 600 L/h) and therefore were interpreted as situated in a possible aquitard. Due to low yield (600 L/h), the boreholes Br9 and Br10 were interpreted as situated in a possible aquitard, while Br2, Br5, Br7, Br9 and Br12 were interpreted as situated in aquifers due to the high yield (more than 900 L/h).

Discussion

The task of siting a borehole for water extraction in consolidated rock areas is challenging and a proper approach should be considered. This study considered both social and technical issues that would lower the failure rate. Community participation in water-well siting has been proposed in water and sanitation projects (Glicken 2000) where the community should interactively participate throughout the process. This approach can improve results, since all proposed activities and

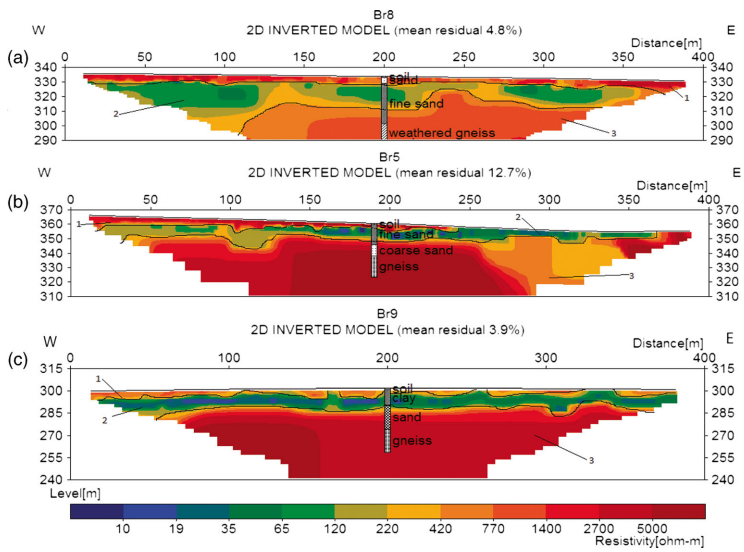

Fig. 8 ERT result of successful and unsuccessful boreholes in three different communities: **a** represents an unsuccessful borehole; **b**–**c** represent successful boreholes

Table 2 Geological and hydrogeological classification of each surveyed boreholes in Rapale District

Group	Symbol	Rock type	Borehole	Yield (l/h)	Drilling depth (m)	Hydrogeological classification
Culicui	P2Nmga	Augen gneiss, with charnockite	Br1	No yield	47.75	Aquitard
			Br9	600	47.65	Aquitard
			Br11	No yield	29.4	Aquitard
			Br12	1,960	45.42	Aquifer
	P2Nmal	Streaky augen leocogranitic gneiss	Br4	No yield	44.99	Aquitard
			Br5	1,200	38.44	Aquifer
			Br7	5,300	33.76	Aquifer
			Br10	600	38.61	Aquitard
Mocuba	P2NMmd	Hornblende-bearing granodioritic gneiss	Br2	1,920	45.9	Aquifer
			Br6	998	30.17	Aquifer
			Br8	No yield	38.46	Aquitard
	P2NMa	Amphibole, mafic gneiss	Br3	No yield	26.5	Aquitard

outcomes are well aligned with community's expectations. Although the results of this process are generally appropriate and sustainable, it is not a simple task. The effective participation is difficult to plan, implement and develop throughout the project (Juan et al. 2002). Many unsuccessful boreholes are related to the first option of the community, which often coincides with the community leader's house. The leaders have influenced the siting of the well close of their house aiming to control it. Using an alternative, scientific based, approach would most likely increase the success in groundwater-well siting, e.g. producing a map with indication of potential areas for siting boreholes based on results of pre-investigation and presented to the community to choose preferred sites.

VES was the geophysical method used in the well drilling project to assess if places selected by the communities had favourable conditions for drilling (Salomon Lda, unpublished report, 2010). The VES site selection was thus not based on geological criteria, which may have significant consequences for the outcome. The VES results did not give the precise depth to drill, therefore, all the unsuccessful boreholes were drilled to large depth when compared with the successful borehole except Br3. Probably the extra drilled depth is in attempt to find water; however, it has economic consequences because the driller is paid for each drilled meter.

By performing an ERT measurement that gives information of lateral variation around the drilled well, it was possible to detect, in several cases, the reasons for failure. The one obvious reason is the presence of high-resistivity zones that are caused by solid rock close to surface as shown in Figs. 6 and 7. Figure 6 illustrates well the difference in thickness and resistivity values of the boreholes at Br11 and Br12. The resistivity values of these resistive zones are higher than 220 ohm-m, which is in accordance with Owen et al. (2005) for granite rocks.

The interpretations of the resistivity values were based on the work of Palacky (1987), Acworth (2001) and Muchingami et al. (2012). As many common earth materials span large resistivity value spectra that overlap, and there are uncertainties on how well the interpretation of the results reflects reality; therefore additional information was used to improve the interpretation. Hydrogeological, geological and lineament maps were used as a base for plausible interpretation of the geophysical results in this study. The result is that granite and gneisses from Nampula block are the basement rocks in the study area.

The thickness of the weathered layer varies significantly at each borehole site but not the resistivity value, which is in range of 19–220 ohm-m. The ERT method could not resolve the precise limit of the weathered layer because the change is gradual. The variation of the resistivity values, from a high resistivity value of fresh rock to low values due to saturation with groundwater or presence of clay layer, was the only way to infer the lower limit. Available information about fractures and faults are on a regional scale, which makes it more difficult to assess the role of these factors and a mapping campaign at local scale would give more information to understand their role in groundwater occurrence. However, in some communities (Fig. 7) the groundwater is strongly controlled by the fractures and other lineaments.

The geophysical layers 2 and 3, in successful boreholes, are considered as unconfined aquifers. The layer 2 is the weathered zone, labelled as c according to Acworth (1987; Fig. 3) and layer 3 is the fractured zone labelled as d (Fig. 4). Due to low yield of Br9 and Br10 (Table 2), the geophysical layer 3 was interpreted as an aquitard. The spatial variation of these two productive units and the aquitard of Mocube Group is in accordance with the model described by Acworth (2001) that varies in 3D in terms of thickness and also the variation of its resistivity value.

Figure 9 shows the main features controlling the thickness of the main hydrogeological units in the study area. Faults and

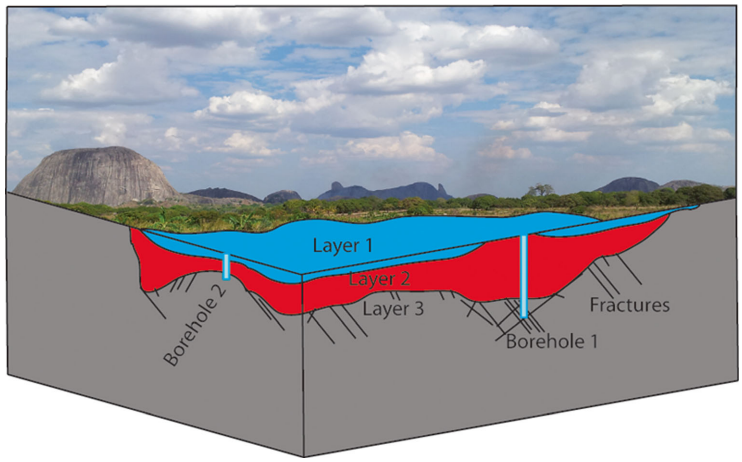

Fig. 9 The conceptual model illustrating the optimal location to site a water well (*borehole 1*) and an unfavourable place (*borehole 2*). *Layer 1* is the upper layer (soil A and soil B), *layer 2* is the soil C, and *layer 3* is the fresh rock

proximity to rock outcrops and the degree of weathering are the main factors controlling the groundwater occurrence. The larger the thickness of the weathered material or the more highly fractured the zone is, the more favourable it is to site a borehole there.

Several of the dry boreholes are placed on or just at the edge of the fresh rock. It is likely that if an ERT survey had been made instead of VES such a placement could have been avoided due to more comprehensive information on the 3D character of the geology: however, there are some successful boreholes placed on high resistive zones. The resistivity values suggest the boreholes may have intersected a fractured zone that is too small to be resolved by the ERT. The site at Br4 (Fig. 7a) is a good example of importance of use of ERT because it indicates that in the first 100 m of the profile there are good conditions to site a borehole.

The reason for successful/unsuccessful boreholes could possibly have been explained with MRS results with an indication of the amount of free water molecules in a specific site; however, the method did not work because the MRS signal-to-noise ratio (Perttu et al. 2011) was too low. The low signal level was caused by low intensity of earth magnetic field and low porosity of the unweathered rock; furthermore, the variation of magnetic field due to variation of rock properties gave a variation of the signal within the loop. The high noise level is mainly due to solar radiation (Vouillamoz et al. 2007). It can also be noted that even if the signal-to-noise levels would have more favourable, the results could have been difficult to interpret due to the strong lateral variation in aquifer properties shown by the ERT results.

There are some uncertainties in this study because of limited access to relevant reference data and uncertainty in the available reference data; however, it has been shown that a scientific approach including a conceptual geological model, comprising tectonic setting and weathering pattern, followed by ERT would improve the outcomes of the project. The CDNRWPI program drilled a total of 271 boreholes in Nampula province with a failure rate of 33%. The mean drilled depth is 40 m. The installation and removal, drilling operations and borehole construction costs, give approximately a rate of USD 100 per drilled meter. In total, around USD 4,000 was paid for each unsuccessful borehole, which is equivalent to a cost of USD 356,000 for all 89 unsuccessful boreholes. Even if taking into account the difference in cost for using a scientific approach and carrying out ERT instead of VES, the total cost is likely to be substantially reduced.

Conclusion

The geological structure of the investigated area is geometrically complex with vertical and lateral variations that can better be described by the ERT method compared to VES. The use of ERT could likely lower the failure rate of water wells if applied with a scientific approach and not using the community preference as base for where to do the investigation. MRS was tested but did not yield any useful results due to a combination of low signal levels, high noise levels and a laterally varying magnetic field.

The variation of resistivity values are in accordance with what can be expected from the local geology (granite and gneiss of Nampula complex) and resistivity values of different rock materials. The variation decreases from the surface downward crossing the zone with low permeability consisting of clay

and clayey materials and then increases from this zone down to the fresh rock where the highest values were recorded.

Two significant hydrogeological units were identified: one altered zone with disintegrated rock fragments characterized by intermediate porosity and permeability, and the fractured zone with low porosity and high permeability. The spatial variation of the units is controlled by the proximity to the unweathered basement, presence of faults and fractures, and the degree of weathering process. There is no direct relationship between rock type and the yield, which means that the thickness of the aquifer and the occurrence of open fractures are the most important factors.

The decision of the community members in siting borehole has to be based on a conceptual geological model and geophysical information that indicates potential areas for siting a borehole. This approach would reduce the influence of the leaders and reduce the failure rate as well. The potential areas for siting a borehole should be identified based on ERT surveys due to the complexity of the geology of the area. It is also recommended to perform geophysical borehole logging to collect information that can improve the interpretation of hydrogeological conditions.

Acknowledgements We would like to thank Cowater International Inc. and Salomon Lda for technical and logistical help for supporting the survey. We also would like to thank Eduardo Mondlane staff for all kinds of support during the survey and the (MFS) Minor Field Study students Erik Sjöstrand and Oskar Enkel. Furthermore we gratefully acknowledge that SIDA has funded the study as part of the bilateral cooperation framework between Eduardo Mondlane University (UEM) and Sweden. We acknowledge that Nils Perttu was responsible for the MRS field tests and ensured that these were made according to highest technical and scientific standards, and wish to thank him for the good cooperation.

References

Acworth I (1987) The development of crystalline basement aquifers in a tropical environment. Q J Eng Geol Hydrogeol 20:265–272

Acworth I (2001) The electrical image method compared with resistivity sounding and electromagnetic profiling for investigation in areas of complex geology: a case study from groundwater investigation in a weathered crystalline rock environment. Explor Geophys J 32:119–128

Clark L (1985) Groundwater abstraction from basement complex areas in Africa. Q J Eng Geol Hydrog 18:25–34

Dahlin T (1996) 2D resistivity surveying for environmental and engineering applications. First Break 14(7):275–283

Dahlin T, Zhou B (2006) Multiple-gradient array measurements for multichannel 2D resistivity imaging. Near Surface Geophys J 4:113–123

Glicken J (2000) Getting stakeholder participation 'right': a discussion of participatory processes and possible pitfalls. Environ Sci Policy 3: 305–310

Juan D, Gomez A, Afamia C (2002) Community participation in water and sanitation. Water Int 27(3):343–353

Kellett R, Steensma G, Bauman P (2004) Mapping groundwater in regolith and fractured bedrock using ground and airborne geophysics: case studies from Malawi and Brazil. In: Integrated exploration in a changing world; 17th ASEG-PESA geophysical conference and exhibition; extended abstracts. Australian Society of Exploration Geophysicists Petroleum Exploration Society of Australia, Sydney

Keating K, Knight R (2010) A laboratory study of the effect of Fe(II) bearing minerals on nuclear magnetic resonance (NMR) relaxation measurements. Geophys J 75(3):71–82

Kumar D (2012) Efficacy of electrical resistivity tomography technique in mapping shallow subsurface anomaly. J Geol Soc India 80:304–307

Kumar D, Ahmed S, Krishnamurthy NS, Dewandel B (2007) Reducing ambiguities in vertical electrical sounding interpretation. J Appl Geophys 62:16–32

Lächelt R (2004) Geology and mineral resources of Mozambique. DGN, Maputo, Mozambique, 515 pp

Legchenko A, Valla P (2002) A review of the basic principles for proton magnetic resonance sounding measurements. J Appl Geophys 50:3–19

Loke MH (1999) Res2dinv ver. 3.4 for Windows 3.1, 95 and NT. Rapid 2-D resistivity and IP inversion using the least squares method. Software manual. http://www.abem.se. Assessed April 2016

Macdonald A, Calowb RC (2009) Developing groundwater for secure rural water supplies in Africa. Desalination 248:546–556

Macey P, Ingram BA, Cronwright MS, Botha GA, Roberts MR, Grantham GH, de Koks GS, Maré LP, Botha PMW, Kota M, Opperman R, Haddon IG, Nolte JC and Rower M (2006) Map explanation: sheets 1537, 1538, 1539, 1540, 1637, 1638 and 1639-40 scale 1:250,000. Council of Geoscience, Pretoria, South Africa

Macey P, Miller J, Rowe C, Grantham G, Siegfried P, Armstrong R, Kemp J, Bacalu J (2013) Geology of the Monapo Klippe, NE Mozambique and its significance for assembly of central Gondwana. Precambrian Res 233:259–281

Mogaji KA, Aboyeji OS, Omosuyi GO (2011) Mapping of lineaments for groundwater targeting in basement complex area of Ondo State using remote sensing and geographic information system (GIS) techniques. Int J Water Resour Environ Eng 3(7):150–160

Muchingami I, Hlatywayo DJ, Nel JM, Chuma C (2012) Electrical resistivity survey for groundwater investigations and shallow subsurface evaluation of the basaltic-greenstone formation of the urban Bulawayo aquifer. Phys Chem Earth 50–52:44–51

Owen R, Gwavava O, Gwaze P (2005) Multi-electrode resistivity survey for groundwater exploration in the Harare greenstone belt, Zimbabwe. Hydrogeol J 14:8

Owen R, Maziti A, Dahlin T (2007) The relationship between regional stress field, fracture orientation and depth of weathering and implications for groundwater prospecting in crystalline rocks. Hydrogeol J 15:1231–1238

Palacky G (1987) Resistivity characteristics of geological targets. In: Nabighian M (ed) Electromagnetic methods in applied geophysics, vol 1. Soc. Explor. Geophysicists, Tulsa, OK, 55 pp

Perttu N, Wattanasen K, Phommasone K, Elming S (2011) Characterization of aquifers in Vientiane Basin, Laos, using magnetic resonance sounding and vertical electrical sounding. J Appl Geophys 73(3):207–220

Plata J, Rubio F (2002) MRS experiments in a noisy area of a detrital aquifer in the south of Spain. J Appl Geophys 50:83–94

Sander P, Minor TB, Chesley MM (1997) Groundwater exploration based on lineaments analysis and reproductibility tests. Groundwater J 35(5):888–894

Srivastava PK, Bhattacharya AK (2006) Groundwater assessment through an integrated approach using remote sensing, GIS and resistivity techniques: a case study from a hard rock terrain. Int J Remote Sensing 27(20):4599–4620

Shemang EM, Chaoka TR (2003) Two-dimensional electrical resistivity study of the basement aquifers of the Moshupa Wellfield area, Botswana. J Environ Eng Geophys 8:179–186

Thomas RJ, Ueda KM, Jacobs J, Matola R (2011) Late tectonic evolution of the Nampula Complex, NE Mozambique. In: 23rd Colloquium of African Geology, Johannesburg, South Africa, 8–14 Jan 2011, Geological Society of Africa, Addis Ababa, 395 pp

Vouillamoz JM, Baltassar JM, Girard JF, Plata J, Legchenko A (2007) Hydrogeological experience in the use of MRS. Bol Geol Min 118(3):531–550

Paper IV

Environ Earth Sci (2017)76:36
DOI 10.1007/s12665-016-6364-0

ORIGINAL ARTICLE

Reconstructing the formation of a costal aquifer in Nampula province, Mozambique, from ERT and IP methods for water prospection

F. J. Chirindja[1,2] · T. Dahlin[1] · D. Juizo[2] · F. Steinbruch[3]

Received: 25 October 2016 / Accepted: 23 December 2016

Abstract In continental margin basins, the hydrogeological setting is complex due to transgression/regression events that removed old sediments in the basin and formed new geologic units. Due to the geological complexity, the use of vertical electrical sounding has proven to be insufficient for groundwater explorations. The lack of understanding the geological underground has resulted in many boreholes with low yield or poor water quality. By performing electrical resistivity tomography (ERT) and induced polarization (IP) measurements in 11 villages in Mongicual district, three different layers covering the basement were identified: a weathered autochthon layer, a weathered allochthon layer (paleo-coastal dune) and eolian white sand layer. The drilling at successful boreholes penetrates formations where the resistivity value is between 220 and 770 Ωm, whereas at unsuccessful boreholes the lower parts of the drilled range have resistivity values higher than 770 Ωm. Also, the thickness ratio of the weathered and semi-weathered layer in the unsuccessful boreholes is less than 1/3, whereas in all successful boreholes the ration is higher than 1/2. The difference between autochthon and allochthon layers was detected by heavy minerals content in the red eolian sand layer (Tupuito formation) that increased the chargeability value. The groundwater with a conductivity higher than 2000 µS/cm is linked to the white eolian sand. The surface extension of white eolian sand layer is small to be mapped; therefore, by mapping the eolian white sand formation and the use of ERT and enhanced with IP method would lower the failure rate.

Keywords Electrical resistivity tomography · Hydrogeology · Induced polarization · Margin basins

Introduction

The majority of people in Mozambique lives in rural areas and only 29% in rural areas have access to an improved source of drinking water (AMCOW 2012). In response, the Mozambique Government embarked on the Rural Water Point Installation Program (RWPIP) in the provinces of Nampula and Cabo Delgado in northern Mozambique. During a period of 3 years, a total of 600 wells were installed including all facilities and sanitation costing approximately US$ 200 million (MCA 2013). The program had to deal with boreholes failing to supply fresh water. The failures are caused by very low yield in the crystalline basement areas as well as saline water in sedimentary formations located distant to today's coastal zones. An approach toward dealing with such reasons of failures will be presented in this paper.

The occurrence of groundwater in crystalline basement is controlled by the thickness of the weathered layer and fractures (MacDonald and Calowb 2008). However, it becomes complex when transgression/regression events form new aquifer systems on top of the basement along the continental margins. The basement aquifers in Africa have developed in Precambrian metamorphic and plutonic igneous rocks that occur in many Sub-Saharan countries (MacDonald and Calowb 2008) and are related to the various weathering-erosion cycles which have shaped the

✉ F. J. Chirindja
farisse.chirindja@tg.lth.se

[1] Lunds Universitet, Lund, Sweden

[2] Eduardo Mondlane Uninversity, Maputo, Mozambique

[3] Ara Centro, Beira, Mozambique

Published online: 30 December 2016

African continent (Clark 1985). Although these hard rock aquifers occur regionally, they are discontinuous and the thickness varies with the degree of weathering and exposure to processes of erosion (Wright 1992). Lateral variation in thickness is an important factor to the productivity of the wells (MacDonald and Calowb 2008). Continuity, thickness and preservation of the weathering profile of a productive basement aquifer determine the likelihood of success or failure of water drilling projects. It is therefore important to reconstruct the geological evolution of a particular area from the perspective of the potentials for the formation and preservation of aquifers.

Some ambiguity exists in the interpretation of vertical electric sounding (VES) results as for example, a low resistivity layer can be explained either by the presence of clay or the presence of saline water (Slater and Lesmes 2002).

The aim of this study is to reconstruct the aquifer formation in the study areas based on the results of geological and geophysical investigation. The obtained hydrogeological model would be used to explain the causes of borehole failures and suggest improved methodology to select drilling locations for future projects.

Study area

The study area

The study area is Mongicual district situated in the Eastern part of Nampula province of Mozambique, between Motomonho River to the North and Metomode River to the south, and bound by Meconta and Mugovolas districts to the West and the Indian Ocean to East (Fig. 1). The district is drained by Mongicual River where people go to fetch water. In this Mongicual River, the water dries out during the dry season when the groundwater level decreases. Wells will potentially provide water with improved chemical and bacteriological quality to people and provide water throughout the dry season.

Under the RWPIP, 40 boreholes were drilled in this district for ca 11,000 inhabitants which live widely scattered in family clans (Design Report 2010). The RWPIP designed that one borehole should supply water for approximately 500 inhabitants and have a water-yield of at least 900 l/h to be determined as sufficient for completion. A lower yield was defined as acceptable when less than 500 people in a community were served (Design Report 2010).

Regional geology

The study area is located at the transition of the Precambrian basement complex formed by Nampula and Monapo Complexes and a marginal sedimentary basin (Lächelt 2004). Nampula Complex is described as a complex of migmatite-granitoid group of rocks (Lächelt 2004) that belongs to the Mozambique orogenetic units with ages of 1100–850 Ma. These rocks outcrop in form of Inselbergs that are small residual hills which stand in isolation above the general level of the surrounding erosional plains (Singhal and Gupta 2010). The Mesoproterozoic rocks form the basement of a relatively small sedimentary basin in the study area (Allan et al. 1990; Macey et al. 2007).

This marginal sedimentary basin is evolved between two major Mesozoic-Cenozoic basins, Rovuma Basin to the North and Mozambique Basin to the South (Salman and Abdula 1995). They are formed as a result of the breakup of Gondwana and the formation of the Indian Ocean at the end of Mesozoic (Salman and Abdula 1995; Macey et al. 2013). In the study area, the intrabasin is shallow with less than 50 m depth increasing toward the Indian Ocean (Macey et al. 2007). The basement is covered by the Pleistocene allochthon weathered reddish brown paleocoastal dune ridge (Tupuito formation) in an east-facing slope described by Macey et al. (2007) as an erosional feature or Pediment (Singhal and Gupta 2010). The sand dune (Tupuito formation) was deposited during the transgressions in the late Pleistocene and Holocene in a coastal environment. The red color is a result of oxidation of iron and other heavy minerals (Macey et al. 2007). Oxidation is a part of chemical weathering process going on in this formation which resulted in a heavy mineral deposit in Moma district (Macey et al. 2007). However, the decreasing with depth of pH and magnetic susceptibility values suggest that the fersiallitic pedogenesis and weathering is most intense within the upper part of the soil profile (Macey et al. 2007). The Tupuito formation is covered by eolian white sand dunes and quaternary alluvial sediments composed by gravel, sand and clay (Macey et al. 2007).

Regional hydrogeology

The hydrogeological map of Mozambique, scale 1:1,000,000 derived from Ferro and Bouman (1987), shows three different quaternary hydrogeological units above the basement (pEG) (Fig. 1). The pEG is covered by the paleocoastal dune (QpE) constituted by fine to medium red sand, the eolian white sand (Qd) constituted by coarse to medium sand, and the alluvial clay and sand (Qal) (Ferro and Bouman 1987). Little is known about the fractured aquifers at a depth of >50 m. Fractured aquifers are all related to basement aquifers. According to Ferro and Bouman (1987), all Quaternary units are permeable and the yield measured from boreholes varies from 5000 to 10,000 l/h, whereas the basement unit has low permeability and the yield is less than 3000 l/h.

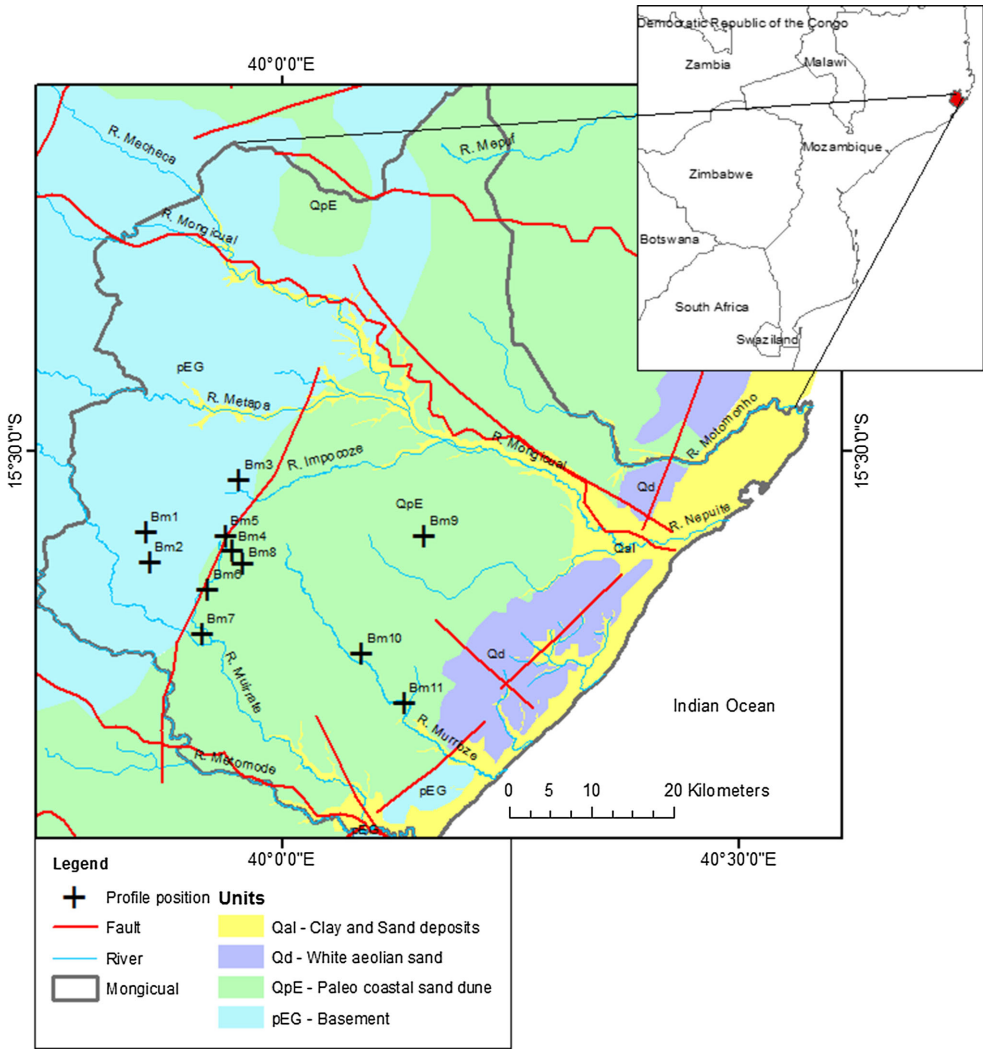

Fig. 1 Location of the research area (*red color*) and the hydrogeological map (adapted from Ferro and Bouman 1987) showing the positions of surveyed *lines* (Bm1–Bm11)

Hydrogeological processes

The hydrogeological setting of the study area is related to the evolution of sedimentary basins which are common in all East Africa. The evolution of these sedimentary basins was divided in two stages (Salman and Abdula 1995): (1) Gondwana stage comprised a period between 300 and 157 Ma ago (Late carboniferous to Middle Jurassic). This stage was characterized by the development of sedimentary basins within the single Gondwana continental mass. (2) Post-Gondwana stage beginning in Upper Jurassic 157 Ma and continuing to the present. This stage was a period of an

active breakup of Gondwana and the formation of continental margins of today's Indian Ocean.

Post-Gondwana stage was subdivided in three phases (Salman and Abdula 1995): (1) the breakup of Gondwana—during this period Gondwana split into two major blocks: West Gondwana (Africa and South America) and East Gondwana (Antarctica, India and Sri Lanka, Madagascar, Seychelles and Australia); (2) stabilization—comprised the stabilization of the East African continental margins accompanied by volcanic activities resulting in the deposition of thick volcanogenic and volcanogenic-sedimentary sequences; (3) neorifting—began 35 million years ago lasting till present.

In Oligocene, the African block rose, accompanied by marine regression. In the Miocene transgression the shallow-water marine environment was restored over a wide shelf. Active rifting of East Africa was also reflected along the continental margins. During Quaternary, the shallow-water shelf of the Miocene sea underwent regional uplifting and those sediments form presently outcrops on the coastal plains (Salman and Abdula 1995).

The Mesoproterozoic gneiss is the basement for the basin in the study area (Allan et al. 1990). The sedimentary cover is composed by eolian sand of different ages and fluvial deposits. The fluvial deposits of reworked gneiss in the West are composed of gravel sand and clay deposited in fluvial environment (Allan et al. 1990). The Valley of Mapane, Monotomo and Mongicual Rivers (Fig. 1) is well developed and cutting into Precambrian formations and therefore might be resting on a zone of weakness and being a river system that may have existed during Mesozoic.

Three hydrogeological units with different aquifer properties can be identified: the basement aquifer (pEG), red coastal dune ridge aquifer (QpE) and white eolian sand aquifer (Qd). pEG underlays the study area with outcrops to the West and plunging eastwards. The permeability depends on the fracture density and the thickness of the weathered layer. The yield is less than 3000 l/h and may reach 5000 l/h in favorable zones (Ferro and Bouman 1987).

The QpE extends over the entire survey area and it is expected to be a more productive aquifer because the permeability and porosity is likely to be high (Ferro and Bouman 1987). In such a case, the yield will depend on the thickness of this formation.

Qd consists of discontinuous units (lenses) controlled by the altitude which can be explained by the ongoing uplifting of Nampula block (Macey et al. 2007) as well as by the climate-controlled sea-level changes. The expected permeability and porosity is high and so the yield.

Rock decomposition and expected geophysical signal

When rocks are exposed to the earth atmosphere, weathering takes place. As a result, weathered and semi-weathered layers known as regolith (Kumar et al. 2016; Wright 1992) form on top of the bedrock (Fig. 2). The regolith is composed by duricrust, saprolite and saprock (Fig. 2) (Acworth 1987). The duricrust is a near surface layer composed of re-concentrated and undissolved minerals of Fe, Al and Si. Saprolite is composed of weathered products of the bedrock and precipitation of leached products from duricrust. At the base of the saprolite lies the saprock which is composed of large blocks of unweathered bedrock surrounded by a matrix of slightly weathered materials (Acworth 1987). The thickness and degree of weathered material are closely related to cycles of relative tectonic stability and the type of the primary rocks (Sharp 2014). In former Gondwana areas which had remained stable since Mesoproterozoic the regolith can extend to depths as great as 90 m for granite and gneiss (Strahler 1971). In the classical profile, the thickness of the weathered layer is 1/3–1/2 of the semi-weathered zone (Sharp 2014). A

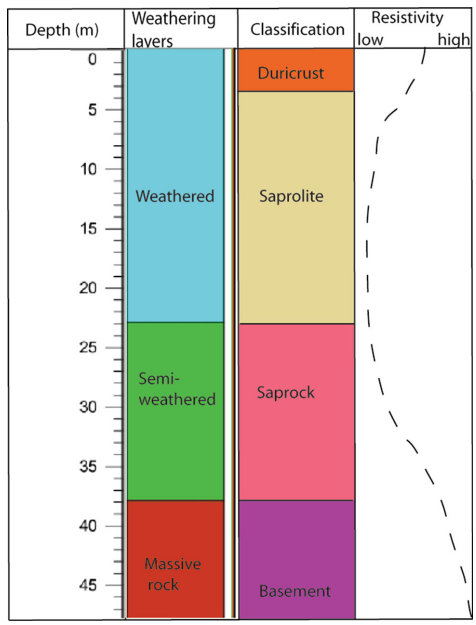

Fig. 2 An example of schematic weathering profile and tentative geophysical resistivity model of each zone. Adapted from Acworth (1987) and Kumar et al. (2016)

change in this ratio is attributed to the removal of the weathered layer by erosion or the addition of material by allochthon sediments.

According to Acworth (1987), soluble minerals are leached from the weathered layer (duricrust and saprolite) downward. The thickness of the weathered layer varies with the degree of weathering and it has high porosity and permeability. The semi-weathered layer (saprock) is characterized by an accumulation of secondary minerals formed in situ by ion exchange (smaller atoms by larger) and hydration (complexation) leached from the weathered layer. Therefore, the permeability and porosity will decrease in the uppermost part of this layer. The bottom of the semi-weathered layer is characterized by laminated fractures and fissures; hence, the permeability will increase and the porosity decreases.

Water percolating through the weathered material will leach all soluble chemical elements and moves clay fine particles present from the upper near surface and precipitate when the chemical conditions change. This process takes actively place at the boundary of the phreatic-vadose zone. As a result of this leaching and mineral precipitation, the initially favorable hydraulic conditions for an aquifer in the laminated fissure zone are lost (Sharp 2014).

The expected variation of resistivity values is presented in Fig. 2. High resistivity values are expected at the surface. Dry and unconsolidated coarse sediments have high permeability and porosity which yield a high resistivity value (Acworth 1987; Palacky 1988). The resistivity value decreases downward from the surface to saprolite due to compaction of the sediments that decreases the porosity, while the clay and water content increases. The resistivity values will increase again when moving from the saprolite layer to the basement due to reduction of weathered material. In the basement, the primary porosity and permeability are low and groundwater is found only in fractures. A reduced value of resistivity compared to the massive rock is expected when a fracture is struck.

Materials and methods of data acquisition

Boreholes: ground control points

The choice of drilling sites within RWPIP was based on VES results. In total 56 borehole were drilled from which 71% had enough yield for village water supply and were equipped as water wells. For each drilled borehole under the RWPIP, a report with information about the drilling rate, geological logging, well completion and water quality exists. The authors collected the reports of the 11 wells used as ground control sites to validate the ERT models. The center point of each ERT profiles was set to coincide with borehole position.

The choice to survey these boreholes was based on the fact that Bm1, Bm2 and Bm3 are located in basement and Bm4, Bm5, Bm6, Bm7, Bm8, Bm9, Bm10 and Bm11 are located in the basin filled with continental and marine sediments. Bm1 and Bm10 were abandoned, as negative well, because no water was found up to the depth defined by the drilling contract. Unfortunately as it often happens, log reports were not archived and water quality parameters not documented for the dry boreholes.

Field measurements and data analysis

In June 2014, combined ERT and IP measurements were made at drilling sites in 11 communities. Two perpendicular lines were measured at each site. The profiles were made perpendicular to describe the variation in three dimensions. At Bm4 only one profile was taken because the terrain was too rough to set the second profile. The lengths of each survey profile were 400 m with a depth penetration of around 70 m.

The used Terrameter LS measures both resistivity and chargeability. The instrument was connected to electrode cables with 5 m spacing between the electrodes. In total 81 electrodes were used which make a full spread of 400 m. The current is passed into the ground, and the potential is measured up to 12 channels which speeds up the measurements. The data were collected as 2D resistivity tomography using the roll-along system (Dahlin 2001). The survey was measured using a multiple gradient array which has an advantage in fast data acquisition with good signal to noise ratio, in combination with a good ability to resolve geological structure (Dahlin 2001; Dahlin and Zhou 2006).

The data quality was checked by visual observation of the pseudosection in Erigraph software and edited in Res2Dinv. After field data quality check, the data were inverted and produced 2D models using the software Res2Dinv. The model is an idealized mathematical representation of the measured subsurface (Reynolds 2011). Each model has information of both IP and resistivity. For the interpretation, the IP results were presented as normalized chargeability (MN).

Results and interpretation

Surface geology

Two sand formations (Fig. 3) were identified in the field and are also shown on the national level hydrogeological map. A white eolian Quaternary (Qd) sand formation

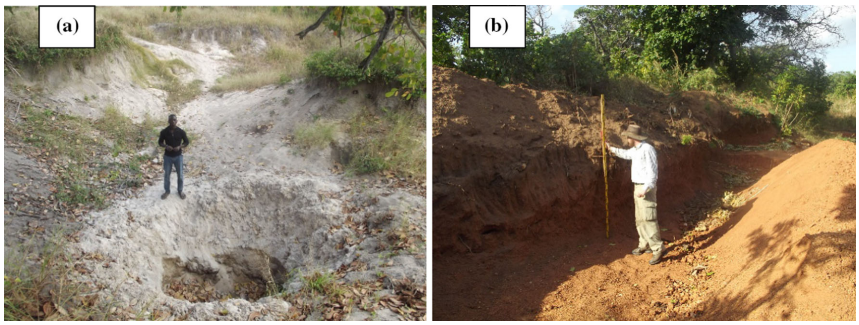

Fig. 3 Two different sand layers occur in the study area. **a** *White sand* close to Bm3 and **b** *red sand* close to Bm7

(Fig. 3a) was picked up in some areas at the scale of the national geological and hydrogeological maps while left out in others. Being the only map source available at this time, this cartographic principle (scale dependent simplification of map contents) probably caused the misinterpretation of previous geophysical results at local scale by the field team of RWPIP. A reddish sand formation (Fig. 3b) which is common in the study area is indicated in Fig. 1 as fossil dune of Tupuito formation (QpE).

Geological log

The comparison of the weathering profile thickness of surveyed sites based on the geological borehole logging report is presented in Table 1. The white sand layer is only present at Bm3, Bm6, Bm8 and Bm9 with a thickness varying from 7 to 25 m. The thickness of the weathered layer varies from 6 m at Bm1 and Bm9 to 29 m at Bm11 and the thickness of semi-weathered layer varies from 7 m at Bm9 to 31 m at Bm1 (Table 1).

The weathering profiles shown in bolded values (Table 1) had additional sediments placed on top of the weathered basement. The additional sediments are eolian white sand and red coastal dune ridge (Fig. 1). The italicized values indicates the boreholes with WL/SWL ratio less than 1/3 which is caused by erosion of the top weathered layer. It coincides also with the unsuccessful boreholes except Bm2.

Interpretation of geological and drill log

The drilling report includes the description of the cuts from the drilling on which the interpretation of the drilling log was based. The cuts were described in terms of color, texture and geological material. The spatial variation of the described geology was made by correlating boreholes in three different profiles.

Figure 4 shows the correlation of the surveyed boreholes in three different profiles AB, CD and EF directed W–E, N–S and NW–SE, respectively. The depth to the

Table 1 Thickness of different layers from borehole logging information and its relationship with the weathering profile of Fig. 2

Material	Thickness (m)										
	Bm1	Bm2	Bm3	Bm4	Bm5	Bm6	Bm7	Bm8	Bm9	Bm10	Bm11
Sand layer	0	0	***9***	0	0	***7***	0	***25***	***21***	0	0
Weathered layer	*6*	**17**	**12**	**24**	**25**	**12**	**12**	**10**	**6**	*7*	**29**
Semi-weathered layer	*31*	**25**	**9**	**9**	**12**	**9**	**8**	**15**	**7**	*28*	**16**
Basement	*23*	**3**	**3**	**0**	**0**	**15**	**25**	**2**	**11**	*10*	**5**
Total drilled depth	60	45	33	33	37	43	45	52	45	45	50
Bottom elevation (masl)	90	90	72	97	93	57	30	73	85	25	10
Ratio WL/SWL	0.19	0.68	1.33	2.63	2.12	1.33	1.50	0.66	0.86	0.25	1.81
Yield (l/h)	–	1200	1400	2800	800	1000	1500	800	1200	–	1100

Italics partially disturbed (removal/replacement with allochthon material), *bold* allochthon cover and *bolditalics* marine sediments. WL stands for weathered layer, and SWL stands for semi-weathered layer

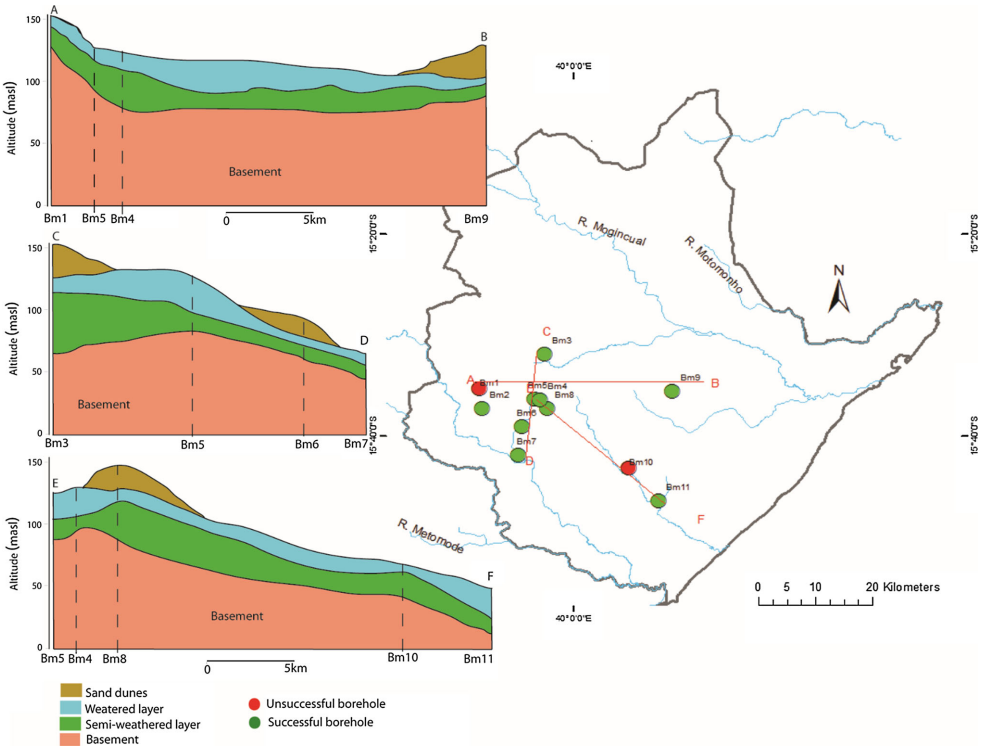

Fig. 4 Geological sections based on borehole logging from the ground truth points, and a map of the location of the boreholes and cross sections

basement is generally increasing eastward as seen in the profiles AB and EF (Fig. 4). Weathered and semi-weathered layers are continuous layers that are present in all boreholes. However, the thickness (Table 1) varies from borehole to borehole. The eolian white sand formation is a discontinuous layer that occurs on top of the weathered and semi-weathered layers. It mainly occurs above the 100 masl contour line.

Surface geophysics

Figure 5 shows all inverted ERT models and the position of the water wells that were used as ground truth. The L1 inversion method has been used as it gives a strong contrast in resistivity mainly between soil and fresh rock. The inverted models have a low residual error ranging from 1.0 to 2.4%. The perpendicular ERT models reveal similar variation in resistivity and thickness of the layers.

In the bottom of the models, there is a resistivity layer with resistivity value between 220 Ωm and more than 5000 Ωm which was interpreted as the basement. The strong lateral variation of the resistivity values within the basement is an indication of variation in depth of the weathered zone and degree of fracturing. This variation must be expected to have a profound impact on the occurrence of groundwater due to the variation in fracture density and secondary porosity.

The basement is overlain by a layer with a resistivity value in the range of 10–120 Ωm indicating a weathered zone. The thickness of this layer varies from 5 m in Bm6 to more than 60 m in some positions of Bm4 and Bm9 profiles. The near surface layer in the models shows high resistivity values ranging from 120 to 1400 Ωm indicating unconsolidated and dry sediments. The thickness of this layer is less than 15 m.

The target layer for water abstraction, as demonstrated by depth of the drilled boreholes (Table 1), has resistivity value in range of 220–770 Ωm. The borehole Bm4 with the maximum yield of 2800 l/h (Table 1) ends in a resistivity layer of 220–420 Ωm. Also for Bm2 and Bm9, the drilled

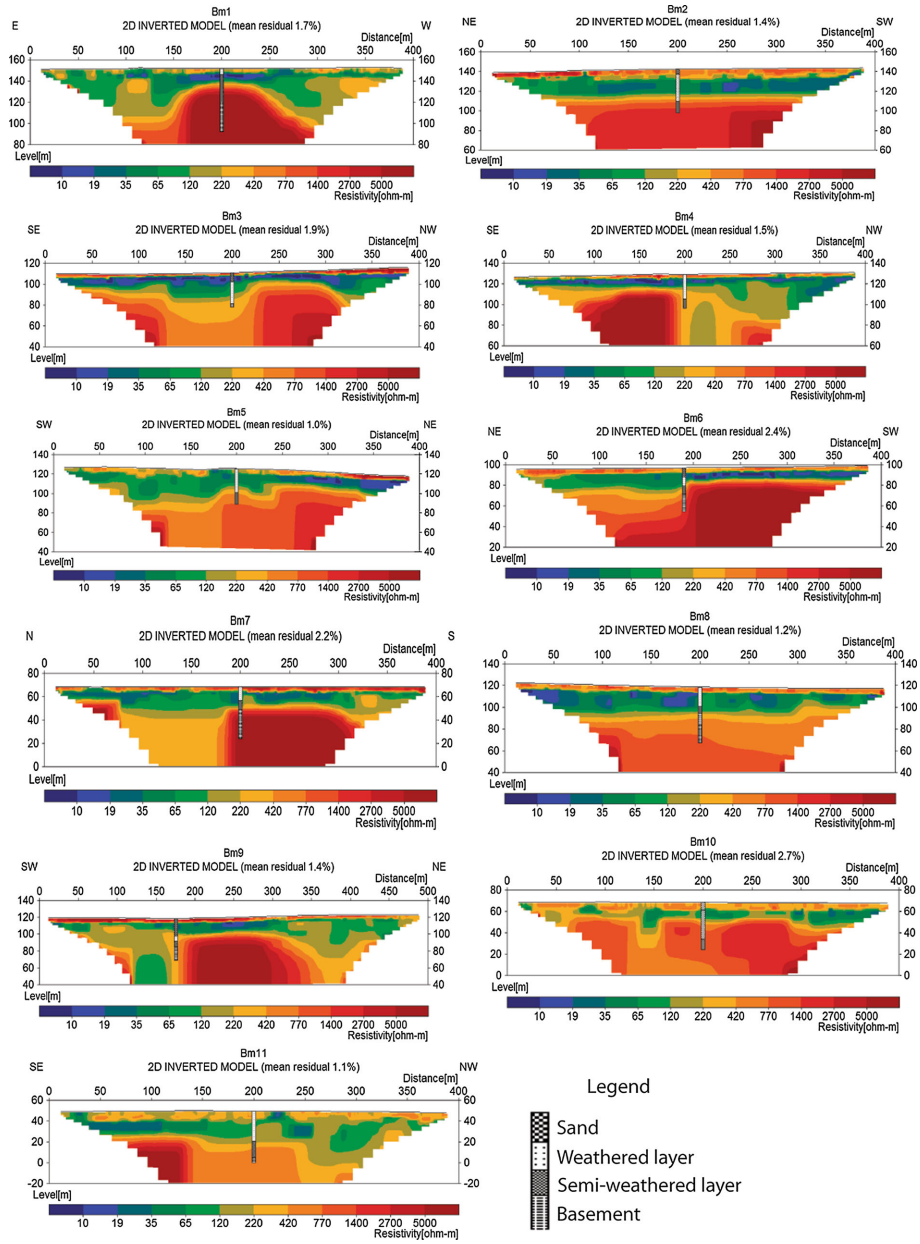

Fig. 5 Resulting models of ERT including the position of the wells

borehole ends in the same resistivity range. Borehole Bm1 which ends in higher resistivity turned out unsuccessful, whereas borehole Bm7 has a yield of 1500 l/h. The latter may be explained by the increased ratio WL/SWL at Bm7 (Table 1).

Normalized chargeability results

Three models representing normalized chargeability values of the pEG, QpE and Qd areas (Fig. 1) are shown in Fig. 6 where the models can be divided into three parts with high, intermediate and lower values of normalized chargeability. The mean residual error is between 1.5 and 3.6% which is an indication of acceptable inverted results.

From the bottom of the inverted IP models, the normalized chargeability is low (<0.025 mS/m) where basement has been documented from the drilling. Immediately above the parts with shallow basement there is a layer with high normalized chargeability value (0.025 to <1 mS/m). The thin shallowest layer has normalized chargeability of 0.016–0.063 mS/m, classified as dry sand in the drilling reports, which is probably not so well sorted because it is in situ weathered.

In the areas outside the shallow basement occurrences, the normalized chargeability is generally intermediate, with values in the range 0.04–0.16 mS/m. This can be interpreted as being related to the higher degree of deep weathering and associated leaching of clay minerals from the shallow parts of the formation.

The high chargeability layer has a more discontinuous character at Bm9, but the reason for this is not known. Here the shallowest layer has a normalized chargeability is lower than for the other lines, being less than 0.01 mS/m, which may be interpreted as well sorted dry sand.

The high normalized chargeability layers and low resistivity value in profile Bm1 and Bm11 suggest the overburden may contain organic material, precipitated minerals or clay content. As indicated by the borehole documentation, the clay layer coincides with this zone (Fig. 6). On the other hand, it was expected that for Bm9 the normalized chargeability would be lower due to the presence of a thick layer of sand. The high chargeability appears in this case to be caused by the presence of heavy mineral sand, in which it is likely that metal precipitation products that make the formation act as a disseminated ore. The high electrical conductivity of the groundwater may in turn be caused by dissolution from the mineral content of the soil.

Water quality

Basic water quality indicators were measured in all boreholes except the dry ones (Bm1 and Bm9). The physical parameters pH, conductivity and temperature were

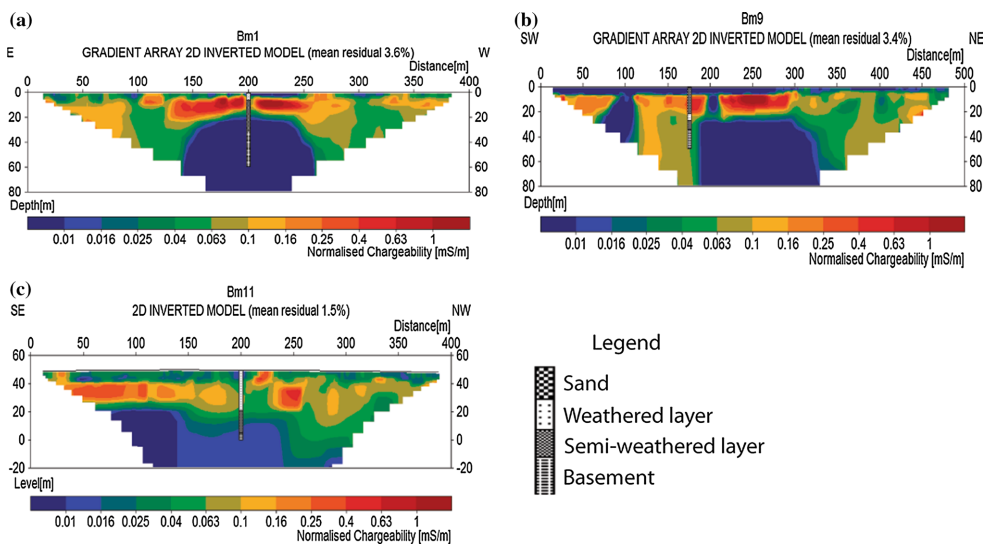

Fig. 6 Inverted IP models showing the normalized chargeability: **a** Bm1, **b** Bm9 and **c** Bm11

Table 2 Result of measurement of physical parameters of groundwater quality at different boreholes (pH, temperature and conductivity)

Borehole	PH	Temp (°C)	Cond. (µS/cm)
Bm2	6.44	27	1444
Bm3	6.87	28.6	2600
Bm4	6.4	28.5	1278
Bm5	6.25	27.9	595
Bm6	6.62	25.8	2240
Bm7	6.84	27	382
Bm8	6.43	28.5	360
Bm9	6.41	28.5	2820
Bm11	5.97	30	470

measured using the ExStik EC510 equipment and the results are presented in Table 2.

The pH of water at Bm3 and Bm7 is in the range of 6.5–8.5 which is the Mozambican standard guideline for potable water. For all other borehole, the measured value of pH is below the standard range which indicates that the water is acidic. The standard value of conductivity for domestic water is below 2000 µS/cm (Portal do Governo 2016). This value is exceeded at Bm3 and Bm6 (Table 2).

Discussion

Combined interpretation of geophysical and geological data

The study area was affected by eustatic Mesozoic/Cenozoic sea-level fluctuations as result of neorifting (Salman and Abdula 1995) characterized by uplifting of Nampula block and formation of a shallow margin sedimentary basin. The Miocene regression wiped out the weathered horizons (Allan et al. 1990; Macey et al. 2007) and continental sediments (eolian) were deposited directly on top of the plane surface of the basement (Macey et al. 2007). The marine sediments were deposited on top of the continental sediments in the following Pleistocene transgression. Adding information of the borehole geological logging report and the inverted ERT models, the reconstruction of the geological history can be summarized in five different events: (1) pre-Gondwana supercontinent; (2) breakup of Gondwana; (3) neorifting event; (4) Cenozoic sand dunes formation (Tupuito formation); (5) uplifting of the African block and deposition of eolian white sand in Pleistocene.

The weathered layer of Mesoproterozoic gneiss (Fig. 7a) was removed during the transgression caused by breakup of Gondwana supercontinent during the Jurassic. As consequence pediments were formed (Fig. 7b). When the sea level was lowered due to rifting 35 Ma ago, the pediments were covered by coastal sand dunes (red sand ridge in Fig. 7c). The cycle of transgression/regression which occurred during Tertiary (Salman and Abdula 1995) resulted in deposition of coastal sand dunes (Macey et al. 2007). This deposit underwent chemical weathering (oxidation) resulting in red sand locally known as Tupuito formation (Lächelt 2004; Macey et al. 2007). This paleo-sand dune ridge forms a steep seaward slope, and it has an erosional feature been covered locally by eolian sand or thin wind redistributed sand cover (Fig. 7e).

The inverted ERT models interpreted together with borehole logging information have improved the geological understanding of subsurface in the study. All resistivity layers have irregular thickness most likely caused by erosion (Bm1 in Fig. 5) and deposition processes (Bm3, Bm4, Bm5, Bm6, Bm7, Bm8; Bm9 and Bm11 in Fig. 5). In Bm1 and Bm10, the thickness ratio of the weathered layer to semi-weathered layer is less than 1/3 (see Table 1) indicating that the weathered layer was eroded (Sharp 2014). The additional geological material on top of the weathering layer, where the ratio is higher than 1/2, is the red sand dunes and white eolian sand (Bm3, Bm6, Bm8 and Bm9).

The degree of fractures in the basement is indicated by the variability of the resistivity values and the yield. The resistivity value of the basement at Bm4 (Fig. 5) is in a range of 220 to >5000 Ωm with a yield of 2800 l/h. At Bm3, Bm5 and Bm9 (Fig. 5), the resistivity value is in the same range as in Bm4 but with yields much less than 2800 l/h (Table 1). According to Acworth (1987), a higher yield would be achieved by increasing the depth of the borehole by fully penetrating the fractured zone.

Aquifers of the study area

The inverted ERT models gave indication of layers with similar properties; however, the geological material might not be the same. There are differences in deposition environment or origin which can be seen in the geological borehole logging and the description of surface geology.

The pEG limited potential for groundwater extraction was confirmed by unsuccessful boreholes at Bm1 and Bm10. Boreholes Bm1and Bm10 were dry because of the nearly absent weathered layer. The WL/SWD ratio at both sites is less than 1/3 (Table 1) which is an indication that the weathered layer was eroded. However, when the fractured zone is hit indicated by decreasing in resistivity as in Bm2 and Bm7 the borehole yield can reach 1200–1500 l/h.

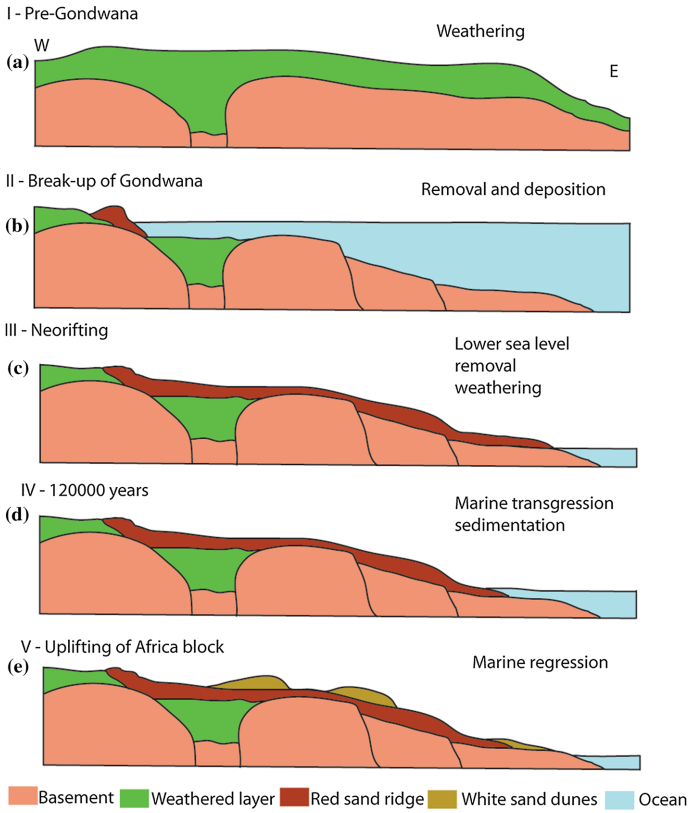

Fig. 7 Profiles with W–E orientation showing five different phases of the geological evolution as result of sea-level fluctuation. **a** Weathering of the basement during pre-Gondwana breakup. **b** Breakup of Gondwana. **c** Regression and preposition coastal dunes. **d** Marine transgression and sedimentation and **e** ongoing uplifting of African block and deposition of eolian *white sand*

Also, when the layer with resistivity value in range of 220–420 Ωm is hit, the obtained yield is high (see Bm3, Bm4 and Bm9 in Fig. 5). The more productive well is Bm4 yielding 2800 l/h (Table 1) where the pEG is covered by QpE. The thickness of QpE varies following the basement shape. The permeability of QpE is highly influenced by ongoing weathering process where the fine material has been leached reducing the permeability toward depth. The QpE is partially covered by Pleistocene/Holocene white sand dune with thickness varying from 9 to 25 m. Macey et al. (2007) includes the eolian colluvium to this Qd. This cover layer was observed in Bm3, Bm6, Bm8 and Bm9. As the layer is thin, the drilling continued reaching the QpE and pEG. An intercommunication between these three units is likely and causing a mixing in water and probably a leaky aquifer response. The mixing also occurs during the infiltration of the rain water (recharge). The aquifers are recharged locally during the rainy season from November to March (Ferro and Bouman 1987).

Interpretation of water quality of found aquifers

The few available data for groundwater quality indicate two different types of water. A low and high mineralized water. The intermediate values could be an indication that the different aquifers are interconnected. Although the pH value is below the standard range for drinking water, the obtained values are also found in groundwater of similar geological environments (Singhal and Gupta 2010). This range of pH does not indicate recent saltwater intrusions or recent exchange with ocean water. It indicates, however, the exchange with rain water.

The IP measurement at Bm9 (Fig. 6) shows the effect of mineralized water. When one measures the resistivity by using VES, the low value usually is related to clay content as expected in a weathering profile (Acworth 1987). At Bm1 and Bm11, the increase in normalized chargeability in the shallow parts is explained by the presence of clay, as Slater and Lesmes (2002) demonstrated, where low

resistivity values correspond with high normalized chargeability can be considered as areas with the presence of clayey sediments. However, at Bm9 the clay is not expected (as seen in Table 1); therefore, the increase in normalized chargeability can probably be explained by the presence of heavy minerals and oxidized iron. The presence of this geological material can also affect the mineralization of the groundwater.

Groundwater management in Mongicual district

A deep understanding and interpretation of hydrogeological processes which led to the formation of the three types of aquifers in the study area is important to understand how the aquifers can be utilized and managed. The extraction of water at the boreholes in the basement will use first groundwater stored in the fissured layer of the basement which will trigger a retarded response of vertical flows from QpE or Qd, where present. Therefore, the water quality and quantity of these two aquifers will affect the well functions. It is important to map carefully the white eolian sand formation to prevent the contamination from the groundwater with elevated electric conductivity values as seen in Borehole Bm3, Bm6 and Bm9 (Table 2).

Because the sand and the weathered layer are highly permeable, the rain water will infiltrate and recharge the aquifers easily. However, with increasing population and semi-urbanization the infiltration area will reduce due to the sealing of the ground and less water will reach the aquifers.

As all rivers dry out during the dry season, the population currently relies on groundwater for a continuous water supply and therefore, it is important to protect the fragile aquifer systems through good management.

Uncertainties

Geological logging of the drill cuttings has its drawbacks, when using rotary percussion with air lifting method. Finer particle compounds may be underestimated or not documented. The depths positioning of lithological breaks will be smudged. In addition, the interpretation was neither made by a geologist nor on complete drill cores in the RWPIP drilling program and therefore it occurs that weathered gneiss is mistaken as coarse sand or pebbles and vice versa. Experts were called in only, when problems had hit. This means that the uncertainty of the borehole data is significant and should be taken into account in the geological interpretation. Had these interpretations been made by a trained geologist their validity would have been less questionable. It would also have made it easier to validate the ERT measurements with actual geological data.

Conclusions

The tendency in large-scale national drilling programs is to deploy a geophysical technique as a stand-alone method; normally using the VES 1D approach to identify suitable sites for water boreholes has proven to be insufficient. This investigation demonstrated that the boreholes when placed above or on the edge of a high resistivity zone with the ratio of weathered and semi-weathered layer less than 1/3 are likely to be unsuccessful. Also the yield of some borehole would have been increased if drilled in locations with more fractured rock and deep weathering. The findings suggest that such a faulty placement could have been avoided, if an ERT survey had been made instead of VES since there would have been more comprehensive information on the 3D character of the geology to make hydrogeological interpretations from. This is equally important in order to understand the geological context and hydrogeological processes which have shaped the area resulting in the formation or destruction of aquifers in order to interpret the geophysical results correctly.

Combining this understanding with the combination of ERT and IP would likely lower the rate of borehole failure and more boreholes could have been drilled from the same budget. Instead of drilling boreholes in areas identified as having poor conditions for hosting aquifers, initiative of rainwater harvesting and surface water management could be prioritized.

The basement, paleo-sand dune ridges and eolian white sand dunes formations are the three hydrogeological units in Mongicual district. They are recharged during the rainy season. Therefore, they are sensitive to climate change and also to human activities on the surface. The increasing population and semi-urbanization will reduce the infiltration area and, as consequence, deplete the groundwater.

Acknowledgements We would like to thank Cowater International Inc. and Solomon Lda for technical and logistical help for supporting this survey in the Nampula province. We also would like to thank B. Andersson, T. Björkström and Eduardo Mondlane staff for all kinds of support during the survey. Furthermore we gratefully acknowledge that Sida has funded the study as part of the bilateral cooperation framework between Eduardo Mondlane University (Mozambique) and Lund University (Sweden).

References

Acworth RI (1987) The development of crystalline basement aquifers in a tropical environment. Q J Eng Geol 20:265–272

Allan E, Nairn M, Lerch I, James E (1990) Geology, basin analysis, and hydrocarbon potential of Mozambique and Mozambique channel. Earth Sci Rev 30:81–124

AMCOW (2012) Water supply and sanitation in Mozambique—turning finance into services for 2015 and beyond—an AMCOW Country Status Overview

Clark L (1985) Groundwater abstraction from basement complex areas in Africa. Q J Eng Geol 18:25–34

Dahlin T (2001) The development of DC resistivity imaging techniques. J Comput Geosci 27:1019–1029

Dahlin T, Zhou B (2006) Multiple-gradient array measurements for multichannel 2D resistivity imaging. Near Surf Geophys 4:113–123

Design Report (2010) Internal report, prepared by: Cowater Inc and Salomon Lda. Submitted to: Millenium Challenge Account—Mozambique and the National Directorate of Water/Rural Water Department. Unpublished report

Ferro BPA, Bouman D (1987) Explanatory notes of the hydrogeological map of Mozambique, scale 1:1,000,000. Project of the hydrogeological map of Mozambique. National Directorate of Water Affairs, Mozambique

Kumar D, Mondal S, Nandam Harimi P, Soma Sekhar BMV, Sem MK (2016) Two-dimensional electrical resistivity tomography (ERT) and time-domain-induced polarization (TSIP) study in hard rock for groundwater investigation: a case study at Choutuppal Telangana, India. Arab J Geosci 9:355

Lächelt R (2004) Geology and mineral resources of Mozambique. Direccao Nacional de Geologica Moçambique, Maputo. ISBN 1-919908-52-8

MacDonald A, Calowb RC (2008) Developing groundwater for secure rural water supplies in Africa. Desalination 248:546–556

Macey P, Miller J, Ingram BA, Cronwright MS, Botha GA, Grantham GH, Robert MR, Kock GS, Mare LP, BothaPMW, Kota M, Opperman R, Haddon IG, Rower C (2007) Map explanation: sheets 1537 Alto Molócuè, 1538 Murrupula, 1539 Nampula, 1540 Mogincual, 1637 Errego, 1638 Gilé and 1639–40 Angoche, Ministério dos Recuursos Minerais e Energia, Direção Nacional de Geologia, Maputo, Mozambique and Council for Geoscience, Pretoria, South Africa, 392 pp

Macey P, Miller J, Rower C, Grantham G, Siegfried P, Armstrong R, Kemp J, Bacalu J (2013) Geology of the Monapo Klippe, NE Mozambique and its significance for assembly of central Gondwana. Precambiran Res 233:259–281

MCA (2013) Millenium challenge account. http://www.mca.gov.mz/m/documents/special/en/MCA_Mozambique_Special_Report_RuralWater.pdf. Accessed Sept 2016

Palacky G (1988) Resistivity characteristics of geologic targets. SEG 1:53–129

Portal do governo (2016) Official publication of the republic of Mozambique: Ministerial diploma nr 180/2004 of September, 15th (I serie—number 37). http://portaldogoverno.gov.mz/por/Governo/Legislacao/Boletins-da-Republica. Accessed Sept 2016

Reynolds JM (2011) An introduction to applied and environmental geophysics, 2nd edn. Wiley-Blackwell, Chichester. ISBN 978-0-471-485360

Salman G, Abdula I (1995) Development of the Mozambique and Rovuma sedimentary basins, offshore Mozambique. Sediment Geol J 96:7–14

Sharp JM (2014) Fractured rocks hydrogeology. CRC Press, USA

Singhal BBS, Gupta RP (2010) Applied hydrogeology of fractured rocks, 2nd edn. ISBN 978-90-481-8798-0, pp 139–154

Slater LD, Lesmes D (2002) IP interpretation in environmental investigations. Geophysics 67(1):77–88

Strahler A (1971) The earth science. A Harper International edition, 2nd edn, CDN 78-127335

Wright EP (1992) The hydrogeology of crystalline basement aquifers in Africa. Geol Soc Spec Publ 66:1–27